2015-09-28

Permeable Pavement in Cold Climates - Improving Hydraulic and Water Quality Performanc

Huang, Jian

UNIVERSITY OF CALGARY

Permeable Pavement in Cold Climates – Improving Hydraulic and Water Quality Performance

by

Jian Huang

A THESIS

SUBMITTED TO THE FACULTY OF GRADUATE STUDIES

IN PARTIAL FULFILMENT OF THE REQUIREMENTS FOR THE

DEGREE OF DOCTOR OF PHILOSOPHY

GRADUATE PROGRAM IN CIVIL ENGINEERING

CALGARY, ALBERTA

SEPTEMBER, 2015

Abstract

The application of permeable pavements has been promoted to reduce pressures on traditional stormwater management systems and enhance urban water. However, the performance of permeable pavement under cold climate context is still uncertain. This thesis focused on assessing the hydraulic and water quality performance of permeable pavements based on field and laboratory experiments and developing a modeling approach for assisting engineering design of permeable pavements.

In a series of field experiments, simulated 100-year storm events with durations of 20 minutes were applied to the pavement surfaces in order to examine and compare the hydraulic and environmental performance of the three permeable pavement types under cold climate conditions. Results demonstrated that PA, PC and PICP are all effective in mitigating storm runoff under cold climate conditions. All pavement types in general have the same level of performance in removing TSS, TP, TN, and heavy metals.

A series of laboratory experiments were designed to assess the ability of the three pavement types to remove TSS, TP and TN within their surface and sub-surface layers individually. PA, PC and PICP with sub-surface layers consisting of different gravel sizes were investigated at various thicknesses. The lab-scale pavements were also compared with the field-scale pavements in terms of pollutant removal. Superior performance in removing pollutants was found in the PC surface layer compared to surface layers of PA and PICP. A regression model based on these results was developed to provide estimates of water quality performance in the field.

A mathematical model for predicting hydraulic and water quality performance in both the short- and long-term is proposed based on field measurements for the three types of permeable pavements. The proposed model can simulate the outflow hydrographs with a coefficient of

determination (R^2) ranging from 0.762 to 0.907, and normalized root-mean-square deviation (NRMSD) ranging from 13.78% to 17.83%. Comparison of the time to peak flow, peak flow, runoff volume and TSS removal rates between the measured and modeled values in model validation phase had a maximum difference of 11%.

Acknowledgements

I would like to thank the City of Calgary, Natural Sciences and Engineering Research Council of Canada and Urban System Ltd. for their financial support of this research. I would also like to thank LaFarge and Harald von Langsdorff from UNI-GROUP U.S.A. for donating test materials and Canada Lands Company for assisting with land use.

I would also like to gratefully thank my supervisor Dr. Caterina Valeo for giving me the opportunity to get involved in such a fabulous research team as well as a great research project. I will never forget the constant guidance, patience and understanding you have given during my life in the University of Calgary.

I would like to express sincere thanks to my co-supervisor Dr. Jennifer He for her valuable inputs and discussions, as well as critical suggestions and valuable feedback on my chapter reviews. I would also like to express all these thanks to my previous co-supervisor Dr. Angus Chu, for his knowledge, guidance, and insight throughout my field and laboratory experiments. All your unselfish help has carried me every step and changed my life.

I also want to show my gratitude to all the people in the City of Calgary who were involved in this research. Thanks to Pamela Duncan, Bert van Duin for their helpful suggestions, guidance and support on the direction of this research. Thanks to Philip Jerome, Heather Feil and Ian Huybregts for assistance with the field experiments.

All my thanks are extended to the technical staff in the University of Calgary. Thanks to Terry Quinn, Donald Anson and Mirsad Berbic for their assistance on wood frame construction, field and laboratory equipment preparation, and moving of heavy objects. Thanks to Daniel Larson and Derek Wilson for their great laboratory support in my water quality analyses.

Dedication

I wish to dedicate this dissertation to my parents for all their wholehearted devotions to carrying me to this stage, and my wife Ningning, for her encouragement, understanding, love, and ongoing support on everything.

Table of Contents

List of Tables

List of Figures and Illustrations

List of Symbols, Abbreviations and Nomenclature

Symbol	Definition
PA	porous asphalt
PC	porous concrete
PICP	permeable inter-locking concrete paver
PSD	particle size distribution
LID	low impact development
TSS	total suspended solid
TN	total nitrogen
TP	total phosphorus
SIR	surface infiltration rate
A	surface area of pavement (m^2)
$A_{orifice}$	cross section area of orifice (m^2)
b	water balance coefficient
C	concentration of pollutant (mg/L)
C_0	initial concentration of pollutant (mg/L)
C_{TSS_in}	average TSS concentration of inflow (mg/L)
C_{TSS_out}	average TSS concentration of outflow (mg/L)
d	gravel diameter (m)
d_p	particle diameter in TSS (m)
d_{pond}	ponding depth (mm)
$F_{surface}$	pollutant removal rate by surface layer (%)
g	gravitational acceleration (m/s^2)
H	water level in pavement (m)
h	water depth in infiltrometer (mm)
h_{in}	water depth through infiltration (m)
h_{out}	water depth through discharge (m)
h_{63}	thickness of 63 mm gravel (mm)
h_{40}	thickness of 40 mm gravel (mm)
h_{12}	thickness of 12 mm gravel (mm)
h_{in}	inflow water depth (m)
h_{out}	discharge water depth (m)
k	Boltzmann constant = 1.3805×10^{-23} (J/K)
L	thickness of pavement structure (m)
M_{in}	inflow TSS load (mg)
M_{out}	outflow TSS load (mg)
M_{TSS}	cumulative TSS load (mg)
M_{TSS_out}	cumulative TSS load in outflow (mg)
m	porosity of gravel layer
m_b	porosity in the boundary layer
n	number of measurements
p_r	peak flow reduction (%)
Q_0	initial flow rate (L/s)
Q_{inflow}	inflow rate (L/s)
Q_{out}	outflow rate (m^3/s)

$Q_{out\_measured}$	measured outflow (m^3/s)
$Q_{out\_modeled}$	modeled outflow (m^3/s)
Q_p	peak outflow rate (m^3/s)
$Q_{p\_measure}$	measured peak outflow (m^3/s)
Q_{p_model}	modeled peak outflow (m^3/s)
P	porosity of a specific layer
$P_{surface}$	surface porosity
P_{base}	base porosity
$P_{sub\text{-}base}$	sub-base porosity
R^2	coefficient of determination
R_{TN}	removal rate of TN (%)
R_{TN_63}	removal rate of TN by 63 mm gravel (%)
R_{TN_40}	removal rate of TN by 40 mm gravel (%)
R_{TN_12}	removal rate of TN by 12 mm gravel (%)
R_{TP_63}	removal rate of TP by 63 mm gravel (%)
R_{TP_40}	removal rate of TP by 40 mm gravel (%)
R_{TP_12}	removal rate of TP by 12 mm gravel (%)
R_{TSS}	removal rate of TSS (%)
R_{TSS_63}	removal rate of TSS by 63 mm gravel (%)
R_{TSS_40}	removal rate of TSS by 40 mm gravel (%)
R_{TSS_12}	removal rate of TSS by 12 mm gravel (%)
R_{TSS_out}	overall removal rate of TSS (%)
T	absolute temperature of stormwater (K)
T_p	pavement temperature (℃)
t	infiltration time (hr)
t_d	discharge time (min)
t_p	time to peak (min)
t_{pond}	ponding time (min)
V_{in}	volume of inflow (L)
V_{out}	volume of outflow (L)
v	flow velocity (m/s)
X	operation time (month)
Y	maintenance time (month)
α	contact efficiency
δ	transient loss coefficient
η	total single collector efficiency
η_d	single collector efficiency by diffusion
η_{in}	single collector efficiency by interception
η_s	single collector efficiency by sedimentation
μ	kinematic viscosity of water (m^2/s)
ρ	density of water (m^3/kg)
ρ_p	density of particle in TSS (m^3/kg)
φ	sphericity of gravel

Chapter One: Introduction

1.1 Research Background

When natural pervious landscapes are replaced by impervious areas due to urbanization, rainfall-runoff processes are altered and thus, negatively affect urban water environment in terms of both water quantity and quality. The impervious areas mainly consist of constructed surfaces such as rooftops, sidewalks, roads and parking lots that are covered with impermeable materials such as asphalt, concrete and stone. These materials prevent precipitation from infiltrating into underlying soil, which leads to water quantity problems such as high peak flows and surface runoff volumes, and loss of groundwater recharge. In addition, the increased surface runoff contains various pollutants and becomes a potential source of pollution for receiving water bodies. (Pratt 1995, Brooth and Leavitt 1999)

Traditionally, stormwater management has been addressed by replacing the lost functions of soil with stormwater detention facilities such as detention and retention ponds. This approach leads to the natural hydrologic cycle being altered by development practices (Brattebo and Booth 2003). Stormwater runoff is transported through storm sewer systems to these facilities where water is temporarily stored and then discharged to receiving streams. However, stormwater detention facilities only control peak flows and still allow increases in water volume compared to pre-development conditions. In addition, these facilities address the concerns of poor water quality when treating storm runoff. Other than consideration of water quantity and quality, the effectiveness of land use and associated construction cost are also of concern when constructing stormwater detention and retention ponds (Dietz 2007). The accelerated urbanization leads to the

requirement for continuous expansion of these facilities, which results in ineffective land use and budgeting issues due to increasing number and sizes of ponds.

Although stormwater ponds are still widely accepted in urban stormwater management, many professionals consider source control of stormwater as a more effective approach for urban stormwater management. Stormwater source control facilities can reduce stormwater runoff volume and simultaneously mitigate stormwater pollution on site. By applying these facilities, urban lands can also be saved for other usage as they are easily integrated into urban development (Brabec 2002). Low impact development (LID) is a popular technology that employs the source control concept. LID is an onsite design strategy with the target of maintaining, as much as possible, pre-development hydrologic characteristics through the use of design techniques to create a functionally equivalent landscape. By applying LIDs, hydrologic functions such as runoff infiltration and storage, and discharge volume, are maintained through techniques such as stormwater detention area, reduction of impervious surface, and the lengthening of flow path and runoff time (Jacobson 2011).

One LID technology that can effectively reduce surface imperviousness in high density urban areas is permeable pavement. Permeable pavement is not a new concept and was first introduced in early 1970s. However, its popularity and widespread use did not emerge until the past decade in part due to the need to address urban stormwater management issues resulting from rapid urbanization (Scholz and Grabowiecki 2007). There are three types of permeable pavements that are widely used nowadays: porous asphalt (PA), porous concrete (PC) and permeable inter-locking concrete pavers (PICP). Unlike traditional pavements, the surface layer of permeable pavements is intentionally made porous with void spaces to allow infiltration of surface runoff. The infiltrated water is stored and filtered in the gravel layer of the base structure before

discharging to either the stormwater sewer system or the receiving stream through an under drain (Drake et al. 2013). Depending on the design and sub-grade soil conditions, infiltrated water can further infiltrate through sub-grade soil and recharge groundwater. Permeable pavements have been demonstrated to be capable of reducing stormwater quantity in both peak flow and runoff volume and improving stormwater quality by removing various pollutant onsite. In addition, permeable pavements can be easily integrated into existing urban areas and does not take up additional space, which is economically feasible in terms of land use (Elliott and Trowsdale 2007).

Due to the functionality and feasibility of permeable pavements, their implementation has been substantially increased. The quantitative benefits from implementing the technology for stormwater management has therefore become an important topic among stormwater management scholars and researchers. Previous studies have investigated permeable pavements from two main perspectives: hydraulic and water quality performance. In hydraulic performance, parameters such as peak flow and volume reduction, delay in time to peak, discharge time, surface infiltration rate (SIR) and surface porosity have drawn a lot of attention (Brattebo and Booth 2003, Sansalone et al. 2008, LeFevre et al. 2009, Pezzaniti et al. 2009, Roseen et al. 2011, Huang et al. 2012). In water quality performance, most studies have focused on the ability to remove total suspended solids (TSS) and a considerable number of studies have examined the removal of nutrients including total phosphorus (TP) and total nitrogen (TN) (Pratt et al. 1995, Pagotto et al. 2000, Bean et al. 2007a, Brown et al. 2009, Huang et al. 2012). Several studies have also paid attention to several heavy metals, such as lead (Pb), copper (Cu) and Zinc (Zn), which are frequently observed in stormwater runoff (Sansalone and Buchberger 1995, Dierkes et al. 1999, Brattebo and Botth 2003, Fach and Geiger 2005). Although an individual study applies its own methodology to conduct the research,

the methodologies, in general, can be categorized into three main streams: field experiment, laboratory experiment and computer modeling.

Results from previous studies have consistently shown the hydraulic efficiency of permeable pavements; whereas their water quality performance appears to be inconsistent. For instance, the removal rates of TP are found in a wide range from 0% to 80%, and the removal rates of TN are from 0% to 50%. These discrepancies might be the result of many factors such as test methodology, pavement type, local climate condition, etc. Climate condition, especially air temperature, can be an important factor that leads to a variation in water quality performance. Until now, a large number of studies on permeable pavement have been conducted for mild climate condition; but very few studies have investigated the hydraulic and water quality performance of permeable pavements in cold climate conditions. Therefore, investigation of permeable pavements in cold climate is required for wide-scale implementation of permeable pavements in such climate conditions. Many parts of Canada, such as Calgary, experience cold climate conditions (sub-zero weather). Calgary experiences a dry continental climate with long and cold winters. The temperature in winter is usually below 0℃; while it is interspersed with brief warm periods known as Chinooks. The Chinook currents (warming trends during winter) quickly bring the temperature above 0℃ several times over the period of a day in winter. Thus, there are several freeze-thaw cycles in Calgary winters. However, no previous studies provide sufficient information to support wide application of permeable pavements in Calgary and other cold regions in Canada. More importantly, there are no robust modeling tools available for engineering design of permeable pavements considering both hydraulic and water quality performance.

1.2 Research Objectives

As a part of the City of Calgary's new water management strategy, the city has intentions to implement permeable pavements along with other LID technologies to maintain and improve a healthy urban water environment. However, little-to-no local data on the performance of permeable pavements is available to demonstrate their applicability. It has also been questionable to simply transfer the findings between different climate conditions, as climate is expected to play a key role in determining permeable pavement performance and applicability. To the present day, little research has focused on cold climate conditions to support the potential application of permeable pavements in Calgary and other cold regions. Cold climate is characterized as long winter conditions, such as average temperature below 0℃ for several months in winters. Winters in Calgary are cold and temperature is usually below 0℃. But Chinook currents (warming trends during winter) quickly bring the temperature above 0℃ several times over the period of a day in winters. Thus, there are several freeze-thaw cycles in Calgary winters. During these freeze-thaw cycles, considerable amount of surface runoff is formed by snow melt. The surface runoff also carries large amount of pollutants (e.g., TSS) and negatively impacts the urban water environment and receiving water bodies. To fill the identified research gap, this dissertation will undertake an assessment of permeable pavements with regards to hydraulic and water quality performance, provide the fundamental knowledge on relationships between pavement structure and performance, and provide practical and robust modeling tools for assisting in the engineering design of permeable pavements. Therefore, the primary objectives of this dissertation include:

1. Investigating and comparing the hydraulic and water quality performance of different permeable pavements (PA, PC and PICP), especially focusing on the influences of Chinook conditions and sanding materials in Calgary's winters on their performance.

2. Assessing the feasibility of the permeable pavements in terms of hydraulic and water quality performance in Calgary's cold climate condition.
3. Evaluating the influence of pavement surface layer, size of bedding materials and thicknesses of bedding layer on the removal of various pollutants.
4. Developing robust models to predict the performance of permeable pavements.

In order to accomplish the objectives 1 to 2, field experiments on three types of field-scale pavements are carried out with a focus during the winter seasons from 2011 – 2013. Analyses based on the collected data from the field experiments are conducted to determine the feasibility of these pavements in terms of storm runoff mitigation, surface infiltration, and pollutant removal. Objective 3 is accomplished using laboratory experiments. Lab-scale pavement cells of surface layers and base layers with various gravel sizes and thicknesses are used to investigate the linkage between pavement structure and water quality performance. In addition, pollutant removal by lab-scale pavement cells, whose structures are similar to the field-scale pavements, are also compared to that of the field-scale pavements to investigate the transferability of knowledge obtained from lab-scale pavements to lab-scale pavements. For objective 4, both conceptual models and data-driven models (multiple linear regression model) are developed based on observations from both field and laboratory experiments to aid in the engineering design of permeable pavements.

1.3 Dissertation Layout

Following this chapter, Chapter 2 is dedicated as a general literature review of permeable pavements to present key findings and research gaps identified from previous field-based, laboratory-based and computer simulation studies. Chapters 3 to 5 are structured as journal articles. Each chapter presents the results and discussions of the hydraulic and water performance of

permeable pavements under cold climate conditions, the linkages between pavement structure and water quality performance and between field-scale and lab-scale pavements, and the development of a conceptual model, respectively. A description of the study site and detailed methodologies are included in these chapters. In addition, a more specific literature review concerning the subject of each chapter is provided in the introduction section to better illustrate the research objectives. Sections such as materials and methods, results and discussions, and conclusions follow the introduction section in each of the chapters. Chapter 6 states general conclusions and summarizes the novel contributions of this research and recommendations for future study. The coverage of Chapters 3 to 5 is given as follows:

In Chapter 3, the hydraulic and water quality performance of three types of permeable pavements (PA, PC and PICP) are assessed using simulated 1:100 year storm events under Calgary's climate conditions. The assessment is based on field experiments on the field-scale pavement cells. Monitored hydraulic data including inflow and outflow hydrographs, pavement surface ponding, and SIR, are used to determine storm runoff mitigation and degradation of surface infiltration along with time. Measured water quality parameters including TSS, TP, TN, and three heavy metals Cu, Pb and Zn, are used to determine the pollutant removal efficiency of the pavements. Regression analysis is conducted to investigate the change of hydraulic performance with respect to degradation of surface infiltration capacity. The impact of pavement temperature on the TP, TSS, and TN removal rates are also investigated using regression analysis. In order to assess the influence of hydraulic performance on water quality performance of the pavements, correlation analysis is performed to detect potential associations between water quality parameters and hydraulic variables. In addition, comparison on performance is made among the three pavements using statistical analyses including Wilcoxon signed-rank and rank-sum tests, and

Kruskal-Wallis test. The materials in this chapter have been submitted to the Journal of Environmental Engineering – ASCE for publication.

In Chapter 4, water quality performance of individual layers of the three types of pavements (namely, surface layer and sub-surface layer) is assessed using finer scale (lab-scale) cells. The assessment is based on laboratory experiments which are designed to examine the ability to remove TSS, TP and TN by three types of surface layers (PA, PC and PICP), as well as sub-surface layers with various gravel sizes (63 mm, 40 mm and 12 mm) and various thicknesses. Regression analysis is performed to evaluate the dependence of outflow TSS, TP and TN on different gravel layers, and dependence of TP and TN removal on TSS removal. Comparison among different layers is also made in terms of the particle size distribution (PSD) and treatment efficiency. The removal of pollutants including TSS, TP and TN of lab-scale and field-scale pavements is also compared. In addition, regression models, in which the pavement structure parameters (gravel size and thickness of gravel layer) are the inputs, are established to predict TSS and TP removal rates. The materials in this chapter have been submitted to the Journal of Hydrologic Engineering – ASCE for publication.

Chapter 5 proposes a new conceptual model, which integrates modified Kozeny-Carman equation and Yao equation, to simulate the infiltrated flow and TSS through pavement structure. Field experimental data of each pavement type are divided into two groups: one for model calibration and the other for model validation. Some parameters such as porosity of surface and base layers are calibrated by regression models with the measured SIR data from the field experiments. The performance of the proposed model is assessed in several simulated variables including peak flow rate, time to peak, runoff volume and TSS removal rate using model performance evaluation metrics including coefficient of determination (R^2) and normalized root-

mean-square deviation (NRMSD). The materials in this chapter have been submitted to the Journal of Hydrology for publication.

Chapter Two: General Review of Permeable Pavement

2.1 Overview of Permeable Pavement

Low Impact Development (LID) technology is a relatively new stormwater management strategy developed to reduce or eliminate the need for traditional stormwater infrastructure. Conventional stormwater infrastructure can be both environmentally and economically unfavourable. One popular LID is permeable pavement because it can treat stormwater both in terms of water quantity and quality on site. Thus, stormwater is no longer a waste product typically absorbed by receiving waters and depending on how the permeable pavement is constructed and maintained it can be very cost effective (Pratt 1995).

Permeable pavement is a pavement with a high permeability and thus, can collect, store and treat stormwater runoff. It is generally used in pedestrian and vehicular traffic areas such as pathways, driveways, parking lots and access roads (Scholz and Grabowiecki 2007). A permeable pavement system allows stormwater to flow from the surface to its structure (the region spanning from the bottom of surface pavement layer to the top of the sub-grade and includes the bedding layer). The sub-grade is the surrounding soil which may or may not be protected by an impervious liner depending on the design. The water finally reaches a sub-drain or is allowed to further infiltrate into the surrounding sub-grade to recharge groundwater if there is no impervious liner. Stormwater is temporarily stored in sub-structure of the permeable pavement during the duration of the storm and hence, stormwater runoff is reduced. Sediment and pollutants in stormwater are trapped and filtered within the sub-structure and water quality is improved (Drake et al. 2013, Imran et al. 2013).

2.2 Potential Advantages and Disadvantages of Permeable Pavement

2.2.1 Potential Advantages

According to previous studies and applications, some of the potential advantages of permeable pavements include: i) reducing volume of runoff from pavement surfaces and a potential decrease in sizes of storm drainage system; ii) preventing overland runoff from directly reaching water receiving bodies and potentially decreasing peak flows in rivers and streams; iii) assisting in aquifer and groundwater recharge; iv) trapping pollutants that might contaminate receiving waters (Abbott and Comino-Mateos 2003, Brooth and Leavitt 1999, Brattebo and Booth 2003, Ismail et al. 2012); v) removing water from the driving surface to prevent hydroplaning; and vi) reducing traffic noise (Brown 2007).

2.2.2 Potential Disadvantages

There are also some potential disadvantages summarized from previous applications. Due to the existing void space in pavement surface, abrasion and damage are likely to occur under heavy traffic loads. Permeable pavement is also vulnerable to frost heave when moisture is retained in void space during winter time (Dierkes et al. 2002). When permeable pavement is designed for further infiltration into sub-soil and groundwater recharge, a common concern is the potential risk of groundwater contamination by storm runoff pollutants (Legret el al. 1996, Legret and Colandini 1999). Although results from several studies show that this risk is low due to the effective filtration capability, permeable pavement is not recommended to install near stormwater hotspots such as vehicle service and maintenance areas, gas stations and industrial facilities with hazardous waste (Rankin and Ball 2004, Fassman and Blackbourn 2010).

Clogging is also a major issue for permeable pavement, which is primarily led by continuous deposition of sediment on pavement surface without proper cleaning (Tan et al. 2003, Montes and Haselbach 2006). In some cases, pavements lose their surface infiltration capacity when given poor attention to maintenance action. As a result of clogging potential, special cleaning and maintenance methods must be implemented to ensure sufficient infiltration capacity, which may introduce extra costs when compared to conventional pavement (Illgen et al. 2007, Lucke and Beecham 2011).

2.3 Structural Component

Permeable pavements were first developed in the early 1970's. Similar to traditional pavement, permeable pavement can consist of a variety of structural components and configurations. Figure 2.1 shows schematic of PICP structure consisting of different layers. The pavement surface is a permeable layer which directly receives traffic loads and storm runoff. Below the surface layer is the base which increases the overall thickness of a pavement and spreads out traffic loads. Depending on the type of surface layer, the base consist of different layers including bedding and base and sub-base layers that usually contain various sizes of gravel for load distribution and infiltrate storage purposes. Sub-drain system may be placed at the bottom of base layer depending on the condition of sub-grade soil and the possibility for groundwater recharge. In this case, the infiltrated water is usually discharged to a receiving stream through a storm sewer system.

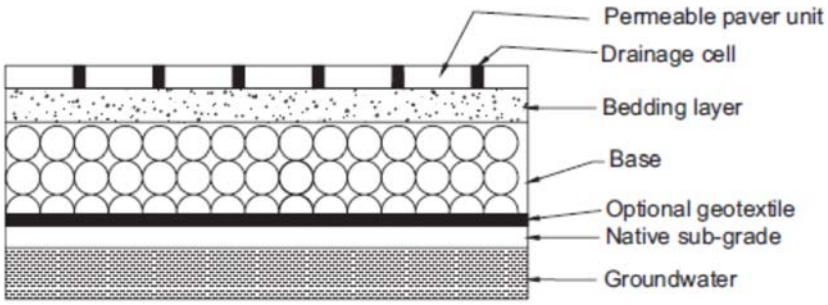

Figure 2.1. Schematic of permeable pavement structure

2.3.1 Surface Layer

There are different types of permeable pavement surface layers with distinguishing physical characteristics. Nowadays the most widely used types are porous asphalt (PA), porous concrete (PC) and permeable inter-locking concrete pavers (PICP) (Ferguson 2005), which are shown in Figure 2.2. People usually name a permeable pavement based on the type of surface layer and this naming strategy is also used in this dissertation.

PA consists of standard bituminous asphalt without the presence of fine materials. Similar to PA, PC is produced by substantially reducing the fines in the mix in order to establish voids for infiltration. Both PA and PC have a coarser appearance than its conventional counterpart (Figure 2.2). PICP consists of inter-locking load-bearing units that are shaped to form open voids when they are laid on ground. The voids are usually filled with small aggregates and grass to maintain structural integrity and aesthetic appearance (Brown 2007). Depending on the pavement use and expected traffic loads, the pavers can also be plastic that are manufactured lattice-like products to create voids for infiltration (Ferguson 2005).

Figure 2.2. Surface layers of permeable pavement

2.3.2 Base Layer

The base layer is constructed above the subgrade soil to provide structural strength and a smooth support for the surface layer. In permeable pavement, this layer typically consists of different sizes of gravel that provide a high level of porosity to temporally store water. Depending on the use of surface layer, the base layer is further divided into more layers of different gravel known as bedding, base and sub-base layers. For instance, PC is a rigid pavement and one base layer can usually provide sufficient structural support. PA is a flexible pavement and it needs both base and sub-base layers for even distribution of traffic loads to subgrade soil (Hein et al. 2010). The thickness and sizes of gravel are dependent on both subgrade soil strength and design storage volume. Poor subgrade soil with low support strength requires thicker base layer(s). Size of gravel in the sub-base layer is usually greater than that in bedding and base layers in order to provide sufficient water storage space. Pollutant removal may also be a concern when determining thickness and gravel size in base layer(s).

A permeable geo-textile fabric is usually placed on top of subgrade soil right below the base layer of permeable pavement. The purpose of this is to: i) maintain the structural integrity of

both pavement and subgrade soil; ii) prevent pollutant migration to subgrade soil and contaminate groundwater, especially when groundwater recharge by infiltrate is expected.

2.4 Hydraulic Performance

2.4.1 Runoff Mitigation

Urbanization leads to increased runoff volumes, peak flow as well as reduced time to peak during storm events. Nearly all these water quantity problems result from one underlying cause: loss of water-retaining function of soil in an urban landscape. Permeable pavement offers a great solution to restore urban perviousness and a considerable number of studies have been conducted on its water quantity performance. Study results show that permeable pavement is capable of reducing surface runoff, attenuating peak discharges and delaying time to peak (Brattebo and Booth 2003, Sansalone et al. 2008, LeFevre et al. 2009, Pezzaniti et al. 2009, Roseen et al. 2011, Huang et al. 2012).

The quantitative degree to which these improvements occur is dependent on various factors such as pavement structure, magnitude of storm and climate condition and hence, the performance of a permeable pavement is unique and site specific (Kuang and Sansalone 2006). Previous studies have covered water quantity performance of various types of pavements under different magnitude storms, and these studies were mostly conducted in warm climate regions. Runoff mitigation by permeable pavement in cold climate regions is not clearly identified and further study is needed to support the applicability. In addition, little research has analyzed the relationship between runoff mitigation and water quality performance, especially under cold climate conditions. Therefore,

further study is suggested to prove the runoff mitigation ability of permeable pavement in cold climate regions.

2.4.2 Surface Infiltration

One major difference between permeable pavement and conventional pavement is the surface layer with porosity to allow water infiltration. Surface infiltration rate (SIR) is a measure of pavement's ability to drain water from its surface into the base and sub-base layers. SIR is the combined forces on water including gravity, negative pore water pressure and drag forces by surface materials (James and Langsdorff 2003). It is believed that SIR is the most fundamentally important measure of a permeable pavement that predominates runoff and peak flow attenuation (Tan et al. 2003, Pezzaniti et al. 2009, Yonget al. 2013). Degradation of SIR, as well as the rejuvenation methods, has been the topic of increasing research in recent years.

Previous studies focusing on SIR show widely varying results on initial and degradation patterns of SIR. Even for the same type of permeable pavement with similar ages, the results can be totally different in terms of SIR changes over time by different studies. For instance, initial SIRs of PICP were reported in a wide range from 200 mm/hr to 30,000 mm/hr. Several studies showed rapid degradation patterns and lost their infiltration due to clogging after 2 years of operation, while some PICP continuously performed in a satisfactory level for up to 9 years' time (Gerrits 2001, Brattebo and Botth 2003, Dierkes et al. 2002, Gilbert and Clausen 2006, Huang et al. 2012). Studies on PA also shared similar findings in which initial SIRs of PA were measured between 2,000 mm/hr to 80,000 mm/hr (Bean et al. 2007a, Brown et al. 2009, Huang et al. 2015, He et al. 2015). The International BMP database 2014 shares similar findings on SIR of PA, PC and PICP (SIR > 2000 mm/hr). Based on the relevant information provided by previous studies,

several factors leading to this wide discrepancy include pavement design (e.g. mix design, surface material), operation environment (e.g. traffic loads, use frequency), geographic locations (e.g. temperature, frequency of storm), and pavement ages (Collins et al. 2008, Deo et al. 2010, Chai et al. 2012).

With combined effects of the above factors, the response to SIR for individual permeable pavements become highly unpredictable. This variability and unpredictability implies that one cannot simply introduce the observation from another study and assume it applies adequately to another scenario. Therefore, in order to examine SIR of a permeable pavement, investigation on a local basis is strongly recommended.

Clogging in permeable pavements has been the topic of many recent studies. In general, it is formed by the accumulation of debris on the surface layer and causes the degradation of SIR for permeable pavement. When clogging is present, the SIR is substantially reduced and eventually to the point of completely negating the hydraulic performance of the permeable pavement (Balades et al. 1995). In terms of the specific characteristics of cumulated surface materials that are responsible for reduced SIR, the deposition of fine sediment appears to the most significant. The mechanisms that lead to this deposition include mechanical wear, brake dust, grinding, rushing and compaction of vehicular traffic, and sediment transport by wind (Bean et al. 2004, Bean 2005).

Previous studies show that proper maintenance can address the clogging issue and restore SIR, which helps to extend the functional life of permeable pavement. Widely accepted maintenance nowadays includes dry/wet vacuum sweeping and pressure washing. These operations focus on the removal of fine materials in the upper section of the surface layer that are responsible for clogging. Previous findings indicate that a successful maintenance operation is dependent on proper determination of maintenance type and frequency to specific pavement types

(Brown et al. 2009, Dougherty et al. 2010, Al-Rubaei et al. 2013). Geological and climate conditions also affect the outcome of maintenance due to different natures of fine deposition (Bean et al. 2004). Therefore, further study is suggested to figure out proper maintenance operation for different types of permeable pavement in a local scale.

2.5 Water Quality Performance

During storm events, various pollutants are carried to receiving streams by surface runoff, which becomes a potential source of pollution to our urban water environment. Major storm runoff pollutants include TSS, TP, TN, and heavy metals according to previous studies on stormwater quality (Pratt 1995, Finkenbine et al., 2000). Instead of stormwater quantity, more attention has been given to stormwater quality in recent years due to rapid urban expansion and deteriorated stormwater quality. Following this trend, recent studies on permeable pavements have been focusing on their ability of removing pollutants. The results indicate that permeable pavement is capable of removing pollutants through mechanisms such as sedimentation and filtration. In this thesis, sedimentation refers to the tendency for solids to settle out of the fluid and rest against on porous media. Filtration is equivalent to the combination of interception and straining and is the separation of solids from the fluid in the voids of porous media.

2.5.1 TSS Removal

TSS is the major pollutant in storm runoff, which is from pavement wear, vehicular tire tracking, and adjacent lands (Rankin and Ball 2004). It is also a critical pollutant that needs to be removed as it increases water turbidity, inhibits plant growth and diversity, affects river biota, and

reduces the overall number of aquatic species (Brown 2007). In addition, several pollutants were found easily attached to TSS such as TP and heavy metals (Balades et al. 1995, Legret and Colandini 1999). Thus, many municipalities in North America use TSS removal as an index in design of stormwater systems. For instance, the City of Calgary requires a minimum of 85% TSS removal rate for stormwater ponds and LID units (The City of Calgary 2011). In Toronto, permeable pavement requires a minimum of 50% TSS removal rate (Toronto and Region Conservation Authority 2010). The City of Portland requires that more than 70% of TSS be removed from storm runoff by permeable pavement (The City of Portland 2014).

Previous studies showed unanimous results on the removal of TSS by permeable pavements. The average reported removal rates were above 75% regardless of pavement types, ages and traffic loads (Pratt et al. 1995, Pagotto et al. 2000, Bean et al. 2007a, Brown et al. 2009, Huang et al. 2012). The primary mechanism behind TSS removal is sedimentation and filtration through pavement structure (Stotz and Krauth 1994). With regards to PSD, effluent from permeable pavements generally has a finer gradation than influent due to aforementioned removing mechanisms (Legret et al. 1996, Legret and Pagotto 1999).

The above summarized findings are mainly based on permeable pavements installed in mild climate areas. Although several studies were conducted in cold climate areas where temperature drops below 0℃ during the winter time (Booth and Leavitt 1999, Bean et al. 2007b), more evidence shall be provided to further support the removing ability of TSS by permeable pavement in cold climate areas. The pavement structure also plays an important role to the removal rate but so far, no research has comprehensively analyzed the relationship between TSS removal and pavement structure. Therefore, study on dependence of pavement structure on TSS removal is necessary to optimize the design from a water quality perspective.

2.5.2 Nutrient Removal

Nutrient components in storm runoff mainly include phosphorus and nitrogen that source from roadside fertilizer applications. Although the concentrations of TP and TN are not as significant as TSS in storm runoff, attention should also be given to them as excessive TP and TN can negatively impact the receiving streams, rivers and lakes. These pollutants cause eutrophication and help algae to grow faster than the water environment can handle (e.g., DO depletion). Significant increases in algae can harm water quality, and deplete oxygen that fish and other aquatic life need to survive (Shuster et al. 2005, Jacobson 2011). Although no strict requirement is announced, several municipalities do recommend that TP and TN be removed from storm runoff. For instance, New Jersey Department of Environmental Protection recommends 60% of TP and 50% of TN be removed by LIDs (New Jersey Department of Environmental Protection 2004). Bureau of Watershed Management in Pennsylvania recommends a permeable pavement should provide 80% and 30% of treatment efficiency on TP and TN, respectively (Pennsylvania Department of Environmental Protection 2006).

Some studies have been conducted to examine the removals of TP and TN by permeable pavement in laboratory and field environments. Unlike TSS, the reported removal rates of TP and TN show a wide range. In general, removal rates of TP were found between 40% and 85%, and no TP removal was observed in some particular cases (Rushton 2001, Gilbert and Clausen 2006, Bean et al. 2007, Tota-Maharaj and Scholz, 2010, Eck et al. 2011). Removal rates of TN were found below 40% in most cases, with a few studies up to 50% (Pagotto et al .2000, Rushton 2001, Bean 2005, Dreelin et al. 2006, Huang et al. 2012). No comprehensive research has yet been done to conclude the removing mechanisms for TP and TN by permeable pavement. But based on previous

findings, TP may be removed by both physical filtration and chemical sorption. The mechanism of TN removal was found complex and suspected to be mainly biological (Collins et al. 2010, Brown et al. 2012).

The above findings indicate that removal rates of TP and TN differ from case to case. This might be ascribed to various factors such as different pavement material, inflow characteristics and climate conditions. In order to obtain a comprehensive performance pattern under Calgary's inflow and climate conditions, there is a need to initiate a study on a local basis. In addition, further evidence shall be provided to prove the removal mechanisms of TP and TN especially under cold climate conditions. Relationship between pavement structure and removals of TP and TN is not clearly understood from previous studies, and further investigation on this relationship is needed for improved water quality design of permeable pavement.

2.5.3 Heavy Metal Removal

Storm runoff often contains significant concentrations of dissolved and particulate-bound fractions of heavy metals. Typical heavy metals found in storm runoff are Cu, Pb and Zn, which come from different sources including vehicular component wear, fluid leakage, engine exhaust, and roadway abrasion and degradation (Brown 2007, Napier et al. 2008). Studies have been conducted on removal efficiency of Cu, Pb and Zn by permeable pavement in different places of the world. In general, permeable pavements are shown to be effective in trapping these pollutants in runoff to some degree.

The reported overall removal rates of Cu, Pb and Zn were above 30% and as high as 90% in some cases. Specific removal efficiencies are dependent on the characteristics of individual pavements and inflows (Sansalone and Buchberger 1995, Dierkes et al. 1999, Brattebo and Botth

2003, Fach and Geiger 2005). As was discussed in TSS removal, these three heavy metals were found to be associated with TSS and the major removing mechanism is through filtration in the upper layers of permeable pavements (Legret and Colandini 1999, Dierkes et al. 2002). Summary of the water quality performance from the studies mentioned above is also provided in Table 2.1.

The above findings show inconsistencies in the removal rates of the three heavy metals due to various factors such as the pavement setups and experimental conditions. In order to obtain this water quality performance in a regional scale, experiments on a local basis with local inflow conditions and testing environment are necessary. Since few studies were conducted in cold climate areas, it is not clearly understood whether temperature can affect the treatment efficiency of heavy metals. Although several studies found that heavy metals were attached and removed with TSS, there is no clear evidence whether similar observations can also be found under cold climate conditions. Therefore, further study on removals of heavy metals under Calgary's cold climate conditions is needed.

Table 2.1. Summary of Studies on Water Quality Performance

Author	Pavement Type	Removal Rate
Pratt et al. 1995	PICP	> 80% for TSS
Pagotto et al. 2000	PA	87% for TSS; 35% for Cu; 78% for Pb; 66% for Zn
Bean et al. 2007a	PICP	75% fot TSS; 43% for TN; 42% for TP; 88% for Zn; 62% for Cu
Brown et al. 2009	PICP and PA	90% for TSS
Huang et al. 2015	PICP, PA and PC	90% for TSS; 80% for TP; 2% – 40% for TN; 80% for Pb; 70% for Cu and Zn
Rushton 2001	PICP	92% for TSS; 88% for Cu; 89% for Pb; 82% for Zn; 40% for TP; 57% for TN
Gilbert and Clausen 2006	PICP	> 80% for TSS; 66% for TP; 50% for TN; 65% for Cu; 67% for Pb; 79% for Zn
Eck et al. 2011	PA	90% for TSS; 66% for TP; 49% for TN; 56% for Cu; 90% for Pb; 87% for Zn
Bean 2005	PICP	72% for TSS; 63% for Cu; 88% for Zn; 65& for TP; 35% for TN
Dreelin et al. 2006	PICP	> 75% for TSS; 80% for TP; 43% for TN; >80% for Zn
Sansalone and Buchberger 1995	PICP	> 90% for TSS; > 60% for Cu, Pb and Zn
Dierkes et al. 1999	PICP	90% for Cu, Pb and Zn
Brattebo and Botth 2003	PICP	89% for Cu; 69% for Zn
Fach and Geiger 2005	PICP and PC	90% for Cu, Pb and Zn

2.6 Modeling of Permeable Pavement

Modeling of permeable pavement is a relatively new topic along with the widespread application of permeable pavement. The purpose of modeling is to simulate the hydraulic (e.g. flow through pavement structure) and water quality performance (e.g. pollutant removal) given a permeable pavement structure, and provide useful information to improve current design. While field and laboratory experiments aim to investigate the current performance, modeling is usually used to predict future performance using proposed model algorithms. In order to yield satisfactory simulation results, measured field and laboratory data are used to calibrate and validate the proposed model. Therefore, both field/laboratory experiments and modeling are of the same importance for a comprehensive study of permeable pavement (Elliott and Trowsdale 2007).

In the last two decades, most permeable pavement studies were based on field and laboratory experiments, and only a few employed modeling techniques. These studies simulated the hydraulic performance using conceptual and data-driven models. The simulations focused on one or several hydraulic parameters such as surface porosity, surface infiltration, hydraulic conductivity and water movement for a specific pavement layer (Zhu et al. 1999, Tan et al. 2003, Montes and Haselbach 2006, Deo et al. 2010, Kuang et al. 2011, Yong et al. 2013). With regards to water quality performance, although a few studies proposed regression models of TSS removal through gravel layers, they were not intended for permeable pavements (Tufenkji and Elimelech 2004, Wong et al. 2004). Several commercial software, such as PCSWMM and XPSWMM, incorporate the stormwater management modeling (SWMM) engine developed by the US Environmental Protection Agency and provide a permeable pavement module for both hydraulic and water quality performance. However, the module cannot visualize important information on water movement and pollutant removal through pavement structure in order to aid in the pavement

design. Based on previous studies on modeling and the limitation of current available modeling tools, there is a need to develop a modeling tool that can simulate movement of infiltrate and pollutant removal by permeable pavement, and utilize the pertinent information to aid in design and predict future performance.

Chapter Three: Three Types of Permeable Pavements in Cold Climates – Field Investigations*

3.1 Introduction

Urbanization often results in an increase in impervious surface area, which leads to increases in both peak flows and surface runoff volumes during storm events. Storm runoff from impervious surface often carries pollutants such as sediments, nutrients and heavy metals into receiving water bodies (Pratt 1995, Legret et al. 1996, Winter and Duthie 1998). To mitigate these adverse impacts, permeable pavement, a type of Low Impact Development (LID) technology, presents a promising solution by allowing stormwater to infiltrate into sub-surface storage that also serves to remove various pollutants (Brattebo and Booth 2003). Commonly used permeable pavements include porous asphalt (PA), porous concrete (PC) and permeable inter-locking pavers (PICP), concrete grid pavers and plastic reinforcing grid pavers (Brown et al. 2011). Among the various types of permeable pavements, PA, PC and PICP have been widely accepted in parking lots, driveways, and access roads (Balades et al. 1995).

Previous studies have assessed the hydraulic performance of PA, PC and PICP in terms of runoff attenuation, peak flow reduction and surface infiltration capacity. Gilbert and Clausen (2006) and LeFevre et al. (2009) found that PICP can effectively mitigate peak flows by 72% and 56% on average, respectively; however, peak attenuation varied with the size of the storm event. Bean et al. (2007a), Brattebo and Booth (2003), Booth and Leavitt (1999) and Pezzaniti et al. (2009) did not observe surface runoff generated on PICP surface from natural storm events. Studies

* The materials in this chapter have been submitted to the *Journal of Environmental Engineering – ASCE* for publication.

on PC in Ohio, U.S.A. (Sansalone et al. 2008) and on PA in Sydney, Australia (Ball and Rankin 2010) found that both PC and PA are effective in reducing surface runoff and peak flows. Collins et al. (2008) compared the hydraulic performance between PC and PICP in coastal North Carolina, U.S.A. and concluded that both PC and PICP are effective in mitigating storm runoff and peak flow ranging from 60% to 75%.The above studies were conducted in mild climate locations where environment temperatures are normally above 0℃. Roseen et al. (2011) observed that PA is still able to reduce peak flows by 86% in cold climate conditions when environment temperature is below 0℃. Huang et al. (2012) observed that peak reduction ranges from 20% to 50% for PICP when environment temperature is below 0℃. As demonstrated in the aforementioned studies, the level of hydraulic performance is not quantitatively consistent, as it is affected by pavement structure, magnitude of storm, and climate condition besides surface porosity, installation location, pavement age and maintenance (Scholz and Grabowiecki 2007, Chai et al. 2012).

Hydraulic performance of permeable pavements is related to surface infiltration capacity, which degrades over time and reduces performance. This degradation can be either gradual, sudden or both depending on the surface. Sansalone et al. (2008) found that the capability of reducing storm runoff and peak flow by a PC in Ohio, U.S.A. is dependent on its surface infiltration rate (SIR). Gonzalez-Angullo et al. (2008) ascribed the reduction of surface runoff attenuation from 90% to 22% for PICP due to decreased SIR after applying construction debris on its surface in a laboratory study. The deposition of sediments on pavement surface is responsible for the degradation of SIR for PA, PICP and PC (Yong et al. 2013, Chopra el al. 2009). A PA in New Hampshire, U.S.A. retained satisfactory SIR even when winter sanding materials were applied (Roseen et al. 2011). Collins et al. (2008) observed that both PC and PICP maintained high SIR within the 1-year monitoring period and no maintenance activity is needed in North Carolina,

U.S.A. Studies conducted in Australia have shown that SIR of PICP can remain sufficiently high after 7 years of continuous service (Lucke and Beecham 2011). Whereas, Al-Rubaei et al. (2013) argued that proper maintenance is needed to restore SIR of an 18-year-old PA in Northern Sweden for ensuring its capability to mitigate surface runoff from 1:100 year storm events of 15 min duration.

Although permeable pavements have demonstrated their hydraulic capability, maintenance indeed is needed to ensure their performance to achieve long-term benefits. Some types of maintenance, such as vacuum sweeping (Brown et al. 2009, Al-Rubaei et al. 2013) and pressure washing (Al-Rubaei et al. 2013) can partially restore SIR for both PA and PICP; while pressure washing was found to be more efficient than vacuum sweeping for PC as fine sediments settling in the voids on pavement surface can be effectively flushed out by pressure washing (Chopra el al. 2009). A study in Alabama, U.S.A. found that pressure washing improves SIR of PC at an average of 20-fold (Dougherty et al. 2010). A study by Bean et al. (2004) in North Carolina, U.S.A. concluded that street sweeping is not effective.

Apart from the hydraulic benefits, permeable pavements also provide considerable water quality improvement by treating and trapping stormwater pollutants (Lucke and Beecham 2011). Depending on the region, total suspended solids (TSS), hydrocarbons, bacteria and fecal coli-forms, nutrients and heavy metals are the primary pollutants of concern to urban stormwater managers. Brabec (2002) suggested that heavy metal concentrations in urban stormwater tend to be dominated by lead (Pb), copper (Cu) and zinc (Zn). Among these pollutants, TSS have been documented to be removed at a high level (in general, higher than 80%) by various permeable pavements (e.g., Pagotto et al. 2000, Bean et al. 2007b, Brown et al. 2009) through physical filtration and sedimentation (Gerrits 2001, Hatt et al. 2007). However, the removal efficiency of

permeable pavements for nutrients and heavy metals documented in previous studies are inconsistent. Bean et al. (2007b) found that a PCIP in North Carolina, USA, is effective for removing total phosphorus (TP) and Zn but not Cu, and reduces total nitrogen (TN) at a moderate level. A study in Texas, U.S.A. showed that PA removes 75% of TP and 60% - 90% of heavy metals (Zn, Pb and Cu), whereas the removal of TN is less than 40% (Eck et al. 2011). Tota-Maharaj and Scholz (2010) also observed a satisfactory removal of TP and moderate removal of TN from PICP in Edinburgh, UK. In addition, Booth and Leavitt (1999) found that PICP could yield satisfactory removal of Cu and Zn after 6-years of service. Welker et al. (2012) observed that both PA and PC installed in Pennsylvania, U.S.A., remove Zn, Cu and Pb at high levels. Ball and Rankin (2010) found that TP, Cu, Pb and Zn removals by PA are higher than 70%. A study conducted in France observed that 35% - 78% of Zn, Cu, and Pb are removed by PA (Pagotto et al. 2000). However, Gilbert and Clusen (2006) demonstrated that PICP cannot mitigate concentrations of TP but can reduce concentrations of TN, Cu, Pb and Zn. Collins et al. (2009) stated that TN was hardly removed from storm runoff by both PA and PICP. Besides geographical location and pavement structure, climate condition is also expected to affect the removal of some pollutants by permeable pavements (Scholz and Grabowiecki 2007). Tota-Maharaj and Scholz (2010) displayed the dependence of removal of TN, but not TSS and TP, by PCIP on pavement temperature.

The City of Calgary in Alberta, Canada, is facing increasing pressure to improve urban stormwater runoff management given the sensitive nature of the Bow River, the primary receiving body for the City's stormwater. Calgary experiences a dry continental climate with long and cold winters interspersed with brief warm periods known as Chinooks. Winter in Calgary is cold and temperature is usually below 0℃. But Chinook currents (warming trends during winter) quickly

bring the temperature above 0°C several times over the period of a day in winter. Thus, there are several freeze-thaw cycles in Calgary winters. Research is needed to assess the performance of permeable pavements under cold climate conditions for evaluating their applicability in cold regions. To date, a very limited number of studies have been conducted to investigate the hydraulic performance and pollutant removal of permeable pavements under cold climate conditions. Furthermore, no research has compared the performance of three common types of pavements, namely PA, PC and PICP, to determine which pavements are suitable for cold regions. The objectives of this chapter are to investigate and compare the hydraulic and environmental performance of three types of permeable pavements, PA, PC and PICP, in Calgary winters. Hydraulic performance is assessed in terms of: (i) storm runoff reduction; (ii) SIR degradation; and (iii) SIR restoration via maintenance (pressure washing). Environmental performance is assessed in terms of removal of: (i) TSS; (ii) nutrients TN and TP; and (iii) heavy metals Cu, Pb and Zn. The methodology for achieving the objectives involves testing in cold climate conditions with prevalence of sanding materials for de-icing road surfaces.

3.2 Study Site and Methodology

3.2.1 Description of Study Area

Three field-scale permeable pavement cells, PA, PC and PICP, are situated in the south west of Calgary, Alberta, Canada (plan view is shown in Figure 3.1). The site normally receives moderate traffic of light vehicles year-round and occasionally heavy duty vehicles. The PICP (Eco-Optiloc®), PA, and PC cells were constructed in September of 2011 and built in series using concrete pads (0.8 m long x 6.0 m wide x 0.08 m thick) to separate each cell. Pavement surfaces

of both PA and PC cells were replaced in Oct. 2012 due to their lower than design value porosities (gravel in the base and sub-base were not replaced). The initial (design) values of surface porosity are 20% - 25%, 15% - 20%, and 10% - 12% for PC, PA and PICP, respectively. The porosity of PICP is estimated by dividing the joint-fill area by the total surface area. Each pavement cell is 6.0 m long and 6.0 m wide with a 1% slope towards the east. The three layers of PA from top to bottom are an 80 mm surface porous asphalt layer, a 70 mm bedding layer of 12.5 mm gravel and a 500 mm sub-base layer of 63 mm gravel. The PICP cell is made up of four layers with 80 mm thick Eco-Optiloc® paving blocks with a void ratio of 12% on the surface, followed by a 70 mm bedding layer of 12.5 mm gravel, a 150 mm base layer of 40 mm gravel and then a 350 mm sub-base layer of 63 mm gravel at the bottom. The PC cell consists of a 150 mm porous concrete on top of an underlying 500 mm sub-base gravel layer 63 mm in depth.

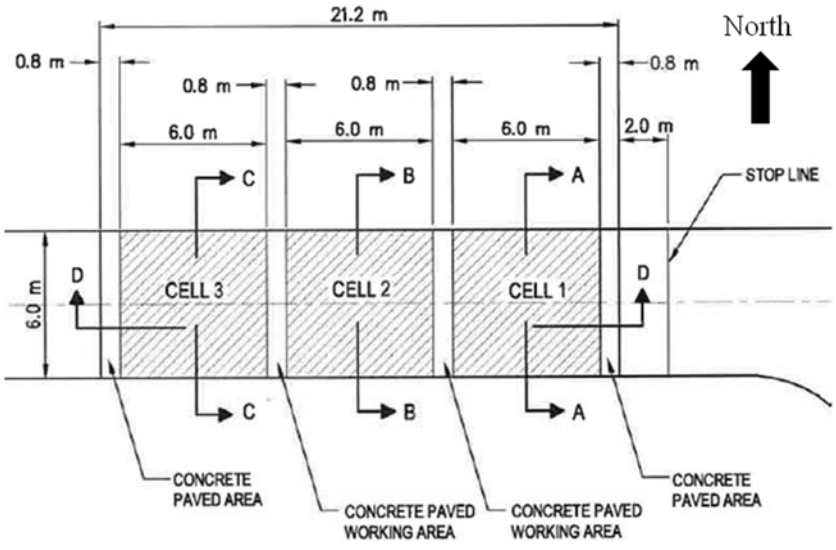

Figure 3.1. Plan view of permeable pavement cell 1) PC; 2) PICP (Eco-Optiloc®); 3) PA

The sub-base layers of the three pavement cells were compacted during construction to ensure approximately 35% of void space for storing storm runoff. All the gravel in the three pavement cells were thoroughly washed before they were levelled out to the base so that fine sediment occurrence would be minimized in the pavements during their construction. A perforated sub-drain pipe of 100 mm in diameter was placed at the bottom of each pavement cell that leads to a nearby manhole for outflow collection. A non-woven geo-textile was placed between the sub-base and sub-grade to prevent pollutants from migrating to the underlying soil. Sub-grade soil is fairly impermeable (measured infiltration rate at 0.58 mm/hr) and hence, infiltration into the sub-grade for groundwater recharge is negligible.

3.2.2 Field Experiments and Laboratory Assay

Two types of field tests were conducted on the three pilot-scale pavement cells: (i) simulated storm runoff, and (ii) surface infiltration tests. Simulated storm runoff tests were used to evaluate the storm runoff reduction and removal of pollutants. Surface infiltration tests were used to assess the surface infiltration capacity. These field tests were performed in the time period from October, 2011 to December, 2013 for PICP, and from October, 2012 to December 2013 for both PA and PC.

3.2.2.1 Simulated Runoff Tests

In the experimental period, six simulated runoff tests for PA and PC and eight tests for PICP were conducted. For each test, stormwater was hauled from a nearby stormwater retention pond to the water storage tank beside the pavements (Figure 3.2). Sediments collected from Calgary roads were manually added into the raw stormwater through the rainfall applicator with

TSS concentrations of approximately 500 mg/L, which is the typical TSS concentration of storm runoff in Calgary. In each field test, a 1:100 year storm event of 20 minutes in duration with 80 mm/hr average rainfall intensity was simulated; thus a total of 4500 L stormwater was used per test. The1:100 year storm events were used because roads, which are also components of the drainage system, should be designed for 1:100 year storm events (The City of Calgary, 2011).The duration of 20 minutes was determined based on the time of concentration of the catchment (Brown et al. 2009). Stormwater was pumped from the water storage tank at a constant rate of 3.7 L/s and then precipitated onto the pavement cells through a runoff applicator (Figure 3.2). The pumping rate was determined to ensure an average rainfall intensity of 80 mm/hr (Brown et al. 2009). Stormwater infiltrating through the pavement cell drained out of the pavement to a nearby monitoring manhole. Outflow from the sub-drain system was continuously monitored using a Sigma 950 flow meter, which was installed in the manhole. Besides flow monitoring at 1-min intervals, other hydraulic parameters were also manually recorded: the ponding depth (d_{pond}), which is the flow depth observed on the pavement surface at the end of the test; and the ponding time (t_{pond}), which is the duration for which the pavement surface is submerged under stormwater since the end of the test. In addition, stormwater temperature was measured using an infrared thermometer. Pavement temperature (T_p) was obtained by the temperature sensor installed in the bedding layer of the pavements. Air temperature was obtained from the weather station at the Calgary International Airport. Negligible differences were found between the pavement temperature and the air temperature during the field work. For each test, the condition of the pavement surface remained undisturbed (e.g., debris and sanding materials) for better representation of the field operation environment. During each simulated runoff test, a total of 8 time-weighted (at 5-min intervals) outflow samples were manually collected from the sub-drain

pipe in the monitoring manhole. The water samples were then delivered to the Civil Engineering Wastewater Laboratory of the University of Calgary for assay. In the Laboratory, 8 composited water samples were prepared based on the measured outflows in each test; then the composited samples were used to determine TSS concentration using a filtration method, and TN, TP, Pb, Cu and Zn concentrations using Hach procedures 8190, 10071, 8033, 8143 and 8009, respectively. These Hach procedures are equivalent to standard methods cited by the American Public Health Association (APHA) for TN, TP, Pb, and Zn. In each test, a total of 3 inflow samples were also manually collected at the rainfall applicator for assaying the same physical and chemical water quality parameters noted above using the same methods.

Figure 3.2. Equipment used in simulated runoff tests

3.2.2.2 **Surface Infiltration Tests**

Surface infiltration tests were conducted to monitor SIR from October, 2011 to December, 2013 for PICP, and from October, 2012 to December, 2013 for PA and PC. Initial SIRs of all three types of pavements were measured right after the construction of the pavements. Due to high SIRs

(> 150 mm/hr) measured on all three pavements and observing no horizontal flow, single-ring infiltrometers were used for the tests. A total of 6 single-ring infiltrometers made of galvanized steel 30 cm in diameter and 25 cm in height were used for PICP from October, 2011 to August, 2012. For easier implementation and better sealing effect, 12 single-ring infiltrometers made of polyvinyl chloride, 15 cm in diameter and 4 cm in height, replaced the galvanized steel single-ring infiltrometers after August, 2012. In a test, a total of 6 or 12 infiltrometers, which are approximately evenly distributed on the pavement surface, were fixed on the surface using fast-curing silicone and plumber's putty. Each ring was topped up with water and the time needed for all water to infiltrate was recorded. These measurements were repeated for each infiltrometer until the recorded drainage time became approximately stable.

Maintenance by pressure washing was conducted on May 13th, 2013 to restore the SIR of all three types of permeable pavements. The equipment used included a powerful water pump creating 1,500 psi water pressure at the outlet of the nozzle. The pressurized water was applied on the entire cell surface of each pavement, and then the surface infiltration test was conducted to determine the restoration of SIR through maintenance.

3.2.3 Analytical Methods

In simulated runoff tests, peak flow reduction is obtained by:

$$PeakReduction = \frac{Q_{inflow} - Q_{outflow\_peak}}{Q_{inflow}} \times 100\% \quad (3.1)$$

where Q_{inflow} is the constant inflow rate [L/s]; and $Q_{outflow\_peak}$ is the peak outflow rate observed from the sub-drain pipe in the manhole [L/s].

The average removal rate of TSS is calculated by:

$$R_{TSS} = \frac{M_{in} - C_{TSS\_out}V_{out}}{M_{in}} \times 100\% \quad (3.2)$$

where R_{TSS} is the average removal rate of TSS [%]; M_{in} is the TSS load of inflow [g]; C_{TSS_out} is the flow weighted TSS concentration of outflow [g/L]; V_{out} is the total volume of stormwater observed from the sub-drain pipe in the manhole [L]. The average removal rates of other pollutants are also calculated using a similar equation.

The surface infiltration rate for each location is calculated by:

$$SIR = \frac{h}{t} \quad (3.3)$$

where SIR is the surface infiltration rate [mm/hr]; h is the initial water depth in the infiltrometer (here 250 or 40mm); t is the time needed for full infiltration of water initially within the infiltrometer ring [hr]. The average SIR of each pavement in a test is calculated by averaging SIRs for all infiltrometers (here 6 or12 infiltrometers).

To compare the performance of pavements under winter and non-winter conditions, the field test results were classified into two groups based on pavement temperature: winter/cold climatic conditions occur when the pavement temperature is less than 5℃. Winter sanding

materials may or may not be present in non-winter conditions and thus, the presence of sanding materials was noted in each test. Pearson correlation was applied to evaluate potential relationships between two variables. In addition, both linear and nonlinear (exponent) regressions were adopted to display the potential dependency of two variables. Several statistical analyses were used to compare the performance of each pavement under different conditions and the performance between/among pavements. Wilcoxon signed-rank test was used to compare two paired samples (e.g., the same parameters in different tests from the same pavement); Wilcoxon rank-sum test was used to compare two independent samples (e.g., the same parameters from different pavements); Kruskal-Wallis test followed by multiple comparisons were used to compare more than two samples. All the statistical analyses and correlation analysis were conducted at a significance level of 0.05 using Matlab statistical toolbox.

3.3 Results and Discussions

3.3.1 Surface Infiltration

3.3.1.1 Initial Surface Infiltration Rate

The initial average SIRs tested from the first infiltration test for PA, PC and PCIP after their constructions are 43,767, 112,886, and 7,548 mm/hr, respectively. Kruskal-Wallis and multiple comparison analysis (sample sizes of 6 for PCIP and 12 for PC and PA) detected that the initial SIR of PC is significantly higher than those of PA and PICP. The high initial SIR of PC can be ascribed to its relatively high design porosity in the surface layer, while PA and PCIP have lower design porosities. These pavements were designed to be capable of infiltrating stormwater runoff generated by a 1:100 year design storm event, which have an average rainfall intensity of

80 mm/hr, without immediate ponding on the surface. The measured initial SIRs of all three pavements are largely greater than the rainfall intensity of 80 mm/hr, which is the required minimum SIR.

3.3.1.2 **Temporal Variation of Surface Infiltration Rate**

Figure 3.3 shows the normalized average SIRs, which are calculated by dividing the measured average SIRs by the initial SIR for each pavement, along with time for PA, PC and PICP, respectively. Gradual degradation of SIR of PC and PA was observed from the initial test until May 2013, when pressure washing was applied to remove sediment clogs from the surface layers of the pavements and to recover pavement surface infiltration. The infiltration rates started declining immediately after pressure washing towards the end of 2013. SIR of PICP also demonstrates similar patterns as those of PC and PA; while SIR of PICP significantly dropped right after the first infiltration test and then SIR slowly reduced until pressure washing after a slight recovery in the summer of 2012. Apart from pressure washing conducted in May 2013 and annual winter sanding material removal, no other maintenance was conducted during the study period. Among these three pavements, measured average SIR of PC are significantly higher than those of PA and PC (Kruskal-Wallis test and multiple comparisons); while SIR of PICP remained the lowest in all the infiltration tests, which are, however, all above the required minimum level of infiltration of 80 mm/hr.

Since the replacement of surface layers of PC and PA was completed a year after construction of the PCIP, the infiltration rates of PICP measured in 2011 were compared with those of PA and PC measured in 2012 for their first year of service. Winter sanding materials were applied on December 20th, 2011, November 6th, 2012 and November 8th, 2013. During the test, it

was observed that finer sediment in winter sanding materials tended to settle in the voids on pavement surfaces where surface runoff was allowed for infiltration. Such effects substantially reduced surface porosity and hence the ability to infiltrate surface runoff deteriorated as illustrated by the substantial degradation of SIR.

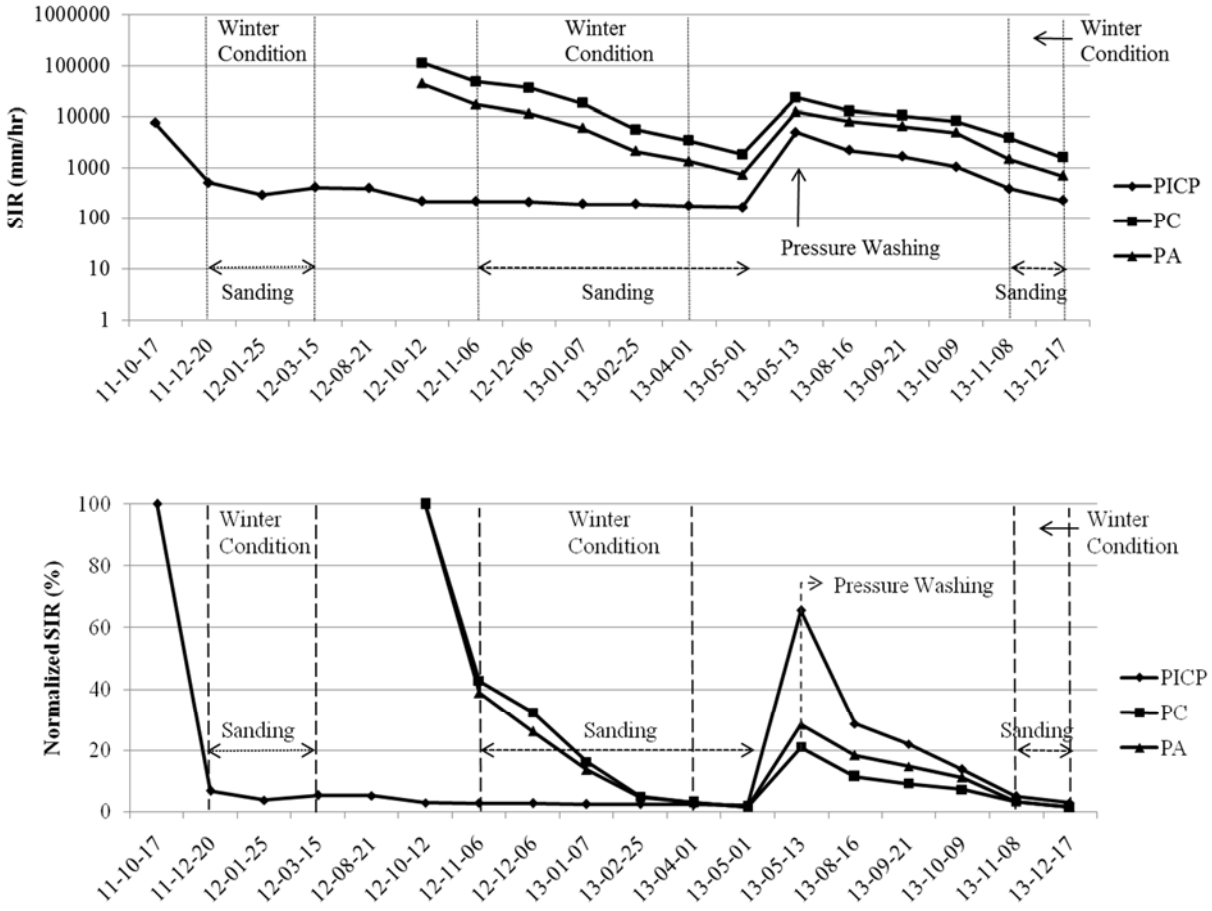

Figure 3.3. Time series of absolute and normalized SIRs for PA, PC and PICP

After pressure washing (discussed in detail in the next section) on May 13th, 2013, the SIRs of the three pavements gradually degraded towards to the end of the study period. During the warm conditions under the absence of sanding materials, SIRs also decreased along with time. Under these circumstances, sediment can still be transported to the pavement surfaces by storm runoff, traffic and possibly wind. During the study period, a residential community was being constructed in the area. This could lead to the degradation of SIRs of the three pavements due to sediment deposition. However, the SIR degradation caused directly by the application of sanding materials appears to be more significant than that caused by traffic and other reasons (e.g., sediments retained in pavements in storm events). For example, the degradation rate in SIR of PA under warm climate conditions in 2013 (1511 mm/hr/month) is lower than that caused by the application of sanding materials in 2012 winter (2711 mm/hr/month). The similar results can be seen for the PC and PICP.

Winter sanding materials were applied on December 20th, 2011, November 6th, 2012 and November 8th, 2013. Since the replacement of surface layers of PC and PA was completed a year after construction of the PCIP, the infiltration rates of PICP measured in 2011 were compared with those of PA and PC measured in 2012 for their first year of service. Due to the application of winter sanding materials in their first year of service, 61%, 57% and 93% of SIR were lost immediately for PA, PC and PICP, respectively. In addition as demonstrated in Figure 3.3, the normalized SIRs before applying sanding materials in the first winter of service were apparently higher than those in the rest of tests (including after pressure washing) throughout the study period for all pavements. During the tests, it was observed that finer sediment in winter sanding materials tended to settle in the voids on pavement surfaces. Such effects substantially reduced surface porosity and hence the ability to infiltrate surface runoff deteriorated as illustrated by the substantial degradation of SIR.

3.3.1.3 **Maintenance**

As demonstrated in Figure 3.3, SIRs of all three pavements are expected to continuously degrade to a degree that would cause surface ponding without effective maintenance to restore their surface infiltration capacity. Thus, regular maintenance is essential for long-term use of permeable pavements. Vacuum sweeping has been documented to be ineffective to remove fine sediments (Bean et al. 2004), and this method was also found to be ineffective in restoring the SIRs of PA and PC in this study. Wilcoxon signed-rank analyses (sample size of 12 because there were 12 locations in the infiltration test) were conducted to compare SIR between, before, and after maintenance for each pavement. The results showed that SIR after maintenance was significantly higher than that before maintenance for all three pavements. SIR of PICP after pressure washing increased 30 times as compared to the SIR before maintenance; while SIRs increased by approximately 11 and 13 times for PA and PC, respectively. Kruskal-Wallis and multiple comparison tests were also conducted to compare SIRs among PA, PC and PICP before and after maintenance, respectively. The tests showed that SIR of PC was significantly higher than PA and PICP both before and after maintenance. However when comparing the normalized SIRs using the same analyses, the normalized SIR of PICP was significantly higher than those of PA and PC after maintenance, while no significant differences were identified before maintenance among the pavements. All these results suggest that pressure washing is an effective measure to restore the SIRs of all three pavements, while this type of maintenance might be more effective for PICP in terms of the recovery of initial SIR. However, a longer study period is recommended for identifying optimal maintenance frequency.

3.3.2 Stormwater Runoff Mitigation

Table 3.1 presents the measurements of variables, including peak reduction (p_r), time to peak (t_p), ponding depth (d_{pond}), discharge time (t_d), pavement temperature (T_p), and the presence of sanding materials for PA, PC and PICP, respectively, in each simulated runoff test. Discharge time denotes the time for infiltrated storm runoff volume to drain out of the pavements, which was obtained from the total time span of the outflow hydrographs. In all the simulated runoff tests, 85% - 90% of inflows were captured at the outlets of the pavements. This minor loss of inflows was likely due to water retention in the pavements (field capacity of the gravel) as well as minor water leakage out of the pavements. Based on the amount of water loss, rainfall events with total volume from about 450 L to 750 L are likely to be "absorbed" by the permeable pavements and no obvious outflows would be generated; however, antecedent rainfall events might also need to be considered as it will affect the outflows..

The results show that peak reduction rates vary over a wide range from 19.0% to 64.3% and an increasing trend (along with time) in these rates was observed for all the pavements. Similar trends were found in time to peak and discharge time. No ponding depth was observed from most simulated runoff tests except for several cases in PICP in which very minor ponding (ponding depth ≤ 5 mm) was observed. Minor to no ponding on the pavement surface suggests that PA, PC and PICP are very effective in reducing surface runoff from 1:100 year storm events under both winter and non-winter conditions. As for peak reduction, Kruskal-Wallis analysis indicates that there is no significant difference among these three pavements. Thus, PA, PC and PICP can provide a similar level of performance in terms of peak reduction. However, both the time to peak and the discharge time of PICP are significantly higher than those of PA and PC according to Kruskal-Wallis and multiple comparison analysis; while both time to peak and discharge time are

not significantly different between PA and PC. These results suggest that the performance of PA and PC are superior to PCIP in terms of mitigating surface runoff. However if the outflow from the pavements are collected by the stormwater drainage system, the quick removal of surface runoff would magnify the peak flow and shorten the time to peak at the downstream drainage system.

Table 3.1. Measured hydraulic variables, pavement temperature and presence of sanding materials in each simulated runoff test for PA, PC and PICP

	Test Date	p_r (%)	t_p (min)	d_{pond} (mm)	t_d (min)	T_p (℃)	Sands applied
PA	2012-10-15	29.2	18	-	40	6.8	
	2013-03-27	39.6	20	-	53	2.4	√
	2013-09-20	39.3	22	-	75	10.7	
	2013-10-08	45.5	23	-	80	4.0	
	2013-11-07	54.7	25	-	84	-3.6	√
	2013-11-27	59.5	30	-	92	0.7	√
PC	2012-10-19	25.5	16	-	35	6.2	
	2013-03-28	33.3	20	-	48	2.1	√
	2013-09-24	36.6	21	-	65	9.8	
	2013-10-10	40.9	22	-	68	2.8	
	2013-11-13	48.6	24	-	72	1.3	√
	2013-11-28	52.7	25	-	76	-0.5	√
PICP	2011-10-19	19.0	14	-	38	10.0	
	2011-10-27	26.8	18	-	52	4.1	
	2011-11-10	35.4	26	2	134	4.5	
	2011-12-14	48.2	28	5	151	-1.0	√
	2012-08-23	59.6	58	3	168	15.8	
	2013-04-02	64.3	65	5	182	0.7	√
	2013-09-26	54.5	40	-	115	6.8	
	2013-10-09	57.2	43	-	122	3.2	

For PA, PC and PICP, hydraulic parameters including peak reduction, time to peak and discharge time showed a common increasing trend with respect to time. When pooling the data of all the pavements together, no strong correlations between pavement temperature and the above parameters were calculated. The correlation coefficients are -0.30 (p = 0.19), 0.09 (p = 0.70) and -0.03 (p = 0.90), respectively. However, the above parameters might be related to the overall porosity of the pavement, in particular surface porosity in addition to the porosity of base and/or sub-base layers. Although the pressure washing is an effective way to restore void space in pavement surface to a certain degree, void space in the base and sub-base layers are expected to decrease with time due to traffic impacts. This consequently would retard flow through these layers and result in lower peak and longer discharge time observed from outflow. Although direct quantification of the impacts of traffic on void space in these layers was not investigated, the decrease in void space may reflect into the pavement surface drop of approximately 5 cm during the study period. In addition, these hydraulic parameters of all three pavements were found to be related to the SIRs as demonstrated in the regression analyses (either linear or non-linear regression) for each pavement (Figure 3.4). The linear regression equations are expressed as follows:

Peak reduction (p_r) and SIR:

$$\text{PA:}\quad p_r = -0.001 * SIR + 54.3 \qquad R^2 = 0.579 \tag{3.4a}$$

$$\text{PC:}\quad p_r = -0.00072 * SIR + 48.9 \qquad R^2 = 0.558 \tag{3.4b}$$

$$\text{PICP:}\quad p_r = -0.0067 * SIR + 61.6 \qquad R^2 = 0.890 \tag{3.4c}$$

Time to peak (t_p) and SIR:

$$\text{PA:}\quad t_p = -4.2 \ln SIR + 47.7 \qquad R^2 = 0.561 \tag{3.5a}$$

$$\text{PC:}\quad t_p = -3.1 \ln SIR + 49.3 \qquad R^2 = 0.753 \tag{3.5b}$$

$$\text{PICP:}\quad t_p = -16.7 \ln SIR + 157.5 \qquad R^2 = 0.780 \tag{3.5c}$$

Discharge time (t_d) and SIR:

$$\text{PA:}\quad t_d = -0.021 * SIR + 172.3 \qquad R^2 = 0.858 \tag{3.6a}$$

$$\text{PC:}\quad t_d = -0.001 * SIR + 74.7 \qquad R^2 = 0.621 \tag{3.6b}$$

$$\text{PICP:}\quad t_d = -0.002 * SIR + 88.4 \qquad R^2 = 0.552 \tag{3.6c}$$

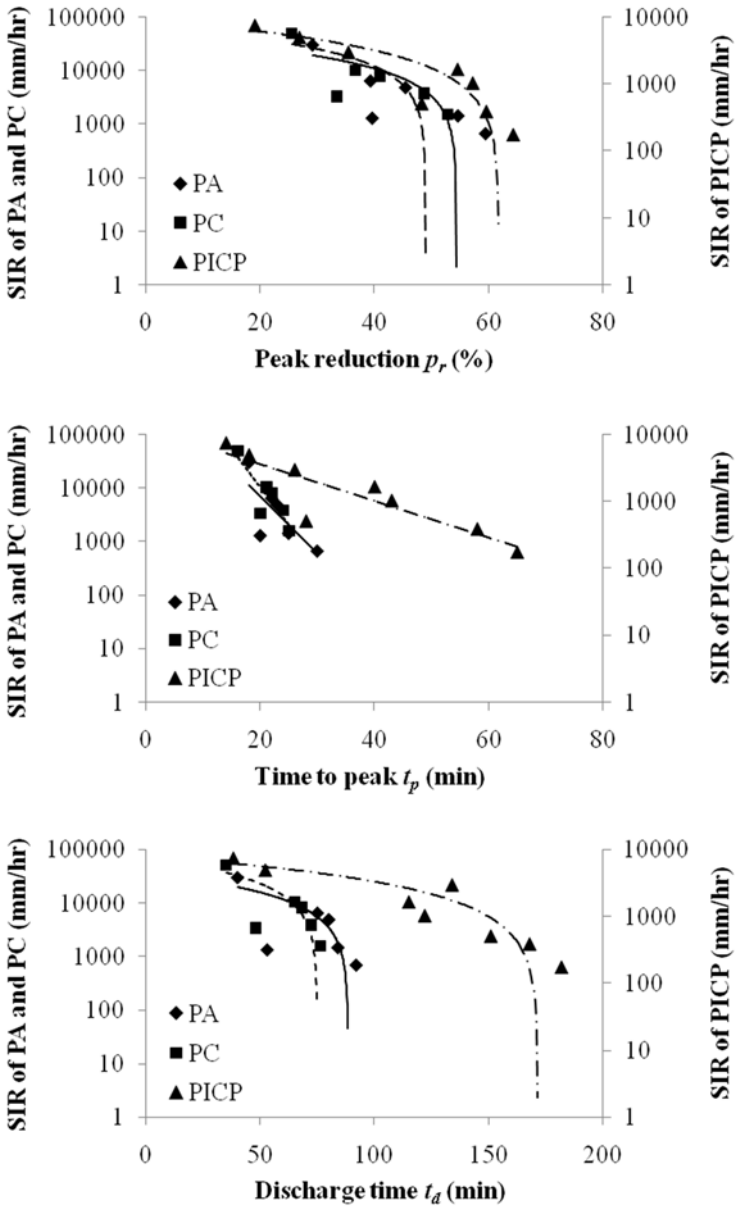

Figure 3.4. Regression analyses of p_r, t_p and t_d on SIR for PA, PC and PICP

These results support the fact that a decrease of SIR, which can be ascribed to the use of sanding materials, traffic, environmental effect and retaining sediments within pavements, leads to an increase in peak reduction and longer time to peak and discharge time of outflow from

pavements. These would benefit in reducing the runoff peak at the downstream and consequently decrease pressures on downstream stormwater drainage systems; however, further decrease of infiltration capacity of pavements, for example SIR < 80 mm/hr, could result in surface ponding and runoff. Therefore, it is essential to consider the trade-off between the advantages of permeable pavements in reducing surface runoff and their disadvantages in increasing pressure on downstream drainage systems when designing the pavements and developing their maintenance schemes. On the other hand, installing control structure (e.g., valve) in the pavement under-drain is also considered a feasible option for mitigating the pressure on downstream drainage systems by allowing pavements to temporarily store infiltrated stormwater runoff in their pavement base and sub-base, while reducing surface runoff.

3.3.3 Water Quality

3.3.3.1 **Inflow Water Quality Characteristics**

Table 3.2 shows the characteristics of the inflows in the simulated runoff tests for PA, PC and PCIP. The inflow temperature ranges from 3.8 ℃ to 10.3 ℃ depending on the test date. Kruskal-Wallis test indicates that concentrations of TSS, TP, TN, Zn, Cu and Pb are not significantly different among 2011, 2012 and 2013 and that the inflow concentrations were not significantly different between tests conducted under both winter and non-winter conditions. When preparing the inflow, only the concentration of TSS was controlled so that TSS concentration varies in a very small range; while relatively large variations were seen in TP, TN, Zn, Cu, and Pb. The larger variations of these water quality parameters reflect their natural variations in the source of stormwater (in the nearby stormwater retention pond).

Table 3.2. Characteristics of inflow for simulated storm runoff tests (sample size n = 20)

Parameter	Unit	Range	Mean	Median	Standard Deviation
TSS	mg/L	491 - 539	508	502	31
TP	mg/L	0.24 - 0.43	0.35	0.36	0.05
TN	mg/L	2.0 - 4.6	3.48	3.65	0.4
Zn	mg/L	0.27 - 0.48	0.34	0.33	0.06
Cu	μg/L	13 - 28	21	20	4.4
Pb	μg/L	17 - 47	30	28	7.6

3.3.3.2 **Total Suspended Solids**

Figure 3.5 demonstrates the removal rates of TSS along with TP and TN in all simulated runoff tests for PA, PC, and PICP, respectively. As shown in this figure, removal rates of TSS remains at a high level for PA varying between 89.6% and 93.2%. The highest removal rate (93.2%) was found under non-winter conditions, while the lowest removal rate (89.6%) was found under winter conditions. Similar to PA, removal rates of TSS for PC and PICP were also stable throughout this research which range from 90.6% to 94.6% and from 86.9% to 94.3%, respectively. For these three pavements, the difference in removal of TSS between winter and non-winter conditions was not obvious. In addition, no significant differences in TSS removal, both under winter conditions among the three pavements and between winter and non-winter conditions for each pavement, were detected in Kruskal-Wallis test and Wilcoxon rank-sum test, respectively. Furthermore, no significant difference in TSS removal was found among the three pavements during this research from 2011 to 2013 in Kruskal Wallis test. All these results demonstrate that these three types of pavements, regardless of the difference in their surface and structure, maintain

a high and similar level of performance in terms of removing TSS under both winter and non-winter conditions and their performance is also similar between these two climatic conditions.

Correlation coefficients between removal rate of TSS and pavement temperature for PA, PC and PICP are0.21, 0.32 and 0.07 respectively; thus indicates that TSS removal is not strongly related to pavement temperature for the three types of pavements. Under winter conditions, the tested pavements did not lose the ability to remove TSS and that the ability remained at the same level as that under non-winter conditions.

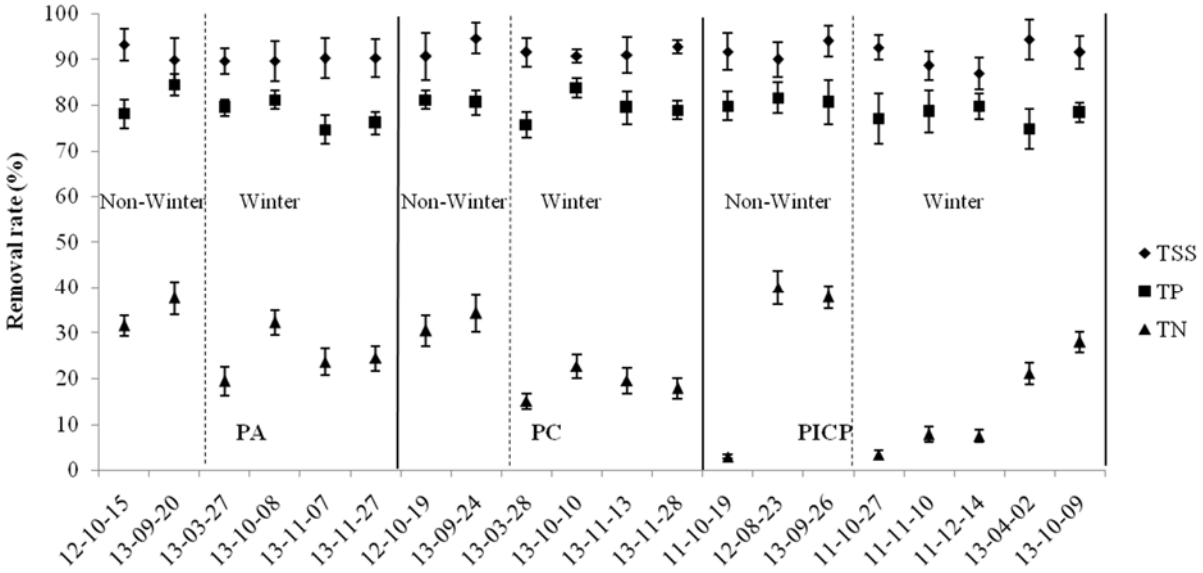

Figure 3.5. Time series of removal rates (mean ± one standard deviation) of TSS, TP and TN for PA, PC and PICP

3.3.3.3 **Total Phosphorus**

Figure 3.5 presents the removal rates of TP for PA, PC and PICP, which range from 74.6% for 84.4%. TP removal appears not to depend on pavement temperature, since no significant correlation was calculated between temperature and the removal rates of TP for each pavement. The correlation coefficients are 0.27, 0.30 and 0.25 for PA, PC and PICP, respectively. Similar to TSS, significant difference was not identified among PA, PC and PICP in terms of both their performance under winter condition and their performance considering all events in Kruskal-Wallis analysis. For each pavement, its performance under non-winter condition did not appear to be superior to that under winter conditions and vice versa.

As demonstrated in Figure 3.5, TP removal appears not to be greatly affected by the sanding materials, since TP removal rates of PA and PC right before and after applying the sanding materials in 2013 (on November 8th) were similar. The same result can be observed for TSS. In addition, TP and TSS removal rates are persistently high throughout the study period; however their correlation coefficient is not significant (-0.21, $p = 0.37$). The absence of strong correlation between them is under expectation, since their removal rates were more or less constant. Both high removal rates might suggest that the removal of TP and TSS might be governed by the same processes. Hatt et al. (2007) argued that TP is removed along with TSS in the pavement structure by sedimentation and filtration.

3.3.3.4 Total Nitrogen

Figure 3.5 shows the removal rates of TN for PA, PC and PICP. Unlike TSS and TP, removal rates of TN were found varying in relatively wide ranges, which were from 19.4% to 37.6% for PA, from 15.0% to 34.2% for PC, and from 2.9% to 40.0% for PICP. The removal rates

of TN under non-winter conditions were, in general, higher than those under winter condition for each type of pavement; while the difference between winter and non-winter conditions was more significant for PCIP, although one of tests under non-winter condition yielded a very low removal rate (2.9%). When pooling all data together for each pavement (except for removal rates of TN of PICP in 2011 due to the reason mentioned below), no significant difference in TN removal rates among the three pavements was detected in Kruskal-Wallis analysis. In addition when only comparing TN removal rates under winter conditions, they also did not significantly differ among the pavements.

Figure 3.6 shows the removal rates of TN, which are grouped in years for PICP. This figure demonstrates that the removal rates of TN in the first year experiments in 2011 were much lower than those in 2012 and 2013, regardless whether the tests were conducted under winter or non-winter conditions. However, such large difference in TN removal was not seen between the experiments conducted in the first year of 2012 and following experiments in 2013 for both PA and PC. Compared to TSS and TP, the overall low removal rates of TN for all three pavements and the differing levels of performance between winter and non-winter conditions could imply that the mechanism governing the TN removal is different from that controlling TSS and TP removal. In wastewater treatment, the removal of TN mainly relies on biological process, which is largely associated with the growth of bio-film, and the process is highly dependent on temperature (Wiesman 1994 and Newman et al. 2002). The construction of PC and PA was initially completed in 2011. Due to a construction flaw in the surface layers of both PA and PC, they had to be replaced in 2012 when commencing simulated runoff tests for these two pavements. The delay of one year for the field experiments for PA and PC may have allowed for the formation of a nitrogen removing bio-film within the base and/or sub-base layers, thus, enhancing TN removal in the experiments

conducted in 2012. The newly constructed PICP had very low TN removal rates (< 10%) in all four tests conducted in 2011 (Figure 3.6) under both non-winter and winter conditions. This might be due to the lack of bio-film within the pavement right after construction with clean gravel. Furthermore, the potential role of bio-film in TN removal is supported by the identified pavement temperature dependence of the TN removal rates as shown in the linear regression analysis for the pavements in Figure 3.7. The linear regression equations are:

$$\text{PA:} \quad R_{TN} = 1.09T_p + 24.29 \quad R^2 = 0.638 \tag{3.7a}$$

$$\text{PC:} \quad R_{TN} = 1.86T_p + 16.53 \quad R^2 = 0.854 \tag{3.7b}$$

$$\text{PICP:} \quad R_{TN} = 1.17T_p + 23.96 \quad R^2 = 0.767 \tag{3.7c}$$

where R_{TN} represents the removal rate of TN [%].

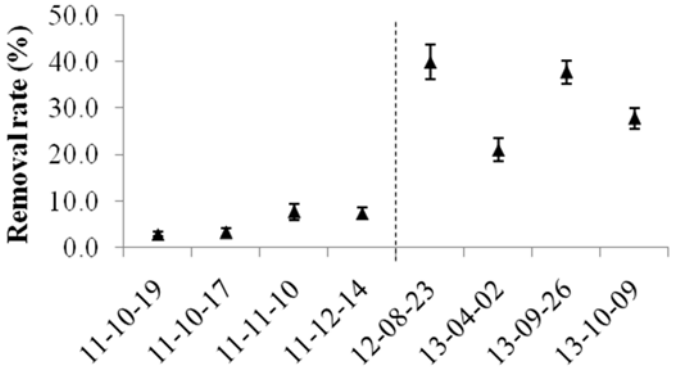

Figure 3.6. Comparison on removal rates of TN by year for PICP

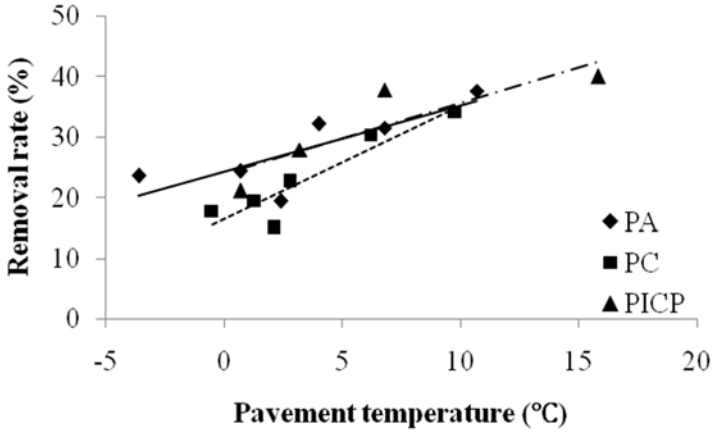

Figure 3.7. Linear regressions of TN removal rate on pavement temperature for PA, PC and PICP during 2012-2013

This result indicates the improvement of TN removal efficiency along with the increase of pavement temperature. As for PICP, TN removal rates obtained from tests run in 2011 were excluded in the analysis as the active role of bio-film was not expected in the first year of experiments for PICP. The investigation of the role of bio-film in TN removal within the pavements is beyond the scope of this chapter, but further research on the bio-film role is required to understand the mechanisms behind the removal of TN and other pollutants by permeable pavements.

3.3.3.5 **Heavy Metals (Cu, Pb and Zn)**

Figure 3.8 shows the removal rates of tested heavy metals for PA, PC and PICP, respectively. In general, for each pavement, the removal rates of Pb were higher than those of both Cu and Zn. The ranges of the rates for all three pavements were from 67.7% to 76.9% for Cu, from 76.3% to 86.1% for Pb, and from 66.2% to 77.3% for Zn. For each metal, the removal rates pooled

all tests for each pavement were not significantly different among the pavements (Kruskal-Wallis analysis). The removal rates of the metals under winter conditions were not largely different from those under non-winter conditions for each pavement (Wilcoxon rank-sum test). In addition, the performance level of the three pavements was also similar under winter conditions. Further water chemistry analyses on these three heavy metals show that Cu, Pb and Zn are largely removed in particulate form rather than dissolved form.

Correlation analyses were conducted between removal rates of heavy metals and pavement temperature for PA, PC and PICP, respectively, and the results are shown in Table 3.3. The results indicate that the removal of heavy metals was not dependent on pavement temperature for PA, PC and PICP, which is consistent with the removal of TSS and TP. The removal rates of TSS, TP, and metals were more or less constant over the study period and independent from climatic conditions and their rates were much higher than the removal rates of TN. Furthermore, removal rates of TSS, TP, and metals were found to be independent from climatic conditions, which were reflected by the absence of both significant correlation with pavement temperature and significantly different performance under winter and non-winter conditions. In stormwater runoff, some pollutants such as TP and metals have usually attached to solids (Hatt et al. 2007). All these may lead to the conclusion that TP and heavy metals are removed along with solids, which are removed by physical processes such as interception and sedimentation within pavements; however TN is removed separately from solids. To verify the findings, investigation on the pollutant removal in different forms, particulate and dissolved forms, is needed.

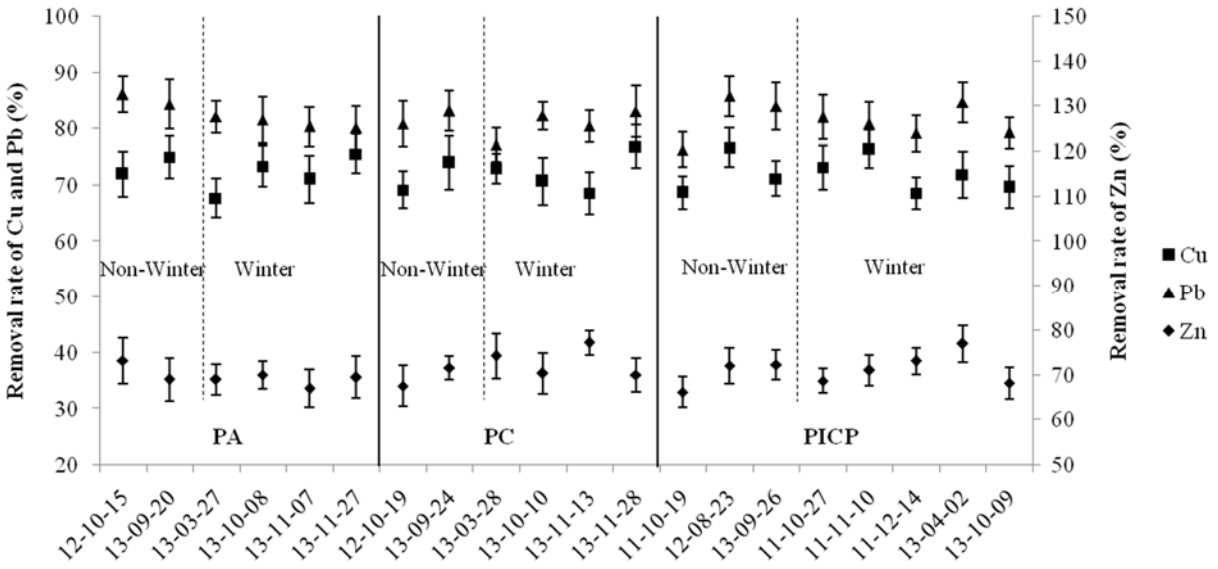

Figure 3.8. Time series of removal rates (mean ± one standard deviation) of Cu, Pb and Zn for PA, PC and PICP

Table 3.3. Correlation coefficients between removal rates of heavy metals and temperature (numbers in parentheses are p-values.)

Pavement	Correlation coefficient		
	Cu	Pb	Zn
PA	0.33 (0.51)	0.21 (0.68)	0.13 (0.80)
PC	-0.12 (0.82)	0.25 (0.62)	-0.31 (0.54)
PICP	0.35 (0.39)	0.24 (0.56)	-0.32 (0.43)

3.3.4 Relationship between Hydraulic and Environmental Performance

Table 3.4 presents the correlation coefficients between the removal rates of all monitored pollutants and hydraulic parameters including peak flow reduction, time to peak, discharge time and SIR for all three pavements. All the calculated correlation coefficients are in the range

from0.23 to 0.4 and are not significant, which indicate weak to no correlation between the examined variables. These results suggest that the environmental performance of the pavements might be independent from their hydraulic performance. The hydraulic parameters vary with SIR (Figure 3.4), which suggests that surface layer of pavements might largely determine their hydraulic performance. However, SIR appears not to affect environmental performance of the pavements, which might be dependent on the entire structure of pavements. These findings are consistent with the study by Gonzalez-Angullo et al. (2008).

Table 3.4. Correlation coefficients between removal rates of various pollutants and hydraulic parameters (numbers in parentheses are p-values.)

Pollutant	p_r (%)	t_p (min)	t_d (min)	SIR (mm/hr)
TSS	-0.01 (0.98)	0.21 (0.37)	0.05 (0.83)	0.08 (0.74)
TP	-0.23 (0.33)	-0.19 (0.42)	-0.13 (0.59)	0.22 (0.35)
TN	0.36 (0.11)	0.32 (0.17)	0.11 (0.65)	0.22 (0.34)
Zn	0.33 (0.16)	0.31 (0.18)	0.29 (0.21)	-0.18 (0.46)
Cu	0.21 (0.37)	0.20 (0.39)	0.24 (0.31)	-0.21 (0.37)
Pb	0.28 (0.23)	0.29 (0.21)	0.26 (0.27)	0.11 (0.63)

3.3.5 Applicability of Three Types of Pavements for Cold Climates

The hydraulic performance of PA, PC and PICP demonstrate that they are capable of mitigating stormwater runoff without or with negligible surface ponding under the extreme design storm event (100-year and 20-minute duration event) even under winter conditions. The degradation of SIR caused by the application of sanding materials, traffic, environmental effects, and aging imply the need for pavement maintenance to restore infiltration capacity to avoid surface

ponding. The three pavements also show high-level removal of all investigated pollutants except for TN under both winter and non-winter conditions. From both hydraulic and environmental perspectives, all the three pavements are applicable under Calgary's special winter conditions and can provide both hydraulic and environmental benefits over the long term provided that effective maintenance will be performed. In addition, consideration of the timing of maintenance is required since a high SIR could result in pressures on downstream stormwater drainage systems by increasing peaks and shortening the time to peak.

3.4 Conclusions and Recommendations

In this chapter, three types of permeable pavements, PA, PC and PICP, were investigated and compared according to their performance in terms of storm runoff mitigation, surface infiltration and pollutant removal, in particular addressing their performance in winters. The SIR of the pavements degraded significantly along with time, especially due to the application of sanding materials in winters. This implies that maintenance for restoring the infiltration capacity of pavements is needed. The pressure washing was demonstrated to be an effective way to restore SIR. In general, the three pavements performed acceptably from hydraulic perspective, since they yielded negligible to no surface ponding under 1:100 year design storms even under winter conditions when the surface of pavements were not frozen and they also presented their capability to attenuate the peak and to delay the time to peak in the outflow.

Regarding environmental performance, all three pavements can effectively remove TSS, TP and heavy metals including Cu, Pb and Zn, under both winter and non-winter conditions. Their removal rates were approximately 70% or higher. The more or less constantly high removal rates

and similar variation patterns of these pollutants might suggest that TP and heavy metals are very likely removed along with solids, which are governed largely by physical processes. However, the removal rates of TN were low (30% in average) and are suggested to depend on pavement age and climatic conditions such as pavement temperature. The different performance implies that the removal of TN might be governed by different process (e.g., biological process), which may be dependent on climatic conditions. To understand the mechanisms controlling TN removal, further research on the role of bio-film within pavements and its removal in different forms (particular and dissolved forms) are recommended. In addition, the water quality performance in this study was captured under 100-year storm event. For smaller magnitude of storm events, the removal rates of the examined pollutants are expected to be higher due to lower flow rate and longer detention time for potential treatment.

Chapter Four: The Influence of Design Parameters on Stormwater Pollutant Removal in Permeable Pavements*

4.1 Introduction

Urbanization leads to increases in a region's impervious surface with roads and rooftops, which in turn leads to significant increases in surface stormwater runoff. This stormwater typically contains a variety of pollutants including total suspended solids (TSS), nutrients such as total phosphorus (TP) and total nitrogen (TN), hydrocarbons and heavy metals that degrade the quality of urban water resources (Ellis et al., 2012; Finkenbine et al., 2000; Kayhanian et al., 2012; Tuccillo, 2006). Among available stormwater management techniques, especially for urban settings, permeable pavements offer a promising solution to the dual problem of increased stormwater runoff and degraded urban stormwater quality (Balades et al., 1995). A permeable pavement commonly contains a porous surface layer, one or more sub-surface gravel layers and in some cases, synthetic geo-textiles above the sub-grade or between pavement layers. Permeable pavements not only allow more stormwater to infiltrate into the ground compared to conventional pavements, but can also simultaneously remove pollutants from stormwater runoff on site; thus, they can play a significant role in mitigating the impacts of stormwater runoff caused by urban development (Pratt, 1995). Among various types of permeable pavements, porous asphalt (PA), porous concrete (PC) and permeable inter-locking pavers (PICP), have been widely used in driveways, parking lots and access roads (Watanabe, 1995).

* The materials in this chapter have been submitted to the *Journal of Hydrologic Engineering – ASCE* for publication.

To investigate the role permeable pavements play in urban stormwater management, a large number of studies have been conducted to quantitatively assess their performance, in particular in removing pollutants. Among the various pollutants of interest in stormwater management, permeable pavements have consistently shown to effectively remove 80% - 95% of TSS from stormwater, primarily by sedimentation and interception (Brown et al., 2009; Pagotto et al., 2000; Pratt et al., 1995; Bean et al., 2007). Unlike TSS removal, the removal rates of TP and TN have been reported to vary widely in previous studies but TP and TN removal are largely the result of chemical sorption and biological activities (Kuba et al. 1993, Wiesmann 1994), respectively. Several studies (e.g., Ball and Rankin, 2010; Eck et al., 2011; Tota-Maharaj and Scholz, 2010) observed that the removal rate of TP is higher than 70%; whereas other works (e.g., Bean et al., 2007; Rushton, 2001) documented low TP removal rates ranging from 40% to 60%. However, Gilbert and Clusen (2006) claimed that permeable pavements can merely remove TP from stormwater runoff. Similar to the removal of TP, the removal of TN reported in previous studies are not consistent either. For example, studies by Bean (2005), Pagotto et al. (2000), and Rushton (2001) found that permeable pavements can remove from 40% to 60% of TN from stormwater runoff; whereas Collins et al. (2009), Dreelin et al. (2006), and Huang et al. (2012) observed very low TN removal rates (<10%).

The reported inconsistent performance of permeable pavements in removing TP and TN might be ascribed to different pavement ages and structure, different testing conditions, such as inflow characteristics (both water quantity and quality) and climatic conditions (Booth and Leavitt, 1999). Field testing and laboratory testing have different advantages and disadvantages. For example, in field-scale tests, the characteristics of storm events that occur are beyond the control of investigators but storm events (i.e., inflow characteristics) are controllable in the laboratory. At

the same time, laboratory investigations are limiting by the very fact that they are a model representation of reality. However, all these should be taken into consideration when evaluating a pavement's performance and optimizing their engineering design for stormwater management purposes. Field investigations provide valuable information for evaluating the water quality performance of permeable pavements. But this information has limitations when attempting to optimize their engineering design. In addition, in some cases the field investigations cannot provide sufficient information to assist in engineering design; for example, when attempting to determine the optimal thickness of sub-surface layer(s) and pavement structure. From an engineering design perspective, there are very few laboratory or field studies conducted to assess the effects of gravel size and the thickness of gravel layers on pollutant removal in permeable pavements.

Hatt el al. (2007) examined the capability of removing TSS, TP and TN with different thicknesses of 10.5 mm gravels, which are typically used in the bedding layer of pavements, and observed an association between the pollutant removal and the thickness of the gravel layer. Another study conducted by Fach and Geiger (2005) concluded that smaller gravel is more effective in removing heavy metals (copper, zinc, and lead) through comparing their removal rates by 5 mm and 45 mm gravel. Brown et al. (2009) found that the gravel layers in permeable pavement could effectively remove sediment with particle sizes greater than 50 μm, and the overall TSS removal rates were dependent on inflow PSD. Davies et al. (2002) confirmed that the surface layer also contributes to sediment removal and suggested that the amount of sediment removed was determined by inflow PSD. The above studies found that both the sub-surface and surface layers act as a filter media and play a role in removing pollutants, and the removal rates (especially on TSS) were related to inflow PSD. Therefore, it is necessary to conduct a quantitative

examination of pollutant removal by different layers (e.g. PA, PC and PICP) in performance assessment of permeable pavements. It is also necessary to examine the PSD with respect to different layers as the inflow PSD also affects the treatment efficiency; many municipalities are paying attention to the PSD of storm runoff for stream health. In addition, to transfer the knowledge obtained from the lab-scale pavements to the field-scale pavements, both the laboratory and field investigations must be comparable in their design. This is often difficult and necessitates the development of modeling tools to link them in order to make the information obtained in anyone's study useful.

Therefore, the objectives of this chapter are to: i) investigate pollutant removal (TSS, TP and TN) with respect to different gravel sizes and thicknesses of gravel layers, which are typically used in permeable pavements, and the particle size distribution (PSD) of outflows; ii) evaluate and compare the ability of removing TSS, TP and TN by the surface layers of three permeable pavements, PA, PC and PICP, and the PSD in the outflows; iii) assess pollutant removal of three different types of permeable pavements, each of which has the same structure as that in the field study (Huang et al., 2015), and the PSD in the outflows; and iv) develop a simple model that can predict pollutant removal by permeable pavements using the knowledge obtained in this study that may be useful for optimizing the permeable pavement design.

4.2 Laboratory Experiments and Analysis Methods

4.2.1 Lab-Scale Modules

In this chapter, three gravel sizes, 12 mm, 40 mm and 63 mm in diameter (100% passing through sieve analyses), were selected, since they are commonly used in the bedding layer, base

layer and sub-base layer of permeable pavements. Table 4.1 shows the detailed gradation of the gravel used for this study. For each gravel size, the gravel layer's thickness was varied according to the following: 12 mm gravel: 30 mm, 50 mm, 70 mm, 90 mm and 110 mm; 40 mm gravel: 50 mm, 100 mm, 150 mm, 200 mm and 250 mm; and for 63 mm gravel: 100 mm, 200 mm, 300 mm, 400 mm and 500 mm. The layer thicknesses were determined to cover the range of required depths of different layers of permeable pavement based on structural and hydrological needs (Ferguson, 2005). Three types of surface layers, PA, PC and PICP (Eco-Optiloc®), which are 80 mm, 150 mm, and 80 mm in thickness, respectively, were chosen due to their popularity and applicability (Scholz and Grabowiecki, 2007). The porosities of the surface layers for PA, PC and PICP are 0.18, 0.23 and 0.12, respectively. In order to meet the structural requirement, the PC surface layer is 150 mm thick and is thicker than those of PA and PICP.

Figure 4.1 shows the schematic structure of gravel layers and surface layers of three types of pavements. It also shows the lab-scale pavements consisting of a surface layer and one or more sub-surface layers. Each gravel layer, surface layer, or pavement was contained in a wood frame, which is 450 mm long by 450 mm wide. The surface area of the wood frame was determined by considering the dimensions of one PICP paving block and selected so that each frame would contain a sufficient number of blocks to create a PICP surface. The wood frames were made of 3/4 inch plywood with waterproof coating on all inner sides and the connections of all four sides were sealed with silicone to prevent potential water leakage. Stainless steel netting (the void size of 5 mm) was placed at the bottom of each testing module to maintain the structural integrity of the testing materials. A tray was placed at the bottom of each wood frame to collect outflow. Prior to each experiment, the testing materials were thoroughly washed using tap water to remove the pollutant residuals from the previous test, thereby ensuring initial conditions were the same prior

to each experiment. The laboratory tests were conducted in the Hydraulic Laboratory of the Department of Civil Engineering, Schulich School of Engineering at the University of Calgary, Alberta, Canada. Regarding the field-scale tests, details on the experimental set-up and pavement structures can be found in Huang et al. (2015).

Table 4.1. Gravel gradation

	Sieve Size *(mm)*	**Percentage by Mass Passing** *(%)*
12 mm gravel	12	100
	10	40 - 75
	5	5 - 25
	2.5	0 - 10
	1.25	0 - 5
40 mm gravel	40	100
	25	95 - 100
	12.5	25 - 60
	5	0 - 10
	2.5	0 - 5
63 mm gravel	63	100
	50	90 - 100
	40	35 - 70
	25	0 - 15
	12.5	0 - 5

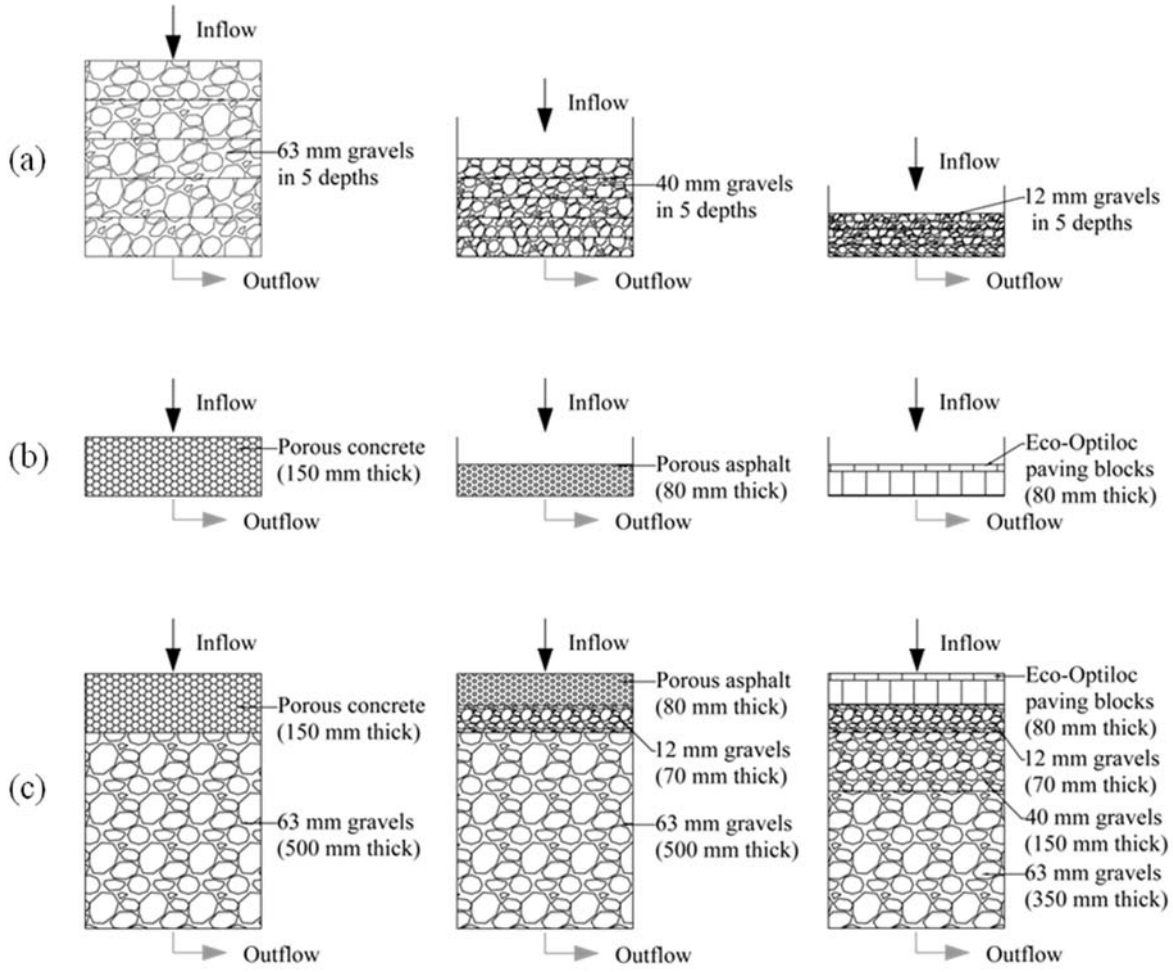

Figure 4.1. Schematic diagram of lab-scale modules: (a) different sizes and thicknesses of gravel (63mm, 40mm and 12 mm gravel); (b) different pavement surfaces (PC, PA and PICP); (c) full lab-scale pavements (PC, PA, and PICP)

4.2.2 Laboratory Experiments

Simulated stormwater runoff tests were conducted to evaluate pollutant removal of TSS, TP and TN by surface layers, gravel layers, and the complete lab-scale pavement with all the layers working together. Given a gravel layer (both gravel size and thickness), a surface layer, or a lab-scale pavement, four experimental tests were conducted. In each test, a 100-year storm event of 20

minutes in duration and 80 mm/hr in intensity was simulated. This storm event was selected due to the fact that: i) permeable pavements are considered components of major drainage systems, which should be capable of draining stormwater runoff for 100-year storm events (The City of Calgary, 2011); and ii) it allows a fair comparison between the lab-scale pavements and the field-scale pavements (Huang et al., 2015) in order to compare information between the laboratory and field scales. Please note that the selection of the storm event was made only considering the hydraulic performance of pavements in the field study. If the pavements are capable of dealing with extreme events, as in the 100-year storm, then they can effectively deal with more frequent and common storms.

In each test, synthetic stormwater runoff, which mimics the urban stormwater runoff in Calgary, was produced by completely mixing 450 L tap water (with 1 mg/L free chlorine) with 230 g of sediment (sizes less than 250 μm), 1.84 g of Nitrogen (as KNO_3) and 1.15 g of Phosphorus (as $Ca_3(PO_4)_2$) in a mixing tank (Figure 4.2(a)). Then a prescribed amount of synthetic stormwater was applied to the experimental modules (Figure 4.2(b)). The concentrations of TSS, TP, and TN of the synthetic stormwater were about 500 mg/L, 2.5 mg/L and 4 mg/L, respectively, which approximates the average water quality level of Calgary's urban stormwater runoff (The City of Calgary, 2011). The initial concentrations of TP and TN are different from those measured in the filed experiments. The values from the field measurement are under 'as is' condition, which are not the same as the reported average values. Sediments were collected from Calgary roads and then sieved to sizes of 250 μm and under. The sizes of sediments were used as they are not only responsible for clogging permeable pavements (Gerrtis, 2001), but also of particular importance to stormwater treatment since pollutants are likely attached to and can thus be easily mobilized and transported by stormwater runoff (Barnes *et al*, 2001). In addition, a previous study by Brown

(2007) found that it is difficult to completely mix the sediments larger than 250 μm with water in a mixing tank. The synthetic stormwater was then pumped from the mixing tank to the rainfall applicator (Figure 4.2(c)) fixed on the top of the lab-scale modules. The pumping rate was kept constant at approximately 0.01 L/s to simulate the 100-year storm event with an impervious to pervious ratio equal to 4 (Huang et al. 2015). The rainfall applicator consists of 16 vinyl tubes (each 4.3 mm in diameter with one hole) that were tightened together using a plastic sheet and connected to the pump outlet. The vinyl tubes were approximately evenly distributed to simulate uniform rainfall on the module surface during the tests.

Figure 4.2. Experimental instrumentation: (a) mixing tank; (b) experimental module; (c) rainfall applicator

In each experiment, 4 time-weighted outflow samples were manually collected at 5-minute intervals from the bottom of the module. The collected water samples were then analyzed for TSS, TP and TN at the Civil Engineering Wastewater Laboratory (room temperature from 19 – 22°C), Schulich School of Engineering at the University of Calgary. Concentrations of TSS were assayed using the standard method (APHA, 1998), and concentrations of TP and TN were assayed using Hach procedures 10071 and 8190, respectively. These Hach procedures are equivalent to standard

methods provided by the American Public Health Association. Particle size distribution (PSD) analysis was performed using a Malvern Mastersizer laser diffraction particle size analyzer. Three inflow samples were manually collected in each test from the rainfall applicator and assayed for same water quality parameters using the same methods described above.

4.2.3 Analysis Methods

In each simulated stormwater runoff test, the removal rate of TSS is calculated by (Huang et al. 2015):

$$R_{TSS} = \frac{C_{TSS\_in}V_{in} - C_{TSS\_out}V_{out}}{C_{TSS\_in}V_{in}} \times 100\% \quad (4.1)$$

where R_{TSS} is the removal rate of TSS [%]; C_{TSS_in} and C_{TSS_out} are the TSS concentrations of inflow and outflow [mg/L], respectively; V_{in} is the total volume of synthetic stormwater pumped from the mixing tank [L]; V_{out} is the total volume of stormwater collected at the bottom of the modules [L]. The removal rates of TP and TN are also calculated using similar equations.

In this chapter, Pearson correlations were calculated to evaluate potential relationships between two variables. In addition, linear regression was adopted to display the potential dependency of two variables. Statistical analyses were used to compare the performance of each type of pavement between field and lab experiments and the performance between/among different layers. Wilcoxon rank-sum test, a nonparametric method, was used to compare two independent samples, while the Kruskal-Wallis test followed by multiple comparisons was used to compare

more than two samples. All the statistical analyses were conducted at a significance level of 0.05 using MATLAB's Statistical Toolbox.

4.3 Results and Discussions

4.3.1 Inflow Water Quality Characteristics

Table 4.2 shows the descriptive statistics of measured concentrations of TSS, TP and TN of inflows in all simulated stormwater runoff tests. As demonstrated in this Table, the standard deviations of each pollutant are less than 10% of their mean values. Kruskal-Wallis analyses were conducted to compare the inflow concentrations of TSS, TP and TN in the tests. No significant differences were detected in all pollutants. In addition, the simulated stormwater runoff successfully mimicked Calgary's stormwater runoff quality as the measured inflow concentrations are similar to the average concentrations measured from the stormwater runoff in Calgary areas, which are 500 mg/L, 2.5 mg/L, and 4 mg/L for TSS, TP, and TN, respectively (The City of Calgary 2011).

Table 4.2. Inflow concentrations of TSS, TP and TN (sample size n = 84)

Parameter	Unit	Range	Mean	Median	Standard Deviation
TSS	mg/L	485 - 538	514	518	23
TP	mg/L	2.46 - 2.89	2.74	2.69	0.20
TN	mg/L	4.05 - 4.61	4.31	4.29	0.27

4.3.2 Dependence of Outflow Water Quality on the Gravel Layer

Figure 4.3 presents the removal rates of TSS, TP and TN, respectively, with respect to the thicknesses of the gravel layers for each gravel size. Given a gravel size, the linear regression line, in which the pollutant removal rate is the dependent variable while the thickness of the gravel layer is the independent variable, are also displayed in these figures. The measured data of TSS, TP and TN were tested, and passed, independence, stationarity and homogeneity tests at a 0.05 significance level prior to conducting the linear regression analysis. The linear regression equations are expressed as follows:

Removal rate of TSS:

63 mm gravel: $R_{TSS\_63} = 0.062h_{63} + 58.11 \quad R^2 = 0.958$ (4.2a)

40 mm gravel: $R_{TSS\_40} = 0.139h_{40} + 48.95 \quad R^2 = 0.921$ (4.2b)

12 mm gravel: $R_{TSS\_12} = 0.330h_{12} + 42.19 \quad R^2 = 0.984$ (4.2c)

Removal rate of TP:

63 mm gravel: $R_{TP\_63} = 0.110h_{63} + 19.75 \quad R^2 = 0.996$ (4.3a)

40 mm gravel: $R_{TP\_40} = 0.085h_{40} + 26.16 \quad R^2 = 0.964$ (4.3b)

12 mm gravel: $R_{TP\_12} = 0.120h_{12} + 23.73 \quad R^2 = 0.973$ (4.3c)

Removal rate of TN:

$$\text{63 mm gravel:} \quad R_{TN\_63} = 0.005h_{63} + 1.577 \quad R^2 = 0.936 \tag{4.4a}$$

$$\text{40 mm gravel:} \quad R_{TN\_40} = 0.004h_{40} + 1.202 \quad R^2 = 0.981 \tag{4.4b}$$

$$\text{12 mm gravel:} \quad R_{TN\_12} = 0.007h_{12} + 0.599 \quad R^2 = 0.926 \tag{4.4c}$$

where h_{63}, h_{40} and h_{12} are the thicknesses of the gravel layer [mm]; R^2 is the coefficient of determination of the regression lines.

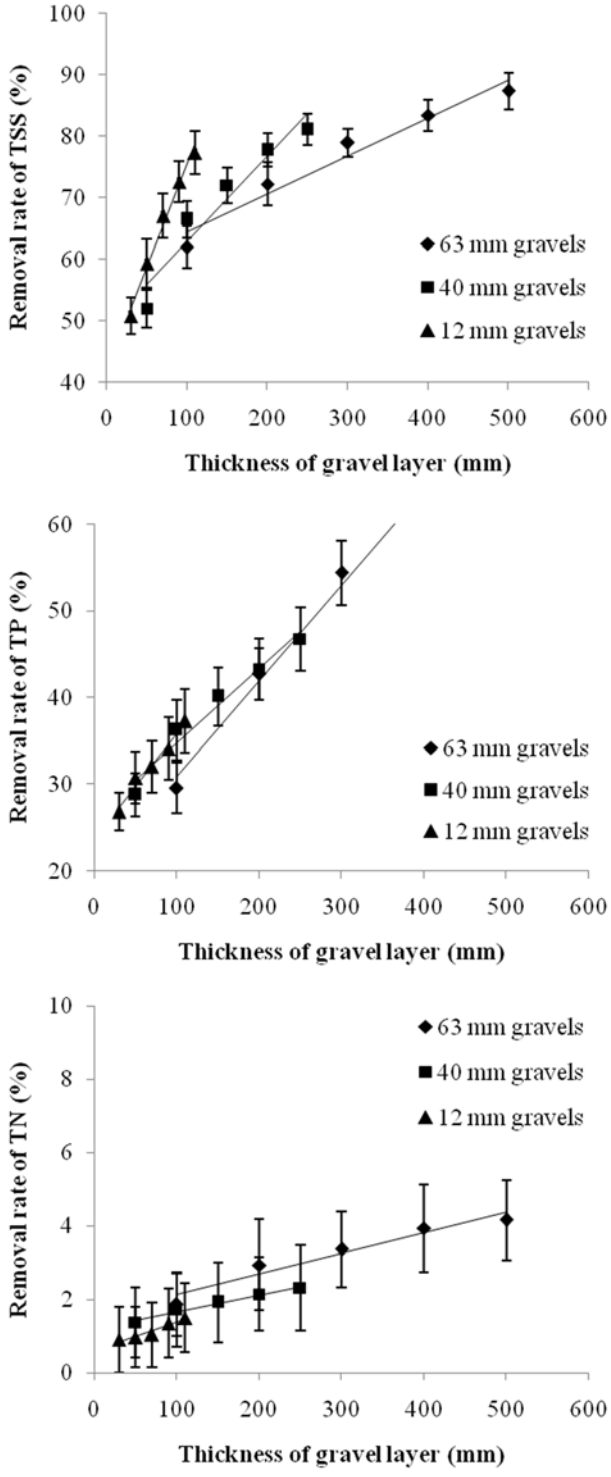

Figure 4.3. Removal rate (mean ± one standard deviation) versus the thicknesses of gravel layers and linear regression lines for each gravel size: (a) TSS; (b) TP; (c) TN (sample size of a given gravel size and layer thickness: n = 4)

As demonstrated in these figures, the removal rates of all three pollutants increase along with increase in the thickness of the gravel layer for a given gravel size. Given a gravel size and thickness of the gravel layer, pollutant removal rates are in the order of TSS, TP, and TN from the highest to the lowest removal. For 63 mm gravel, the removal rates of TSS, TP and TN range from 62% to 87%, from 30% to 74%, and from 1.4% to 2.3%, respectively; the removal rates of TSS, TP and TN by the gravel layer of 40 mm gravel varies between 52% and 81%, between 29% and 47%, and between 1.3% and 2.3%, respectively; while the removal rates of TSS, TP and TN by 12 mm gravel are from 51% to 77%, from 27% to 37%, and from 0.9% to 1.5%, respectively. Regardless of the gravel size and the thickness of the gravel layers, the TN removal rates are very low and all below 5%. This result is under expectations due to the fact that the smaller gravel should have small voids and thus, provide additional benefits in removing pollutants such as TSS by physical processes. However, these smaller gravel diameter layers are prone to clogging in earlier stages than larger diameter gravel. Although the TN removal rate appears to be dependent on the layer thickness for all gravel sizes, its dependence on the layer thickness is not prominently different among the different gravel sizes according to the derived regression slopes. Therefore, increasing the thickness of the gravel layer enhances pollutant removal, which is removed by physical process (for example TSS); whereas, it does not significantly benefit removal of other pollutants, such as TN, which is removed by biological processes (Wiesmann, 1994).

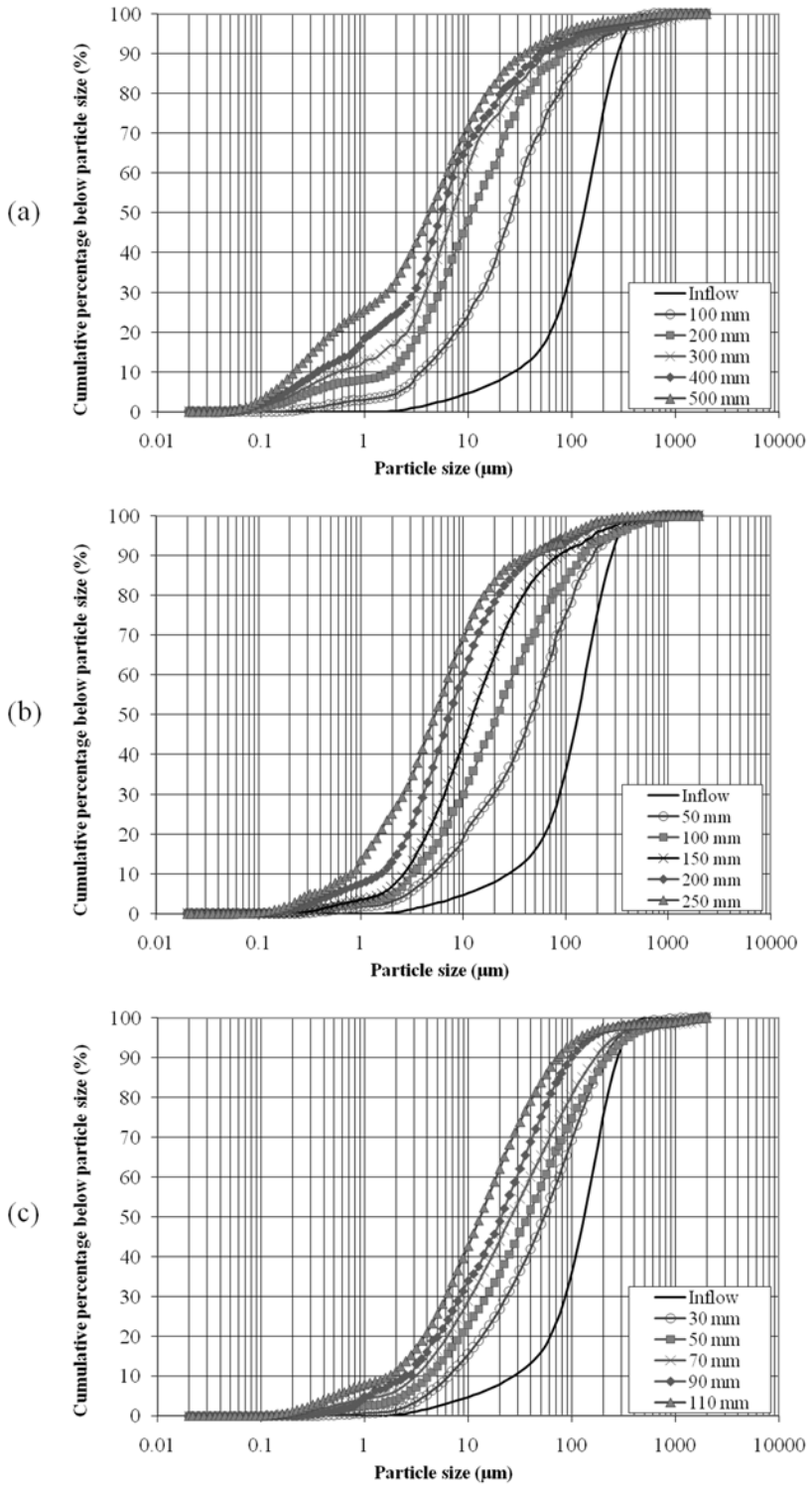

Figure 4.4a. PSD percentage curves of inflows and outflows from various gravel layers for gravel sizes (a) 63 mm, (b) 40 mm, and (c) 12 mm

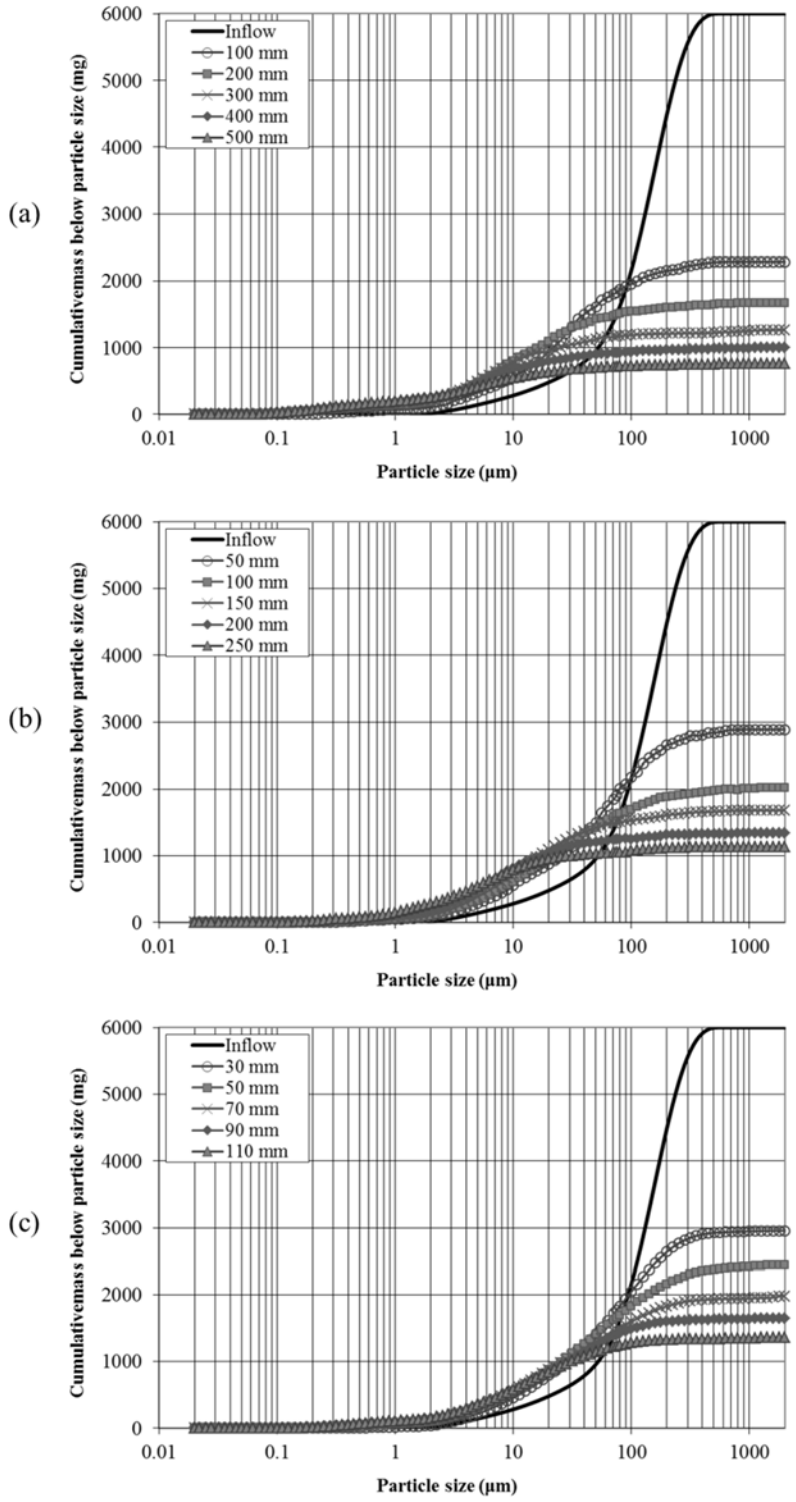

Figure 4.4b. PSD mass curves of inflows and outflows from various gravel layers for gravel sizes (a) 63 mm, (b) 40 mm, and (c) 12 mm

Figure 4.4 presents the results of PSD analyses of the inflows and outflows from various gravel layer thicknesses of 63 mm, 40 mm, and 12 mm gravels, respectively. The y axis of the figures is the cumulative percentage of TSS load no greater than the corresponding particle size in either the inflow or the outflow. The percentage is calculated by dividing the cumulative TSS load up to the particle size by the total TSS load in each event. Given a specific gravel size, the PSD curves of the outflows from all gravel layers obviously deviated from that of the inflow and the particles in the outflows are also finer than those in the inflow. For example, for the 100 mm thick gravel layer of 63 mm gravel, 85% of the particles are less than 100 μm in the outflow, while 85% of particles are less than approximately 250 μm in the inflow. In addition, the thicker the gravel layer is, the higher the percentage of smaller particles that appears in the outflow. Namely, larger particles (in percentage) are removed by thicker gravel layers. These results suggest that increasing the thickness of the gravel layer is effective in enhancing the removal of larger particles instead of smaller particles, along with the increase of the overall TSS removal rate (Figure 4.3). Similar results were observed for both 40 mm and 12 mm gravel.

To compare the performance of the gravel layers with the same thickness but different gravel size, the outflow PSD curves of 100 mm thick layers of 63 mm and 40 mm gravel together with the PSD curve of 110 mm thick layer of 12 mm gravel are provided in Figure 4.5. Kruskal-Wallis and multiple comparison tests indicate that the PSD curve of 12 mm gravel is significantly different from those of 63 mm and 40 mm gravel with the latter two not being significantly different. This means that the size distribution of removed particles by 12 mm gravel is significantly different from those of 63 mm and 40 mm gravel. Similar to what was observed previously in that the thickness of the gravel layer (given a gravel size) affects the PSD of the outflow, the PSD of the outflow is also associated with the gravel size (given a thickness of the

gravel layer). Given a specific thickness, the layer of small gravel tends to remove a relatively high percentage of large particles compared to the layer of large gravel. As presented in Figure 4.3 for these specific thicknesses of the gravel layers, the average removal rates of TSS are 61%, 66% and 77% for 63 mm, 40 mm and 12 mm gravel, respectively. This result demonstrates that given the same thickness of the gravel layers, smaller gravel has the potential to remove more particles.

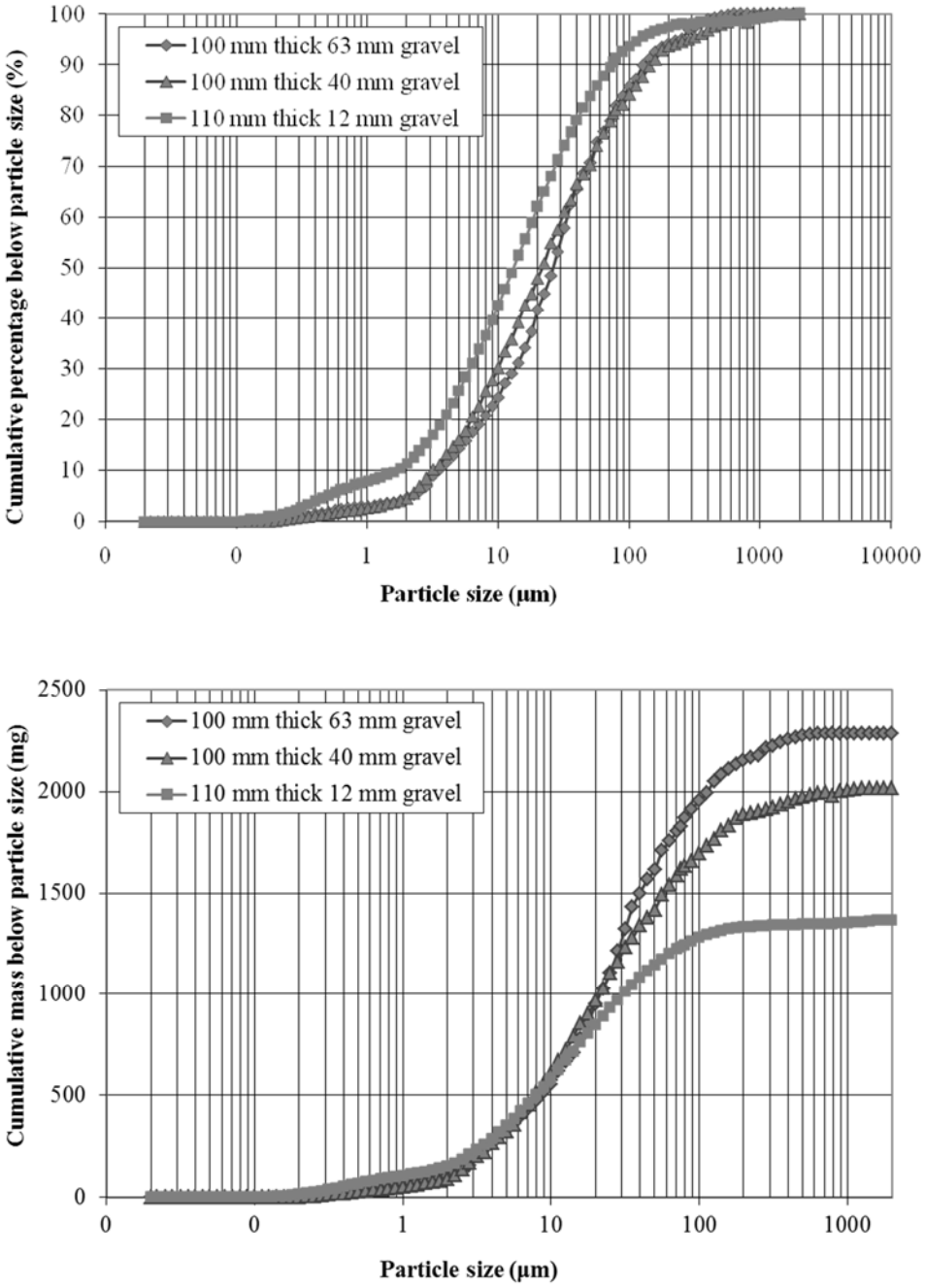

Figure 4.5. PSD (percentage and mass) curves of the outflows from 63 mm and 40 mm gravel layers of 100 mm thickness and 12 mm gravel layer of 110 mm thickness

According to the above findings, it is apparent that both the TSS removal rate and the composition of the particles (in terms of size) of outflows are associated with the thickness of the gravel layer and the size of the gravel. For the engineering design of permeable pavements to improve stormwater runoff quality, a thicker gravel layer is preferable as the increase in layer thickness leads to an increase in TSS removal rates; while the PSD is dependent on both the thickness of the gravel layer and the gravel size. The use of small gravel in the gravel layer benefits the TSS removal rate; however the layer of small gravel is easily clogged compared to that of coarse gravel and thus, more frequent maintenance to restore the efficacy of the pavement is required. These imply the challenge in optimizing pavement design to satisfy the needs for stormwater quality management. Balades et al. (1995) stated that large particles are initially trapped in the top of the pavements and then small particles are pushed through the entire layer by flow. This explains that the physical processes such as sedimentation and filtration are the primary mechanisms governing the TSS removal and the difficulty in removing small particles. Moreover given a gravel size, increasing the thickness of the gravel layer yields a relatively low percentage of removed small particles, although the overall TSS removal rate increases. In addition, a thicker gravel layer requires higher construction and material cost. Therefore, an increase of the thickness of the gravel layer is not always beneficial and economical. Ideally, an optimal thickness of gravel layer is needed to be determined by considering its performance in terms of the overall TSS removal rate and the composition of particles in the outflow, along with other factors such as the need for traffic load and economics.

4.3.3 Dependence of TP and TN Removal on TSS Removal

In stormwater runoff, some pollutants are attached to particles to a large degree. For instance, previous researchers (e.g., Andral et al., 1999; Sartor et al., 1974; Roger et al., 1998) have shown that phosphates are likely largely bounded to particles less than 250 μm in diameter. Therefore, some pollutants can be removed along with the sediments in the stormwater runoff. The study on permeable pavements conducted in the field by Huang et al. (2015) supported the suggestion that TP is likely removed with TSS by sedimentation and filtration, while TN is removed by different mechanisms that are primarily biological. In the laboratory study, strong positive correlations between TP removal and TSS removal, both of which increase along with the increase of the layer thickness (Figure 4.3), were found for all three gravel sizes as shown by the linear regression lines in Figure 4.6. The linear regression equations are expressed as follows:

63 mm gravel: $R_{TP\_63} = 0.677R_{TSS\_63} - 8.622 \quad R^2 = 0.930$ (4.5a)

40 mm gravel: $R_{TP\_40} = 0.598R_{TSS\_40} - 2.792 \quad R^2 = 0.988$ (4.5b)

12 mm gravel: $R_{TP\_12} = 0.360R_{TSS\_12} + 8.645 \quad R^2 = 0.961$ (4.5c)

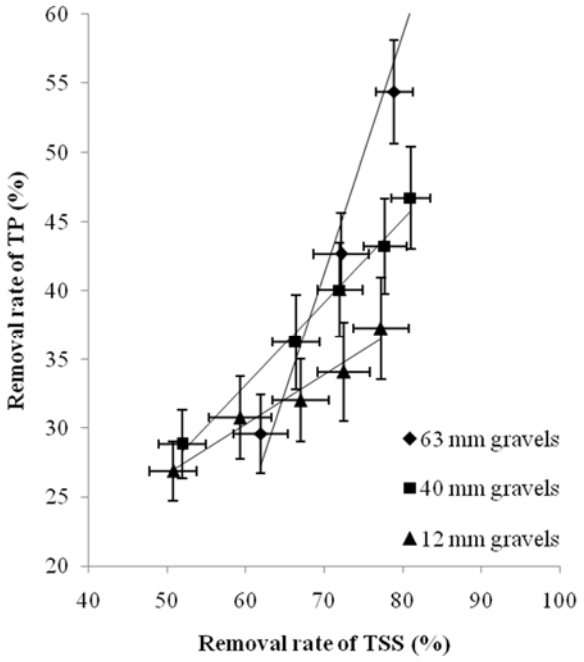

Figure 4.6. Linear regressions of TP removal rates (R_{TP}) on TSS removal rates (R_{TSS}) for different gravel sizes

The correlation coefficients between the removal of TP and TSS are 0.96 ($p < 0.01$), 0.99 ($p < 0.01$) and 0.98 ($p < 0.01$) for 63 mm, 40 mm and 12 mm gravels, respectively. As demonstrated in Figure 4.6, the regression slope for the 12 mm gravel is relatively smaller than those of both 40 mm and 63 mm gravels. Therefore, given the same increase in TSS removal rate, a smaller increase in TP removal with 12 mm gravel would be achieved. The difference in the linear regressive relationships between TSS removal and TP removal for 63 mm and 40 mm gravel is not prominent in their given ranges of layer thicknesses. These results suggest that the increase in thickness of the gravel layer can lead to increases in the removal of both TSS and TP; while the increase in TSS removal is more significant than that of TP removal as shown in the regressive slopes (less than 1).

Correlation coefficients between the TSS removal rates and the TN removal rates were also calculated for all three gravel sizes. The correlation coefficients are 0.99 ($p < 0.01$), 0.98 ($p < 0.01$) and 0.93 ($p < 0.01$) for 63 mm, 40 mm and 12 mm gravels, respectively. However, similar to the field study conducted by Huang et al. (2015), the TN removal rates are significantly lower than those of TSS and TP and appear to be more or less constant (< 5%) in all laboratory tests (Figure 4.3). The difference in removal rates of TSS and TN suggest that TN is removed separately from particles and consequently the TN removal is governed by different mechanisms. While the calculated correlations between the TN removal rate and the TSS removal rate might be explained by the thickness of the gravel layer, as TN is speculated to be removed by biological processes that take place in the void space of pavement structures (Newman et al., 2002; Stotz and Krauth, 1994). A few previous studies have also concluded that the removal of TN is largely associated with the growth of bio-film and is highly dependent on temperature (Wiesman, 1994). In this study, the low removal rates of TN compared to that from field study (Huang et al., 2015) may have resulted from little to no bio-film existing in the gravel since the gravel was thoroughly washed before each laboratory experiment.

4.3.4 The Roles of Pavement Surface Layers

Figure 4.7 presents the box plots of the removal rates of TSS, TP and TN of three pavement surface layers, PA, PC and PICP. The removal rates of TSS vary from 10% to 18%, from 16% to 27%, and from 8% to 18% for PA, PC and PICP, respectively. It is also obvious that the TSS removal rate of PC is relatively higher than those of both PA and PICP; while the TSS removal rates of PA and PICP are similar. The variation in the pollutant removal among PC, PA, and PICP surface layers might be associated with the thickness of the surface layers and the nature of the

pollutants. The surface layer of PC (150 mm thick) is thicker than those of PA and PICP, both of which are 80 mm thick (Figure 4.1). Similarly, the TP and TN removal rates of PC appears higher than those of both PA and PICP, but the difference in the TP and TN removal rates among these three surface layers is not as significant as that in the TSS removal rates. For all three surface layers, the TP and TN removal rates vary in the ranges from 3% to 13% and from 0% to 5%, respectively. By comparing the pollutant removal between the surface and gravel layers (Figure 4.3), similar magnitudes (< 5% difference) in the TN removal rates were observed; whereas the TSS and TP removal rates of the surface layers are much less than those of the gravel layers. The difference in the TSS and TP removal of the surface and gravel layers might be ascribed to their different physical structure, as the surface layers are designed to enhance water infiltration without causing surface ponding under the 100-year design storm event. According to Kruskal Wallis and multiple comparison tests, the TSS removal rate of PC is significantly higher than those of PA and PICP, but no significant difference was found for the TSS removal rate between PA and PICP.

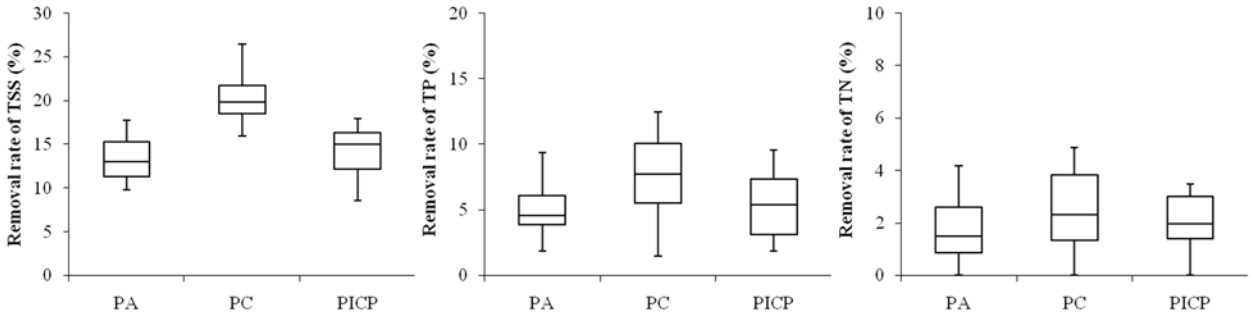

Figure 4.7. Removal rates of TSS, TP and TN for pavement surfaces, PA, PC and PICP (sample size n = 4)

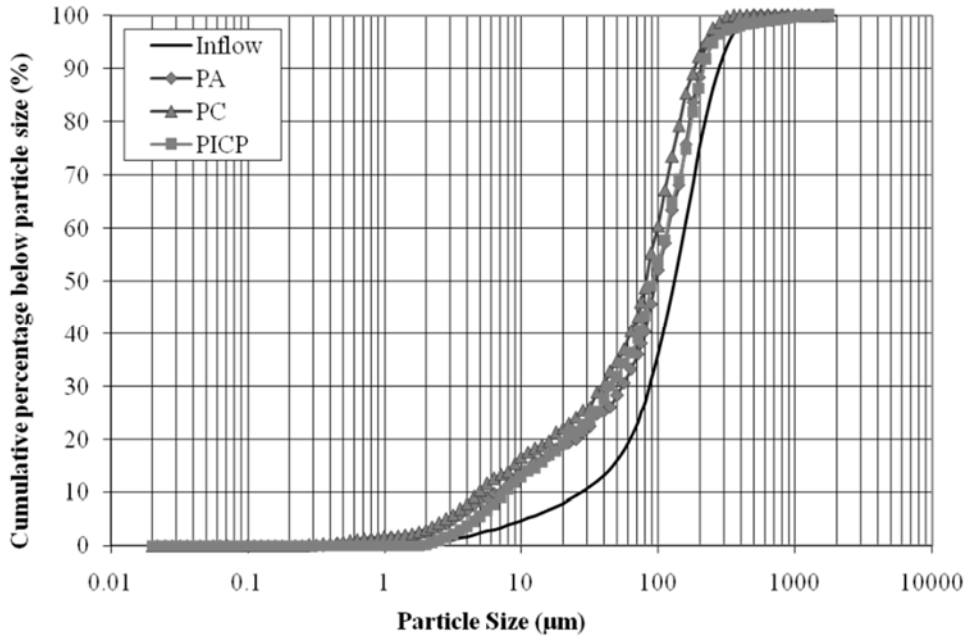

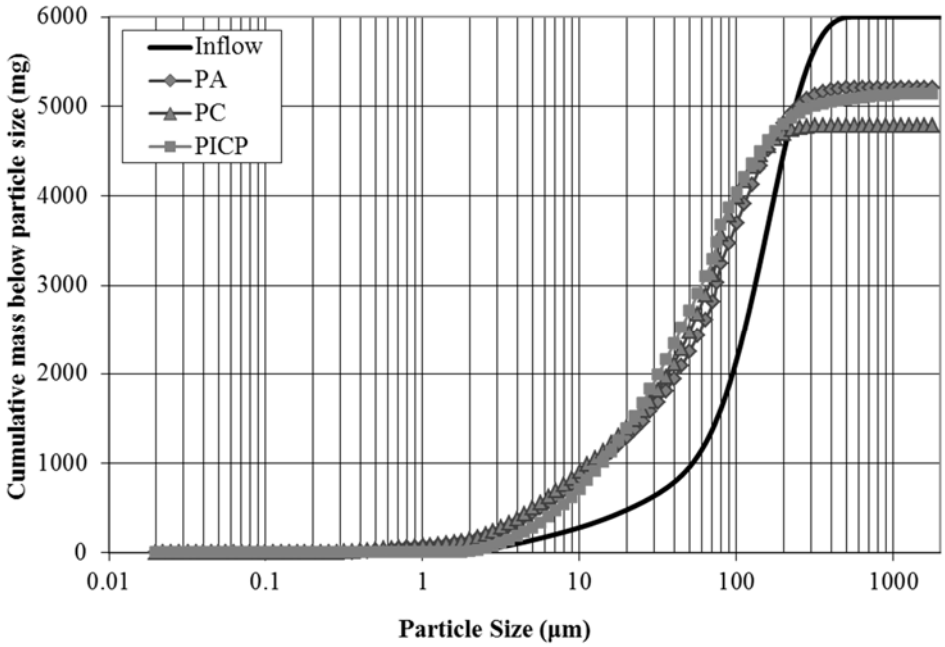

Figure 4.8. PSD (percentage and mass) curves of both the inflow and outflows for the pavement surface layers

The PSD curves of both the inflow and the outflows from the three surface layers are displayed in Figure 4.8. The curves of the outflows are obviously deviated from the inflow PSD curve, in particular in the range of the particle size from 3 μm to 100 μm. This result suggests that the three surface layers tend to trap relatively large particles. There is no significant difference in the outflow PSD curves among these three surface layers.

4.3.5 Pollutant Removal by Lab-Scale and Field-Scale Pavements

All the laboratory experimental tests in this chapter were conducted under room temperature between 19℃ and 22℃, while the field experiments were conducted under both warm and cold climatic conditions (Huang et al., 2015). As concluded in the field study, all three pavements can effectively remove TSS and TP and the removal rates are approximately 70% or higher. The removal rates of TSS and TP are independent of temperature; while the TN removal rate relies on temperature to some degree, however it is largely affected by the age of the pavements. In addition, the removal rates of TSS and TP are independent of SIR, which is over the rainfall intensity of 100-year design storm event, 80 mm/hr, in this study. Therefore, a fair comparison in their pollutant removal between the lab-scale and field-scale pavements can be made for TSS and TP.

The pollutant removal rates of the three lab-scale pavements, PA, PC, and PICP, whose structures are shown in Figure 4.1, are presented in Figure 4.9. To compare the results of the lab-scale pavements with the field-scale pavements (Huang et al. 2015), which have the same structures as those used in this laboratory study, the pollutant removal rates obtained from the field study were also included into the figure. The removal rates of TSS of the three lab-scale pavements range from 87% to 95% and are not significantly different among them (Kruskal-Wallis test). In

addition, no significant differences were detected between the lab-scale and field-scale pavements for each type of pavement (Wilcoxon rank-sum test). According to the PSD curves of the outflows from these lab-scale pavements demonstrated in Figure 4.10, for example, approximately 90% of particles in the outflows and the inflows are less than 40 μm and 300 μm, respectively. This suggests that relatively more small particles appear in the outflows, that is, more of the large particles are removed by the pavements. This finding is consistent with the observations from the gravel and surface layers as discussed previously and indicates the difficulty in removing small particles. By closely observing the PSD curves of the outflows from the lab-scale pavements and various gravel layers (Figure 4.4), it was found that a lower percentage of small particles was removed by the lab-scale pavements (650 mm thick) compared to all the investigated gravel layers (except for the 500 mm gravel layer of 63 mm gravels). The shape of the PSD of the lab-scale pavements is similar to that of the 500 mm thick layer consisting of 63 mm gravels. All these findings imply that the particle distribution of outflow might be more dependent on the thickness of the pavement layers, rather than the gravel sizes.

The removal rates of TP and TN of the lab-scale pavements range from 75% to 89% and from 3% to 10%, respectively. Similar to the results obtained from the gravel layers, the TSS removal rates of the lab-scale pavements are the highest, followed by the TP removal rates, and the TN removal rates are the lowest. In addition, there is no significant difference in the TP removal rates between the lab-scale and field-scale pavements for each type of pavement (Wilcoxon rank-sum test). The TN removal rates of the field-scale PC and PA (in their second year of operation) are obviously higher than that of the lab-scale PC and PA; whereas similarly low TN removal rates were measured in the field-scale PICP in its first year of performance (Huang et al., 2015). This

result demonstrates the effect of the pavements age on their performance in removing TN, which might be related to the governing mechanisms of TN removal in the pavements.

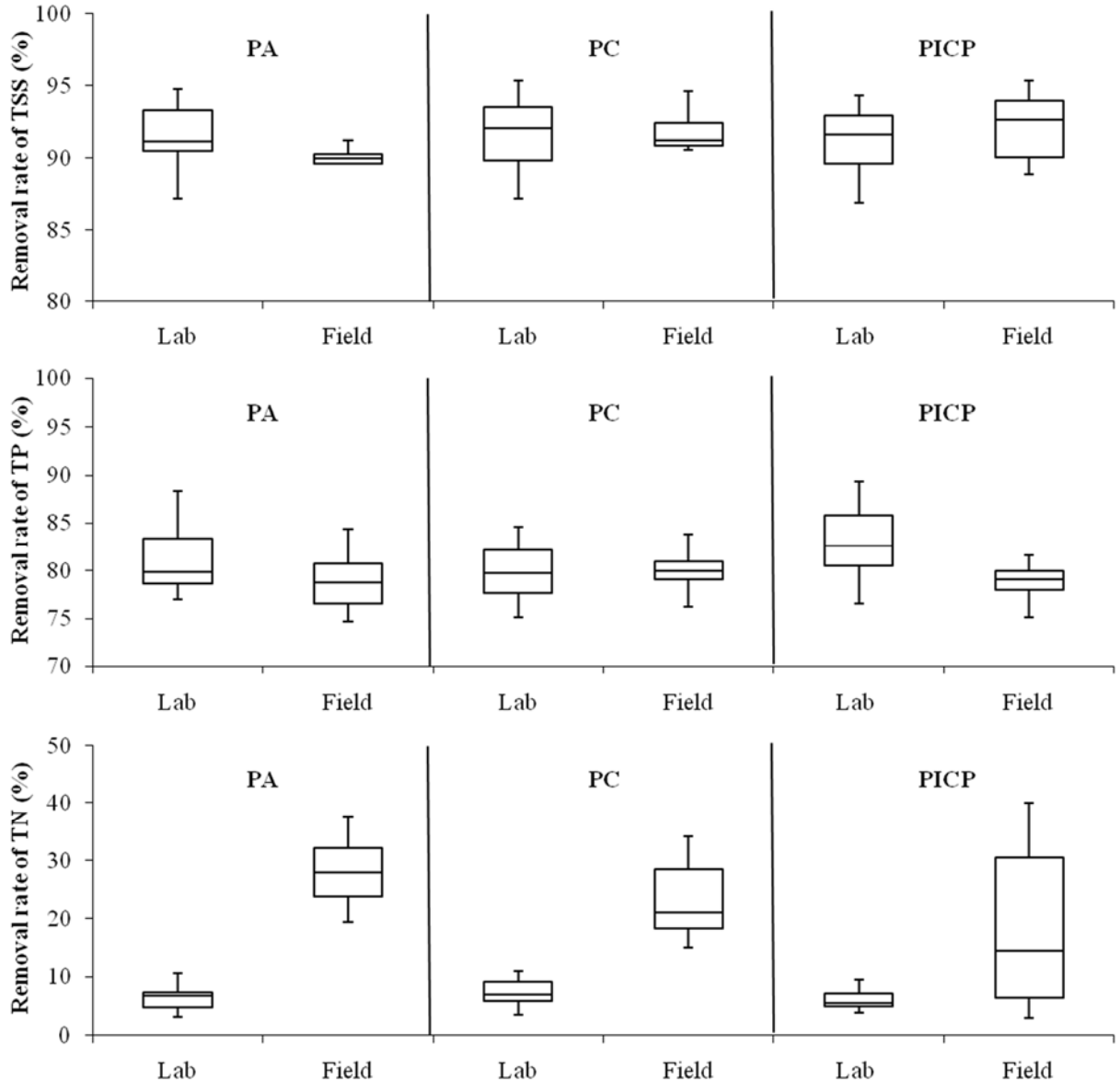

Figure 4.9. Removal rates of TSS, TP and TN for the lab-scale pavements (sample size n = 4) and field-scale pavements (sample size n = 6 for PA and PC, n = 8 for PICP)

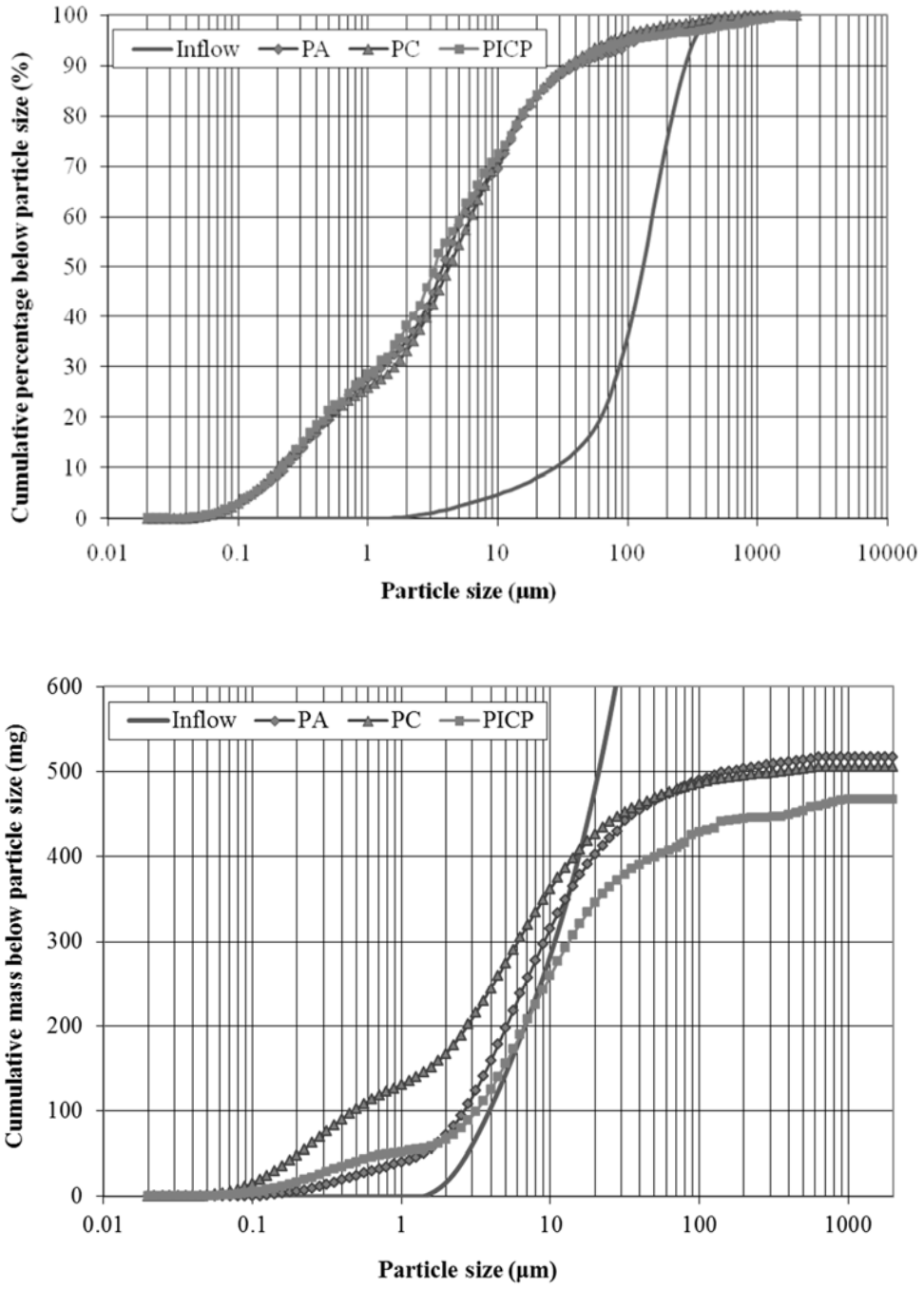

Figure 4.10. PSD (percentage and mass) curves of the inflow and outflows of the lab-scale pavements

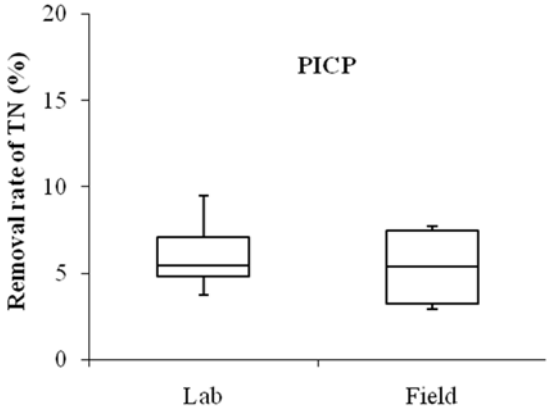

Figure 4.11. Removal rates of TN in the lab-scale PICP and field-scale PICP (in the first year of in 2011) (sample size n = 4 for lab, n = 4 for field)

The difference in water quality performance may be ascribed to the different governing mechanisms removing the pollutants. The results from this chapter along with results from Huang et al. (2015) support that the removal mechanism of TN is likely different from that of TSS and TP and that the TN removal is associated with biological process, which might be largely dependent on the age of the pavement. Since the TN removal rates are speculated to be associated with time, the comparison between the lab-scale pavements and the field-scale pavements in their first year of service (gravel was also thoroughly washed before construction) were conducted to avoid the influence of pavement age on TN removal. Due to the failure of the surface layer of both PA and PC in the first year out in the field, their surface layers were replaced in the next year. Therefore, the comparison was conducted only between the lab-scale and field-scale PICP (Figure 4.11). As shown in this figure, similar TN removal rates were observed in both the lab-scale and the field-scale PICP and no significant difference is detected in the Wilcoxon rank-sum test. Therefore, the performance in removing TN in the laboratory test is similar to that in the field test in the initial year.

4.3.6 Prediction of Pollutant Removal of Permeable Pavements

Using the results obtained from the laboratory study, a practical mathematical model useful for optimizing pavement structure was developed to predict the pollutant removal rates of TSS and TP for permeable pavements. The removal rate of TN is not included in the modeling as it might be largely dependent on the pavement age rather than the pavement structure. The model developed below is applicable to the permeable pavements designed given similar inflow conditions, including hydrological condition and inflow pollutants.

When given a permeable pavement with structural details including surface material, layer thickness and gravel size, the pollutant mass of its outflow can be calculated by the specific removal rates of individual layers:

$$M_{out} = M_{in}\left(1 - F_{surface}\right)(1 - F_{12})(1 - F_{40})(1 - F_{63}) \times 100\% \quad (4.6)$$

where M_{in} and M_{out} are the pollutant mass in the inflow and outflow, respectively [mg]; $F_{surface}$ is the pollutant removal rate of the pavement surface layer (as a fraction $F_{surface} = R_{surface}/100\%$); F_{12}, F_{40} and F_{63} are the pollutant removal rates for gravel sizes of 12 mm, 40 mm and 60 mm, respectively ($F_{12} = R_{12}/100\%$, $F_{40} = R_{40}/100\%$, $F_{63} = R_{63}/100\%$). These pollutant removal rates are functions of the thickness of the gravel layer and are calculated based on the regression equations demonstrated in Figure 4.3 for TSS and TP.

Thus, the overall removal rate of the pollutant (R) by the permeable pavement is:

$$R = \frac{M_{in} - M_{in}\left(1 - F_{surface}\right)(1 - F_{12})(1 - F_{40})(1 - F_{63})}{M_{in}} \times 100\%$$

$$= [1 - \left(1 - F_{surface}\right)(1 - F_{12})(1 - F_{40})(1 - F_{63})] \times 100\% \quad (4.7)$$

Taking the water loss (in quantity) into consideration, the Eq. (4.7) is modified as:

$$R = [1 - b\left(1 - F_{surface}\right)(1 - F_{12})(1 - F_{40})(1 - F_{63})] \times 100\% \quad (4.8)$$

where b is the water balance coefficient [dimensionless] and is calculated by

$$b = {}^{V_{out}}/_{V_{in}} \quad (4.9)$$

V_{out} and V_{in} are the total volumes of outflow and inflow, respectively [L]. According to the water balance analysis for the laboratory experiments (results shown in last chapter), the value of b is approximately 0.95; while b was found in the range from 0.85 to 0.9 in the field study (Huang et al., 2014). Therefore, the value of 0.9 is used in the prediction model (Eq. 4.8) herein.

Table 4.3 demonstrates the predicted removal rates and measured removal rates from the field study conducted by Huang et al. (2015) for each type of pavement. The errors between the model predicted rates (where the model was developed using the laboratory data for each individual pavement layer) and field measured removal rates are also calculated and shown in the Table. The prediction errors range from -1.5% to 4.5%, which shows a good performance of the developed prediction model. When a targeted pollutant removal rate is provided, the model can be used to design the permeable pavement by determining proper thickness of gravel layers. For example, the Pennsylvania stormwater best management practice manual (Pennsylvania

Department of Environmental Protection, 2006) states that permeable pavements should remove a minimum of 85% of TSS from stormwater runoff. The City of Calgary requires stormwater ponds to be capable of removing 85% of TSS (The City of Calgary, 2011), but no specific guideline for permeable pavements has been given yet. Thus, it is generally assumed that permeable pavements must also be designed to meet 85% removal of TSS. The predicted removal rate of the PC is 91.8% given the same structure as the lab-scale and field-scale PC. If reducing the thickness of the 63 mm gravel layer from 500 mm to 400 mm, the designed PC, which has the predicted removal rate of 88.1%, still satisfies the minimum requirement of the TSS removal but substantially reduces the construction and material cost. The above practice demonstrates the capability of using laboratory study results to assist in optimizing engineering design of permeable pavements. However, note that apart from the consideration of the performance in pollutant removal, the structural requirements (e.g., for traffic) of the pavements needs to be taken into consideration for optimizing the pavement structure.

Table 4.3. Measured and predicted removal rates of TSS and TP of the field-scale pavements

Pollutant	Pavement	Measured mean removal rate (%)		Predicted removal rate by model (%)	Error between field and lab (%)	Error between field and model (%)
		Lab	Field			
TSS	PA	91.4	90.5	92.0	1.0	1.7
	PC	91.6	90.9	91.8	0.8	1.0
	PICP	92.2	91.2	95.3	1.1	4.5
TP	PA	81.0	78.9	80.4	2.7	1.9
	PC	80.0	79.9	78.7	0.1	-1.5
	PICP	82.9	78.8	80.4	5.2	2.0

4.4 Conclusions

In this chapter, the removal of pollutants including TSS, TP and TN by the surface layers and gravel (sub-surface) layers with a variety of thicknesses were investigated and PSD analyses were conducted. Three sizes of gravel (63 mm, 40 mm and 12 mm), which are typically used in permeable pavements, were used in the laboratory study. Three types of permeable pavement surfaces, PA, PC and PICP, were examined for pollutant removal. For different surface layers, PA and PICP surfaces, which are of the same thickness (80 mm), have equivalent performance in removing TSS, TP and TN; while the surface layer of PC (150 mm thick) is demonstrated to have superior performance due to its greater thickness. For all three sizes of gravel, the dependence of the removal efficiency of all investigated pollutants on the thickness of gravel layers was found. While given a layer thickness, smaller gravels yield higher TSS and TP removal rates; whereas TN removal does not appear to be significantly different among the diffident sizes of gravel. In addition, strong dependence of the TP removal on the TSS removal was found. According to results of PSD, no significant difference in the PSD curves was observed in the three lab-scale pavement surfaces; but significant difference was found in the investigated gravel layers. Given a specific thickness of gravel layer, smaller gravel is preferred in the design of pavement structure from a water quality perspective.

A comparison of pollutant removal between the lab-scale and the field-scale pavements, both of which have the same structure (surface layers, thickness of all sub-surface layers, gravel sizes), was conducted. In general, their equivalent performance was observed in removing TSS and TP for all pavements; while the TN removal rates of the field-scale pavements were higher than those of the lab-scale pavements on PICP. The difference in TN removal might be due to the effect of the age of the field-scale pavement. Similar TN removal rates were found between the

lab-scale and field-scale pavements after removing the effect of pavement age on TN removal. The laboratory test results along with the field results support the suggestion that TP is removed along with TSS and that TN is removed separately from TSS.

Based on the results from this laboratory study, a mathematical model was developed to predict the removal rates of TSS and TP given a pavement structure. The model showed good performance in predicting the removal rates of TSS and TP through comparing the model results with the lab and field measurements. Therefore, the developed model can be a useful tool for assisting in the design of permeable pavements and the optimization of pavement structures.

Chapter Five: Temporal Evolution Modeling of Hydraulic and Water Quality Performance of Permeable Pavements*

5.1 Introduction

Traditionally, stormwater runoff from impervious surfaces has been intercepted by sewer systems and discharged to receiving water bodies. Due to rapid expansion in recent years, urban areas have experienced an increase of impermeable surfaces such as roofs, roads and other paved surfaces. This change in the impervious-pervious surface balance has caused significant changes to both quality and quantity of stormwater runoff leading to degraded urban water systems (Arnold Jr and Gibbons 1996, Brabec 2002, Finkenbine et al. 2000). Permeable pavement, one of the widely used Low Impact Development (LID) technologies in urban areas, presents a feasible solution to the above issues as it provides in situ restoration of the urban hydrologic cycle and reduces the needs for traditional stormwater facilities. Permeable pavement not only reduces runoff and flooding, enhances groundwater recharge, and filters and treats infiltrating runoff, but also provides the load carrying capacity of the conventional pavement. (Sansalone et al. 2008, Scholz and Grabowiecki 2007). Porous asphalt (PA), porous concrete (PC) and permeable inter-locking pavers (PICP) are currently three very popular permeable pavements and have been widely applied in driveways, parking lots and low-speed roads (Balades et al. 1995, Watanabe 1995).

Due to the massive application of permeable pavement in urban areas, many studies have been conducted to address its applicability on hydraulic and water quality performance. The hydraulic performance focuses on runoff attenuation, peak reduction and surface infiltration

* The materials in this chapter have been submitted to the *Journal of Hydrology* for publication.

capacity, while water quality performance focuses on removal of various pollutants including total suspended solids (TSS), nutrients (i.e. nitrogen and phosphorus), heavy metals (i.e. Cu, Pb and Zn) and hydrocarbons. Most studies of water quality and quantity performance in the literature use field investigations under different testing conditions such as pavement age and structure, inflow characteristics and climates. The results showed that permeable pavement is capable of reducing stormwater runoff and can maintain its surface infiltration capacity at a satisfactory level with proper maintenance after up to 10 years of service (Al-Rubaei et al. 2013, Ball and Rankin 2010, Bean et al. 2007, Booth and Leavitt 1999, Brattebo and Booth 2003, Lucke and Beecham 2011). In water quality performance, permeable pavement has been consistently shown to remove considerable amounts of TSS, heavy metals (Cu, Pb and Zn) and hydrocarbons from stormwater runoff (Brown et al. 2009, Eck et al. 2011a, Newman et al. 2002, Roseen et al. 2011). However, reported performance for removing nutrients (nitrogen and phosphorus) have been inconsistent (Collins et al. 2009, Gilbert and Clusen 2006, Huang et al. 2012, Pagotto et al. 2000, Rushton 2001). Several studies employing laboratory experiments in order to better control testing conditions showed similar finding to those from the field investigations (Fach and Geiger 2005, Huang et al. 2015a, Tota-Maharaj and Scholz 2010).

Previous studies on hydraulic and water quality performance of permeable pavements have primarily focused on the analyses and interpretation of field and laboratory-based observations. This information is critical for understanding performance and thus, necessary for predicting the performance in existing pavement systems and for design of future systems. In order to utilize this information for design purposes, designers need robust modeling tools that can quantitatively predict both the hydraulic and water quality performance over the short-term and long-term horizons before pavement construction. Therefore, this chapter aims to develop a numerical model,

which is accurate and robust and can capture the temporal variation of pavement performance, for the engineering design of different types of permeable pavements. The literature shows that sufficient research has been conducted to understand how permeable pavements function to mitigate water quantity attenuation and mitigation of TSS. Engineering permeable pavements for long-term performance with minimal maintenance requires accurate computer modelling so engineers may be able to determine the appropriate design for the desired mitigation levels. A handful of studies have simulated the performance of permeable pavements by modeling techniques (either numerical or empirical), but fewer still have compared their predictions to data obtained through field investigations and lab experiments.

In modeling hydraulic performance, permeable pavements are often considered as a porous media made of various surface materials (PA, PC and PICP) with one or more sub-surface gravel layers. Previous studies have simulated the hydraulic conductivity and porosity for surface and gravel layers of permeable pavements. Tan et al. (2003) modeled the reduction of porosity in the base layers for permeable pavements using the Kozeny-Carman equation in conjunction with experimental data. Montes and Haselbach (2006) established a quantitative relationship between porosity and hydraulic conductivity of a PC surface using a similar methodology to Tan et al. (2003). Deo et al. (2010) developed a model to simulate the degradation of surface infiltration rates (SIR) for a PC system based on a probabilistic particle capture approach and the experimental data. Kuang et al. (2011) compared the hydraulic conductivity of the surface layer of a PC with that simulated by different models using various pore-structure equations. The comparison showed that Kozeny-Carman equation can successfully simulate the hydraulic conductivity with proper calibration of porosity and tortuosity. Yong et al. (2013) developed a black-box regression model to predict the degradation of porosity for a PA surface using laboratory experimental data.

A few studies have also focused on simulating the surface runoff, infiltration and outflow of permeable pavements. Macdonald et al. (1979) modeled the flow through a gravel media using a revised version of the Ergun equation and the results from the model were consistent with those obtained from lab experiments. Zhu et al. (1999) developed a numerical model based on Smoothed Particle Hydrodynamics (SPH) to describe the flow through a gravel media. Schluter and Jefferies (2002) developed a computer model to simulate the outflow (peak rate and volume) from porous pavement using the stormwater software package ERwin®. Eck et al. (2011b) developed a numerical model using the Boussinesq equation to simulate the surface runoff mitigation during storm events by applying mass conservation for the surface layer of a PA.

In water quality performance, previous studies have modeled pollutant removal (mostly TSS) by filter units of a gravel media in water and wastewater treatment. The removal mechanisms of TSS for gravel are mainly by sedimentation and interception (Yao 1968, McDowell-Boyer et al. 1986, Urbonas 1999). Yao (1971) developed a numerical model in TSS removal for a gravel media, rapid sand filter by assuming that the major removal mechanisms are sedimentation, interception and diffusion. Based on the study by Yao (1971), Tufenkji and Elimelech (2004) developed a regression model to describe the sedimentation, interception and diffusion processes for gravel media and model results were in good agreement with experimental data. Wu (1994) developed a numerical model simulating TSS removal from a gravel media given constant water pressure head. Several studies applied the theory developed from sand filters to stormwater management. Siriwardene et al. (2007) modified the model created by Yao (1971) and applied the modified model to successfully simulate the sediment transport in gravel layers installed in a stormwater pond and sediment basin. Wong et al. (2004) introduced a first order kinetic decay model to estimate the overall TSS removal in stormwater ponds with the presence of a gravel

media. Huang et al. (2015a) developed a regression model to predict the overall TSS removal efficiency for permeable pavements using experimental data. However, no study has applied the developed methodologies from filter units to numerically model the TSS removal in permeable pavements, even though the removal mechanisms between filters and permeable pavement are similar.

The above review shows that the aforementioned hydraulic models mainly targeted one or more hydraulic parameters (e.g. porosity, hydraulic conductivity and outflow) for a specific layer of permeable pavement (either the surface or subsurface gravel layer). From a water quality perspective, the previous models cited above were mostly developed for modeling the treatment efficacy of gravel media in sand filters or stormwater ponds but not for permeable pavements. As permeable pavements become more and more popular and more widely used, design requirements that achieve peak flow reduction will be required, and thus, accurate models that predict performance are required. In addition, pollutant removal becomes an important index for permeable pavement performance and it is necessary to have this information available at the design stage. This necessitates the development of numerical models that can predict both hydraulic and water quality performance of complete permeable pavement systems (both surface and gravel sub-layers) in order to help stormwater engineers optimize design and operation. Therefore, the two-fold objectives of this chapter are to: 1) propose a numerical model for permeable pavement systems that can accurately and realistically simulate both water quantity and quality (focusing on TSS) of outflow, and 2) to prove the applicability of the proposed model by applying the model to simulate three different types of permeable pavements (PA, PC, and PICP), which were tested in a field study in Calgary, Alberta, Canada.

5.2 Mathematical Model Development

A permeable pavement usually consists of a surface layer and one or more sub-surface gravel layers. The material specifics used in the surface layer and sub-surface layer are different due to the structural requirements and the purpose of the engineering structure. The surface layers of PA and PC are normally formed of coarse aggregates that are bonded together by bituminous asphalt and cement, respectively. The surface layer of PICP typically consists of concrete paving blocks with gaps in between, where are filled with small gravel for structural integrity and storm runoff infiltration. Thus, the surface layer of the permeable pavements has a relatively high porosity compared to conventional pavements. The sub-surface layer of the pavements often consists of compacted gravel for bearing load and temporally retaining stormwater. Due to the primary use of gravel in both layers, flow movement within, and sediment removal by the layers can be modeled based on the same theory.

The model development is described in terms of a conceptual flow model shown in Figure 5.1. The permeable pavement system is modelled using a combination of flow equations and treatment equations for each layer.

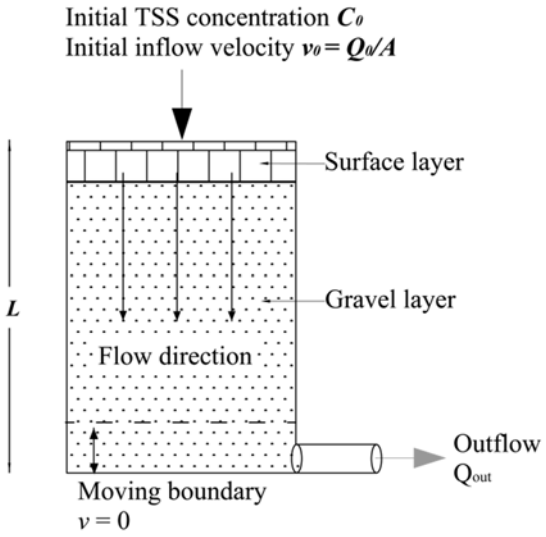

Figure 5.1. Definition sketch

5.2.1 Flow Equation

The modified Kozeny-Carman equation is employed to simulate the infiltrated flow through a permeable pavement structure (Tan et al. 2003, Kuang et al. 2011) by assuming that the infiltrated water only flows in a vertical direction:

$$\frac{\partial v}{\partial L} = \frac{1}{180}\frac{m^3}{(1-m)^2} \cdot (\varphi d)^2 \cdot \frac{g}{\mu L} \tag{5.1}$$

where v is the vertical flow velocity through the pavement structure [m/s]; m is the porosity of surface and gravel layers in the pavement structure [unitless]; φ is the sphericity of gravel, which ranges from 0 to 1 depending on the shape of the gravel [unitless]; d is the gravel diameter [m]; g

is the gravitational acceleration [m/s^2]; μ is the kinematic viscosity of infiltrated water [m^2/s]; and L is the total thickness of the pavement structure [m].

5.2.2 Sediment Removal Equation

Yao et al. (1971) developed a sediment removal model for a sand filter in water and wastewater treatment processes. Based on the similarity of the gravel media in a sand filter and the pavement structure (they are both comprised of various sizes of gravel and properly packed for sediment removal), this developed model can also be utilized to simulate the process of sediment removal for permeable pavements by introducing single collector efficiency, η:

$$\frac{\partial C}{\partial L} = -\frac{3}{2}\frac{(1-m)}{d}\alpha\eta C \tag{5.2}$$

where C is the concentration of TSS [mg/L]; and α represents contact efficiency, which is the number of contacts that succeed in producing adhesion divided by the number of collisions that occur between suspended particles and the gravel media (ranging from 0 to 1). Ideally, α equals to 1 if the suspended particles are completely mixed in water (Yao et al. 1968). The collector efficiency η is defined as the ratio of particles striking different layers by interception, sedimentation or diffusion, to total particles flowing towards the gravel media and is mathematically expressed as (Yao et al. 1971):

$$\eta = \eta_d + \eta_{in} + \eta_s \tag{5.3}$$

In Equation (5.3), η_d, η_{in} and η_s are the portions of η caused by diffusion, interception and sedimentation, respectively. Tufenkji and Elimelech (2004) claimed that these parameters are related to gravel size, flow velocity, water temperature and particle size distribution (PSD) of inflow TSS. The mathematical expressions of these three parameters are:

$$\eta_d = 0.9\left(\frac{kT}{\mu d_p dv}\right)^{2/3} \tag{5.4}$$

$$\eta_{in} = \frac{3}{2}\left(\frac{d_p}{d}\right)^2 \tag{5.5}$$

$$\eta_s = \frac{(\rho_p - \rho) g {d_p}^2}{18\mu v} \tag{5.6}$$

where k is Boltzmann constant (1.3805×10^{-23} J/K); T is absolute temperature of stormwater [K]; d_p is particle diameter in TSS [m]; ρ_p is the density of particles in TSS [kg/m^3]; and ρ is the density of infiltrated water [kg/m^3]. Therefore, the sediment equation (Equation 5.2) can be written in the following form with respect to Equations (5.3) to (5.6):

$$\frac{\partial C}{\partial L} = -\frac{3}{2}\frac{(1-m)}{d}\alpha\left[0.9\left(\frac{kT}{\mu d_p dv}\right)^{2/3} + \frac{3}{2}\left(\frac{d_p}{d}\right)^2 + \frac{(\rho_p - \rho) g {d_p}^2}{18\mu v}\right]C \tag{5.7}$$

5.2.3 Numerical Approximation

The finite difference approximation is employed to solve v in Equation (5.1). The value of v at time step j is expressed by:

$$v_{i+1}^{j} = v_i^{j} + \frac{1}{180} \cdot \frac{{m_i}^3}{(1-m_i)^2} \cdot (\varphi d_i)^2 \cdot \frac{g}{\mu L} \Delta L \tag{5.8}$$

where the subscript *i* indicates the section number after discretization of the pavement depth *L*, and the superscript *j* indicates the time step; and ΔL represents the distance between sections *i* and *i+1*. For a single storm event, the inflow rate Q_0 can be assigned as the initial input (see Figure 5.1) when duration and intensity of the storm are given.

During a storm event, permeable pavement undergoes a "filling process" as water continuously infiltrates into the pavement and is then stored in the gravel layer(s). At the same time, a portion of the stored water is discharged through the under-drain pipe installed in the bottom of the pavement. Therefore, the water level in the gravel layer is unsteady and thus, is the boundary where $v = 0$ moves up or down (Figure 5.1). The stored water level at time step *j* can be estimated based on the water level at the previous time step *j-1* and the change of water storage (in depth) under the current time step *j*:

$$H^j = H^{j-1} + h_{in}^j - h_{out}^j \tag{5.9}$$

where *H* represents the water level in storage [m]; h_{in} is the depth of water that infiltrates into the pavement structure [m]; and h_{out} is the depth of water discharging from the under-drain pipe [m]. Based on the flow velocity near the boundary (v_b^j) and the porosity of the gravel layer (m_b) where the boundary lies in, h_{in} at time step *j* is calculated by:

$$h_{in}^{j} = {bv_b^j \Delta t}/{m_b} \tag{5.10}$$

where b is the water loss coefficient, which indicates the ratio of the volume of inflow, V_{in}, to the volume of outflow, V_{out}, ($b = V_{out}/V_{in}$).

The value of h_{out} at time step j is calculated by:

$$h_{out}^{j} = {Q_{out}^{j} \Delta t}/{A \cdot m_b} \tag{5.11}$$

where A represents the surface area of the permeable pavement [m^2]; and Q_{out}^{j} represents the outflow rate from the sub-drain pipe [m/s] used to simulate the outflow hydrograph, which is calculated by:

$$Q_{out}^{j} = \delta A_{orifice} \sqrt{2gH^{j-1}} \tag{5.12}$$

In Equation (5.12) δ is the transient loss coefficient; and $A_{orifice}$ is the cross-sectional area of the orifice in the under-drain pipe (0.028 m^2 in this study).

When given the velocity profile from Equation (5.8), C at time step j can be solved by applying a finite difference approximation to Equation (5.7):

$$C_{i+1}^{j} = C_i^j - \frac{3}{2}\Delta L \frac{(1-m_i)}{d_i}\alpha \left[\frac{3}{2}\left(\frac{d_p}{d_i}\right)^2 + 0.9\left(\frac{kT}{\mu d_p d_i v_i^j}\right)^{2/3} + \frac{(\rho_p - \rho) g {d_p}^2}{18\mu v_i^j}\right] C_i^j \tag{5.13}$$

After calculating TSS concentrations along the thickness of the pavement structure, the accumulated TSS, M_{TSS}, at location i can be estimated by:

$$M_{TSS_i} = \sum_{j=0}^{t/\Delta t} C_i^j v_i^j A \Delta t \tag{5.14}$$

where t is the duration of the storm event [s] and Δt is the defined time between time step j and $j+1$.

The removal rate of TSS, R_{TSS}, at location i is then determined based on mass balance and thus, can be calculated using Equation (5.15). When location i indicates the bottom of the pavement, the overall removal rate of TSS by the pavement, R_{TSS_out}, can also be calculated using Equation (5.15).

$$R_{TSS_i} = (C_0 Q_0 t - b M_{TSS_i}) / C_0 Q_0 t \tag{5.15}$$

Figure 5.2 shows the flow chart of the proposed model, which indicates the algorithm in obtaining hydraulic and water quality information according to Equations (5.8) to (5.15). In hydrological respects, the velocity and flow rate profile can be determined by Equation (5.8) when rainfall intensity and duration are given. The depth increment due to h_{in} can be calculated by Equation (5.10). Q_{out} and h_{out} are obtained from Equations (5.11) and (5.12). Based on the calculated h_{in} and h_{out}, the water level in storage, H, for the next time step is then calculated using Equation (5.9). TSS concentration along the pavement thickness is calculated by Equation (5.13).

Both the TSS retained within the pavement and the TSS removal rate at some depth is determined by Equations (5.14) and (5.15), respectively. Then, R_{TSS} of the outflow is determined by Equation (5.15). According to the above algorithm, the proposed model was programmed using MATLAB.

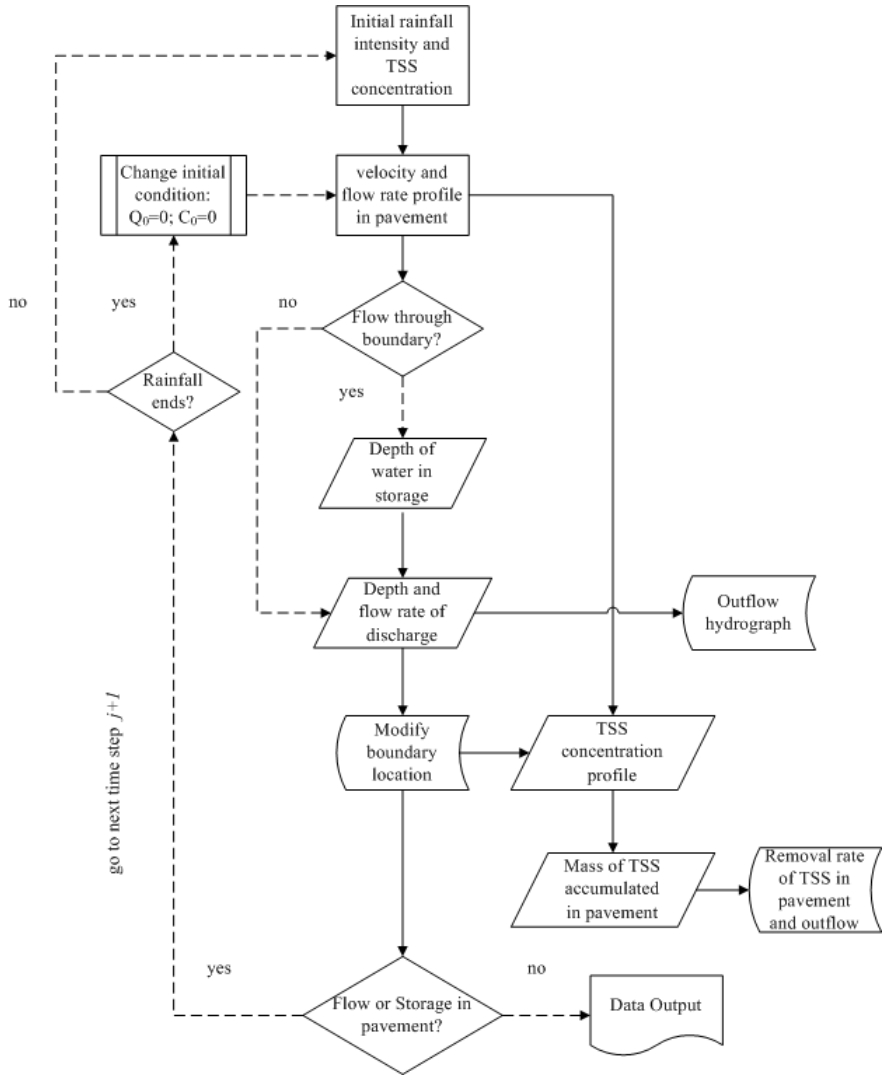

Figure 5.2. Flow chart of the proposed model

5.3 Site Description and Data Collection

The hydraulic and water quality data collected from three pilot-scale permeable pavements, which were installed in the Currie Barracks southwest of Calgary, Canada, were used to calibrate and validate the proposed model (shown in Figure 5.3). Figure 5.4 shows the schematic structure of the three pavements that consist of three surface materials: PC, PA and PICP. PICP was installed in September 2011, while PA and PC were installed in October 2012. For each pavement, the surface is 6.0 m long and 6.0 m wide, with a total thickness of 0.65 m. A perforated under-drain pipe (100 mm in diameter) is placed at the bottom and diverts infiltrated water to a nearby manhole for outflow collection. A layer of non-woven geo-textile is installed between the sub-base and sub-grade to prevent pollutant migration to the underlying soil. The underlying soil proved to be fairly impermeable by infiltration tests (measured infiltration rate = 0.58 mm/hr). Thus, water loss due to infiltration into the underlying soil was considered negligible.

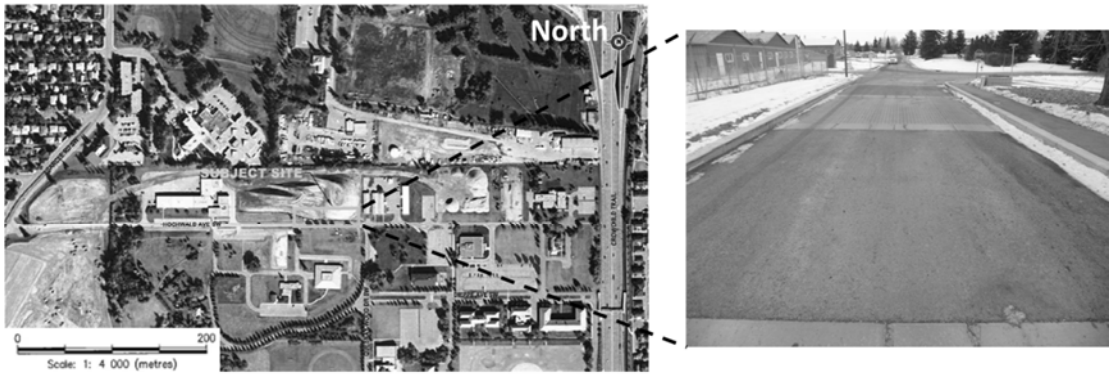

Figure 5.3. (a): Study site location; (b): Field-scale permeable pavements

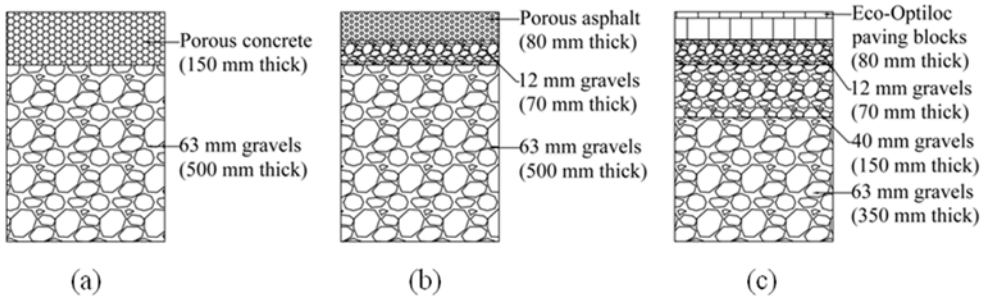

Figure 5.4. Schematic structure of pilot-scale permeable pavements: (a) PC; (b) PA; (c) PICP

5.3.1 Field Data Collection

A total of twenty simulated storm runoff tests were conducted for the three pavements (six for PC, six for PA, and eight for PICP) during the monitoring period from October 2011 to December 2013. The tests were mainly conducted before and during the winter period in order to examine the performance under Calgary's winter conditions. In each test, stormwater was delivered from a nearby stormwater pond and evenly distributed to the pavement surface. A 1:100 year storm event of 20 minutes in duration and 80 mm/hr average rainfall intensity was simulated. The TSS concentration of the stormwater was controlled to approximately 500 mg/L by manually adding street sediment into the stormwater, which is the typical TSS concentration of storm runoff in Calgary (The City of Calgary 2011). Outflow from the under-drain pipe was continuously monitored (at 1 min intervals) using a Sigma 950 flow meter in a nearby manhole. A total of 8 outflow samples were collected from the manhole at 5-minute intervals in each event. The water samples were delivered to the Civil Engineering Wastewater Laboratory of the University of Calgary for assaying TSS. The recorded data that include peak flow (Q_p), time to peak (t_p), b, flow-weighted outflow TSS concentration (C_{TSS_out}) and R_{TSS_out}, are shown in Table 5.1 for each event.

Surface infiltrated tests were conducted to measure surface infiltration rate (SIR) of each pavement. Please note that pressure washing for recovering SIR was conducted on May 13, 2013 during the field study period. More detailed information on the field study can be found from Huang et al. (2015b).

Table 5.1. Field observations of the three field-scale pavements in each simulated storm event

Pavement	Test No.	Test date	Q_p (L/s)	t_p (min)	b	C_{TSS_out} (mg/L)	R_{TSS_out} (%)
PC	1	2012-10-19	2.68	16	0.84	47.3	90.6
	2	2013-03-28	2.40	20	0.88	42.8	91.5
	3	2013-09-24	2.28	21	0.88	27.0	94.6
	4	2013-10-10	2.13	22	0.91	46.0	90.8
	5	2013-11-13	1.85	24	0.85	45.2	91.0
	6	2013-11-28	1.70	25	0.92	36.4	92.7
PA	1	2012-10-15	2.55	18	0.85	29.5	93.2
	2	2013-03-27	2.17	20	0.90	49.5	89.6
	3	2013-09-20	2.18	22	0.83	43.8	89.8
	4	2013-10-08	1.96	23	0.88	45.4	89.6
	5	2013-11-07	1.63	25	0.92	40.9	90.2
	6	2013-11-27	1.46	30	0.90	43.0	90.3
PICP	1	2011-10-19	2.92	14	0.91	38.2	91.7
	2	2011-10-27	2.64	18	0.83	33.6	92.6
	3	2011-11-10	2.33	26	0.89	55.2	88.6
	4	2011-12-14	1.87	28	0.86	61.5	86.9
	5	2012-08-23	1.46	58	0.85	50.1	90.0
	6	2013-04-02	1.29	65	0.91	27.1	94.3
	7	2013-09-26	1.64	40	0.83	30.3	94.0
	8	2013-10-09	1.54	43	0.85	42.5	91.5

5.4 Model Calibration and Application

According to the proposed model, several parameters need to be initially determined as model inputs. Among these parameters, some can be obtained from field and laboratory experiments; whereas others are needed to be determined through model calibration due to a lack of information and/or difficulty in measuring physically. In particular, some parameters (such as porosity) changes with time. The following details the rationale behind various parameter estimates:

- To ensure the stability and convergence of numerical results, Δt and Δl are 1 second and 1 mm, respectively (Marzulli and Trigiante 1995).
- Stormwater temperature, T, of inflow in each event was recorded and the kinematic water viscosity is then determined according to the measured temperature.
- The sphericity of the gravel in the surface and sub-surface layers, φ, is set as 0.1 to account for the irregular shape of gravel (Al-Rousan et al. 2005).
- The mean particle size in inflow sediment, d_p, is 120 μm based on PSD of inflow (Huang et al. 2015a).
- The density of the dry sediment, ρ_p, is approximately 1,090 kg/m^3 from lab measurements.
- The transient loss coefficient, δ, ranges from 0 to 1 and its specific value is determined in model calibration.
- Porosity, m, of the different layers of a pavement is an essential input parameter in the model. For PA and PC, initial surface porosity was measured from their core samples. For PICP, initial surface porosity was estimated based on the ratio of the joint-fill area between paver blocks to the total surface area. The initial porosity for each gravel layer, which is dependent on the gravel compaction in the construction process (for structural integrity),

was provided by the construction company. Estimated initial porosities of each layer of the three pavements are shown in Table 5.2. Unlike other parameters, porosity is not a constant and continuously decreases with respect to time due to compaction by traffic loads and clogging by sediment retention (Scholz and Grabowiecki 2007). It is difficult to obtain estimates of both surface and sub-surface porosity by direct measurement after pavements are put into operation. In the proposed model, the porosity of the surface layer is determined based on the measured SIRs as discussed in the following paragraph; while the porosity of sub-surface layer(s) is determined in model calibration.

Table 5.2. Estimated initial porosities of each layer of PA, PC and PICP

Pavement	PA	PC	PICP
Surface layer	18%	23%	12%
Bedding layer 12 mm gravel	19%	-	25%
Base layer 40 mm gravel	-	-	30%
Sub-base layer 63 mm gravel	30%	30%	35%

Previous studies have demonstrated that SIR can effectively reflect the level of surface porosity of permeable pavement (Wu and Huang 2000, Bean et al. 2007). With the support of the above statement, the surface porosity of the three pavements can be estimated with respect to the measured SIR. For the three field-scale pavements, SIR was measured for PICP from 2011 to 2013, and for PA and PC from 2012 to 2013 (Huang et al. 2015b). The observed SIR indicated a continuous decrease during the time intervals in which maintenance (e.g., pressure washing) was

not applied to recover SIR. Considering the trends of SIR measured in the field, it is initially assumed that the surface porosity is linearly related to the logarithmic SIR. The surface porosity is then modeled as a function of the operation time of the pavements. The surface porosity determined in this way are used in the calibration and also in the verification discussed in the next sections.

Figure 5.5 shows the regression analyses of the surface porosity with respect to operation time for the three pavements, respectively. Types of regression were selected based on the value of the coefficient of determination, R^2. As pressure washing has been demonstrated to be an effective way to recover SIR, the regression analysis was conducted before and after pressure washing (applied to the pavements on May 13, 2013), respectively. Please note that further adjustments on the initially determined surface porosity may be required based on the model performance in the calibration and that a "good" model performance helps in justifying the assumption of the surface porosity.

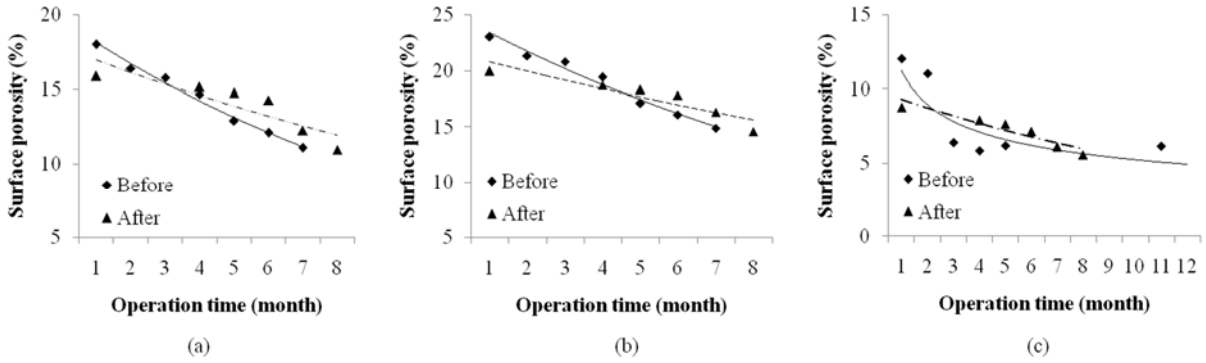

Figure 5.5. Surface porosity degradation with operation time, before and after pressure washing: (a) PA; (b) PC; (c) PICP

The regression equations from Figure 5.5 for the three pavements are as follows:

PA: Before maintenance: $P_{surface} = 19.64e^{-0.08X}$ $R^2 = 0.988$ (5.16a)

After maintenance: $P_{surface} = 17.83e^{-0.05(X-Y)}$ $R^2 = 0.764$ (5.16b)

PC: Before maintenance: $P_{surface} = 25.17e^{-0.07X}$ $R^2 = 0.979$ (5.17a)

After maintenance: $P_{surface} = 21.62e^{-0.04(X-Y)}$ $R^2 = 0.830$ (5.17b)

PICP: Before maintenance: $P_{surface} = 10.45X^{-0.24}$ $R^2 = 0.774$ (5.18a)

After maintenance: $P_{surface} = 9.90e^{-0.06(X-Y)}$ $R^2 = 0.883$ (5.18b)

where X is the operation time [month]; and Y is the maintenance time [month].

Due to a lack of site information, the porosity of gravel layers for the three pavements needs to be calibrated. According to the pavement structure (Figure 5.3), the total number of layers that needs calibration for PA, PC and PICP are 2, 1, and 3, respectively. The recorded events from the simulated storm events (Table 5.1) were divided into two groups for model calibration and verification, respectively. Events 1, 2, 4 and 6 were selected for model calibration, while events 3 and 5 were used for model verification for PA and PC. Events 1, 2, 4, 6 and 8 were used for model calibration, while Events 3, 5 and 7 were used for model verification for PICP. In the proposed model, the parameters to be calibrated include the porosity of sub-surface layer(s) and δ. Before the model calibration, sensitivity analyses were performed to identify the acceptable ranges of the calibration parameters. The models were then calibrated manually using the trial-and-error

approach to determine the above parameters. In the model calibration, the parameters were determined to yield acceptable error (less than 10% here) in a variety of modeled hydraulic and water quality variables, which include t_p, Q_p, V_{out}, and R_{TSS_out}, in each calibration event. The error of Q_p is calculated using Equation (5.19) and errors of other variables are calculated in the same manner.

$$error = \frac{Q_{p\_model} - Q_{p\_measure}}{Q_{p\_measure}} \times 100\% \tag{5.19}$$

where Q_{p_model} and $Q_{p\_measure}$ are modeled and measured peak outflow, respectively [m^3/s].The model performance metrics used in the model calibration include R^2 and normalized root-mean-square deviation (*NRMSD*). *NRMSD* is defined as:

$$NRMSD = \frac{\sqrt{\sum\left(Q_{out\_model} - Q_{out\_measure}\right)^2 / n}}{Q_{p\_measure}} \times 100\% \tag{5.20}$$

where Q_{out_model} and $Q_{out\_measure}$ are modeled and measured outflow, respectively [m^3/s]; n is the total number of measurements.

The modeled and measured outflow hydrographs in each calibration event for PA are presented in Figure 5.6. R^2 ranges from 0.813 to 0.917 and *NRMSD* ranges from 9.32% to 15.04%. These results indicate a good agreement between the measured and simulated results in all the calibration events. Table 5.3 presents the measured and modeled hydraulic and water quality variables (t_p, Q_p, V_{out}, and R_{TSS_out}) along with their errors in each calibration event. As shown in

Table 5.3, the parameters were calibrated to ensure that errors of these variables are less than 10%. The calibration results for PC are shown in Figure 5.7 and Table 5.4; and the calibration results are presented in Figure 5.8 and Table 5.5 for PICP. The calibrated δ for PA, PC and PICP are 0.70, 0.66 and 0.58, respectively. These results also suggest good agreement between measured and observed outflow hydrographs and TSS removal rates for both PC and PICP.

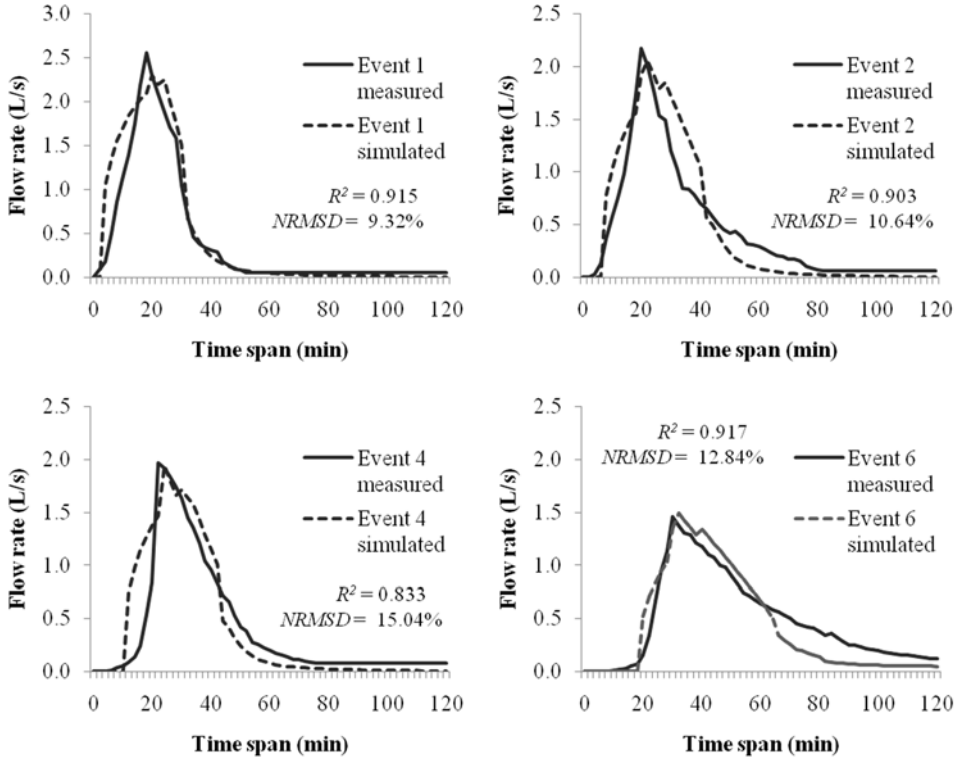

Figure 5.6. Measured and modeled outflow hydrographs for calibration events for PA

Table 5.3. Measured and modeled hydraulic and water quality variables for PA in the model calibration

Event No.	Parameter	Measured	Simulated	Error (%)
1	Q_p (L/s)	2.55	2.3	-9.80
	t_p (min)	18	19	5.56
	V_{out} (L)	3610	3477	-3.68
	R_{TSS_out} (%)	93.2	91.8	-1.50
2	Q_p (L/s)	2.17	2.05	-5.53
	t_p (min)	20	22	10.00
	V_{out} (L)	3560	3406	-4.33
	R_{TSS_out} (%)	89.6	94.7	5.69
4	Q_p (L/s)	1.96	1.94	-1.02
	t_p (min)	23	25	8.70
	V_{out} (L)	3483	3360	-3.53
	R_{TSS_out} (%)	89.6	94.8	5.80
6	Q_p (L/s)	1.46	1.49	2.05
	t_p (min)	30	30	0.00
	V_{out} (L)	3410	3321	-2.61
	R_{TSS_out} (%)	90.3	95.4	5.65

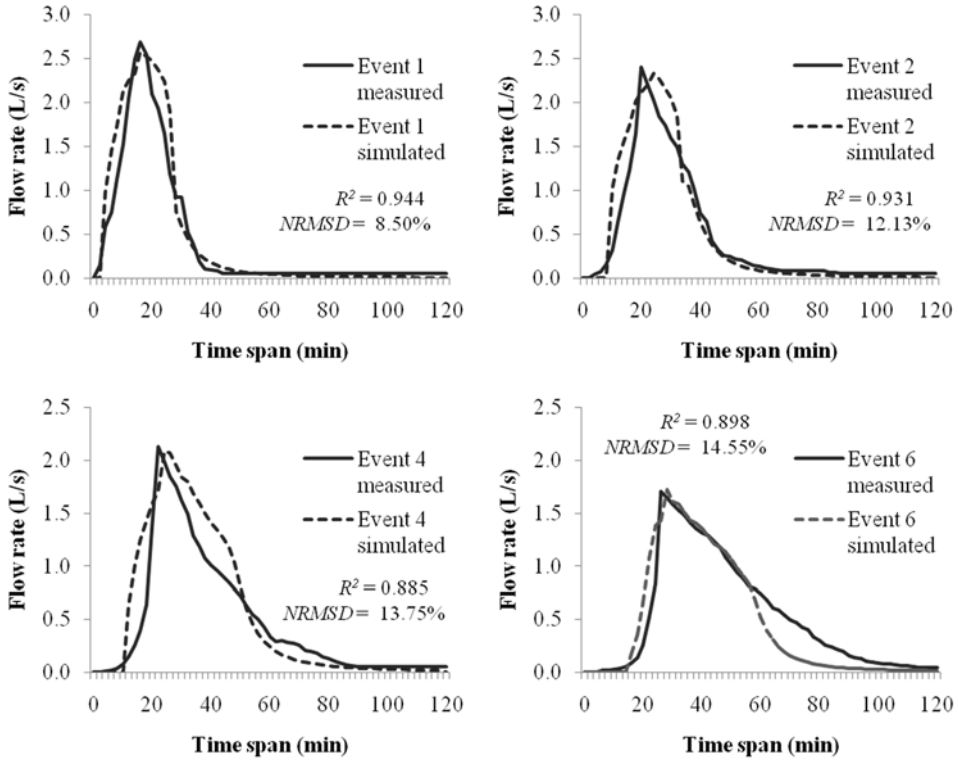

Figure 5.7. Measured and modeled outflow hydrographs for calibration events for PC

Table 5.4. Measured and modeled hydraulic and water quality variables for PC in the model calibration

Event No.	Parameter	Measured	Simulated	Error (%)
1	Q_p (L/s)	2.68	2.58	-3.73
	t_p (min)	16	16	0.00
	V_{out} (L)	3360	3472	3.33
	R_{TSS_out} (%)	90.6	82.9	-8.50
2	Q_p (L/s)	2.40	2.32	-3.33
	t_p (min)	20	22	10.00
	V_{out} (L)	3520	3501	-0.54
	R_{TSS_out} (%)	91.5	84.1	-8.09
4	Q_p (L/s)	2.12	2.08	-1.89
	t_p (min)	21	22	4.76
	V_{out} (L)	3540	3725	5.23
	R_{TSS_out} (%)	90.8	85.4	-5.95
6	Q_p (L/s)	1.70	1.72	1.18
	t_p (min)	26	28	7.69
	V_{out} (L)	3580	3690	3.07
	R_{TSS_out} (%)	92.7	87.5	-5.61

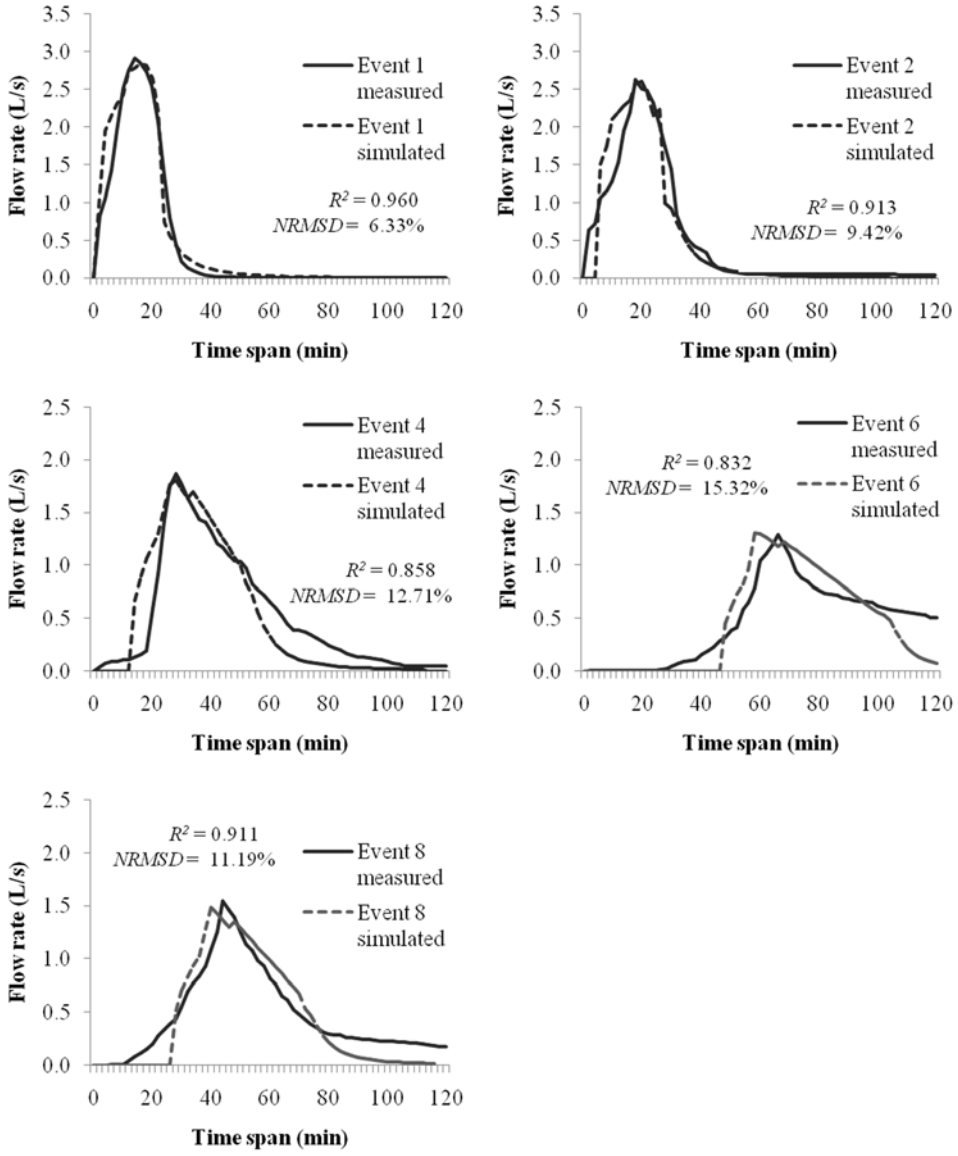

Figure 5.8. Measured and modeled outflow hydrographs for calibration events for PICP

Table 5.5. Measured and modeled hydraulic and water quality variables for PICP in the model calibration

Event No.	Parameter	Measured	Simulated	Error (%)
1	Q_p (L/s)	2.92	2.84	-2.74
	t_p (min)	14	15	7.14
	V_{out} (L)	3405	3598	5.67
	R_{TSS_out} (%)	91.7	89.8	-2.07
2	Q_p (L/s)	2.63	2.578	-1.98
	t_p (min)	18	19	5.56
	V_{out} (L)	3759	3610	-3.96
	R_{TSS_out} (%)	92.6	90.8	-1.94
4	Q_p (L/s)	1.87	1.81	-3.21
	t_p (min)	28	28	0.00
	V_{out} (L)	3842	3623	-5.70
	R_{TSS_out} (%)	86.9	93.5	7.59
6	Q_p (L/s)	1.29	1.3	0.78
	t_p (min)	65	60	-7.69
	V_{out} (L)	3710	3393	-8.54
	R_{TSS_out} (%)	94.3	96.0	1.80
8	Q_p (L/s)	1.54	1.49	-3.25
	t_p (min)	43	40	-6.98
	V_{out} (L)	3685	3376	-8.39
	R_{TSS_out} (%)	91.5	95.7	4.59

Similar to the surface porosity, the porosity of the sub-surface layer is also expected to vary with time. The calibrated porosities of sub-surface layers along with the operation time were plotted for each layer of each pavement in Figure 5.9. As illustrated in Figure 5.9, the degradation of the porosity of sub-surface layers with the operation time were seen from the calibration results for each type pavement.

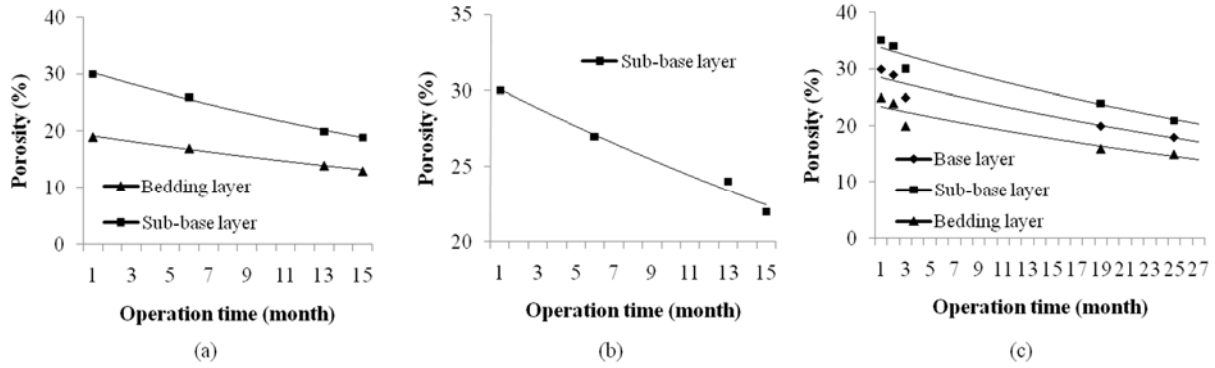

Figure 5.9. Regressions of porosity for various layers with respect to operation time: (a) PA; (b) PC; (c) PICP

Different from the porosity of the surface layer, the porosity of the sub-surface layers is not expected to be largely affected by pressure washing. Thus, the calibrated sub-surface porosity is modeled as an exponential function of time for each sub-surface layer of each pavement. The regression equations from Figure 5.8 are expressed as:

PA: Bedding layer: $P_{bedding} = 19.71e^{-0.02X}$ $R^2 = 0.994$ (5.21a)

Sub-base layer: $P_{sub-base} = 31.29e^{-0.03X}$ $R^2 = 0.996$ (5.21b)

PC: Sub-base layer: $P_{sub-base} = 30.68e^{-0.02X}$ $R^2 = 0.980$ (5.22)

PICP: Bedding layer: $P_{bedding} = 23.81e^{-0.02X}$ $R^2 = 0.898$ (5.23a)

Base layer: $P_{base} = 29.07e^{-0.02X}$ $R^2 = 0.938$ (5.23b)

Sub-base layer: $P_{sub-base} = 34.33e^{-0.01X}$ $R^2 = 0.957$ (5.23c)

The developed regression curves for the sub-surface porosity obtained from the model calibration along with the regression curves for the surface porosity (without adjustments) were used in the model verification (application), as the calibrated model successfully simulated the outflow hydrographs and TSS removal rates in all calibration events.

5.5 Verification and Discussion

Events 3 and 5 were used to verify the calibrated model for PA and PC, while Events 3, 5 and 7 were used to verify the calibrated model for PICP. The surface porosity and porosity of sub-surface layer(s) were determined using the regression equations (Equations 5.16-5.18, 5.21-5.23) according to the field test time of each verification event. The porosities of surface, bedding and sub-base layers of PA are 13.9%, 15.5% and 21.8%, respectively, for Event 3, and 12.5%, 14.9% and 20.5%, respectively, for Event 5. These porosities were then used in the model verification. Figure 5.10 shows the measured and modeled outflow hydrographs of PA. The measured and modeled hydraulic and water quality variables, Q_p, t_p, V_{out}, and R_{TSS_out} along with their errors are shown in Table 5.6. The calculated errors of all hydraulic and water quality variables are all less than 10%. R^2 is 0.835 and 0.879, and *NRMSD* is 14.76% and 14.45% for the two verification events, respectively. These indicate a decent match between the measured and model results. Similarly, a good performance of the model in the model verification can be found from the results for PC and PICP, which are illustrated in Figures 5.11 and Table 5.7, and Figure 5.12 and Table 5.8, respectively. When comparing to PA and PC, the model cannot successfully capture the measured flows at the beginning of hydrographs for PICP. This may be due to the limitation of determining the porosity for PICP surface layer (with a combination of blocks and joint-fill gravel)

by which the porosity change with respect to time cannot be successfully captured, although the monitored parameters (t_p, Q_p, and R_{TSS_out}) are in acceptable errors.

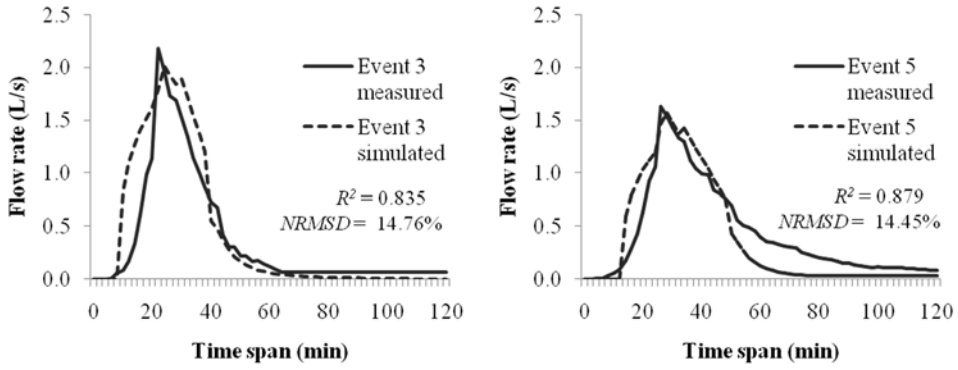

Figure 5.10. Measured and modeled outflow hydrographs for verification events for PA

Table 5.6. Measured and modeled hydraulic and water quality variables for PA in the model verification

Event No.	Parameter	Measured	Simulated	Error (%)
3	Q_p (L/s)	2.18	2.01	-7.80
	t_p (min)	22	24	9.09
	V_{out} (L)	3205	3128	-2.40
	R_{TSS_out} (%)	89.8	94.2	4.90
5	Q_p (L/s)	1.63	1.57	-3.68
	t_p (min)	26	28	7.69
	V_{out} (L)	3348	3200	-4.42
	R_{TSS_out} (%)	90.2	94.6	4.88

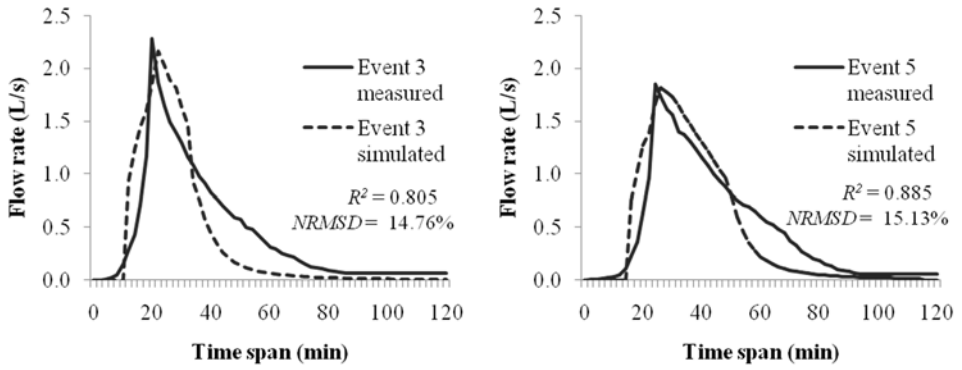

Figure 5.11. Measured and modeled outflow hydrographs for verification events for PC

Table 5.7. Measured and modeled hydraulic and water quality variables for PC in the model verification

Event No.	Parameter	Measured	Simulated	Error (%)
3	Q_p (L/s)	2.28	2.17	-4.82
	t_p (min)	20	22	10.00
	V_{out} (L)	3420	3262	-4.62
	R_{TSS_out} (%)	94.6	85.1	-10.04
5	Q_p (L/s)	1.85	1.820	-1.62
	t_p (min)	24	25	4.17
	V_{out} (L)	3400	3268	-3.88
	R_{TSS_out} (%)	91.0	86.7	-4.73

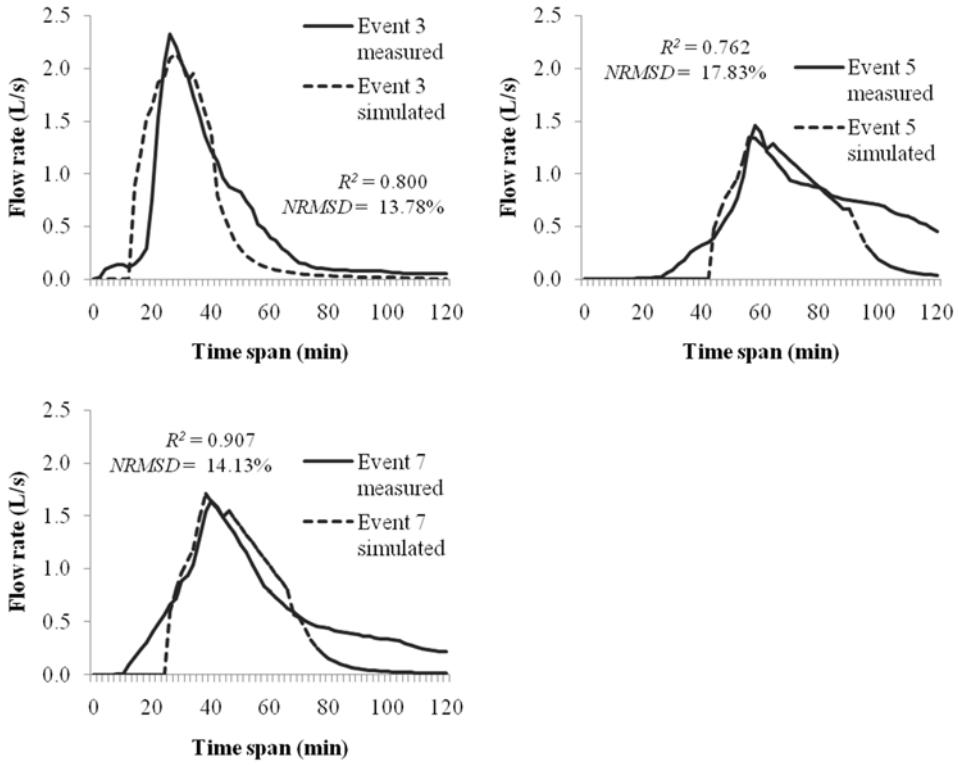

Figure 5.12. Measured and modeled outflow hydrographs for verification events for PICP

Table 5.8. Measured and modeled hydraulic and water quality variables for PICP in the model verification

Event No.	Parameter	Measured	Simulated	Error (%)
3	Q_p (L/s)	2.33	2.14	-8.15
	t_p (min)	26	28	7.69
	V_{out} (L)	3666	3368	-8.13
	R_{TSS_out} (%)	88.6	91.9	3.72
5	Q_p (L/s)	1.46	1.34	-8.22
	t_p (min)	58	56	-3.45
	V_{out} (L)	3695	3310	-10.42
	R_{TSS_out} (%)	90.0	94.0	4.44
7	Q_p (L/s)	1.64	1.71	4.27
	t_p (min)	40	38	-5.00
	V_{out} (L)	3867	3442	-10.99
	R_{TSS_out} (%)	91.5	95.6	4.48

Aside from simulating the hydraulic performance and R_{TSS_out} of the pavements, the proposed model can also predict the amount of TSS retained in different depths of the pavements. Although the retained amount of TSS in different depths cannot be verified through comparing its measurements and modeled results, the good performance in modeling R_{TSS} suggests the retained amounts of TSS modeled in different depths may be realistic. As an example, Figure 5.13 displays the modeled percentage of TSS retained in PC versus the depths (from pavement surface) in Event 3. In the event, the percentage of accumulated TSS retained by PC, namely pollutant removal rate, is approximately 85% but approximately 80% of that TSS was retained in the surface layer. This result suggests that TSS in the inflow was mainly removed by the surface layer of the pavement, which is consistent with findings in the literature (e.g., Balades et al. 1995, Bean et al. 2007).

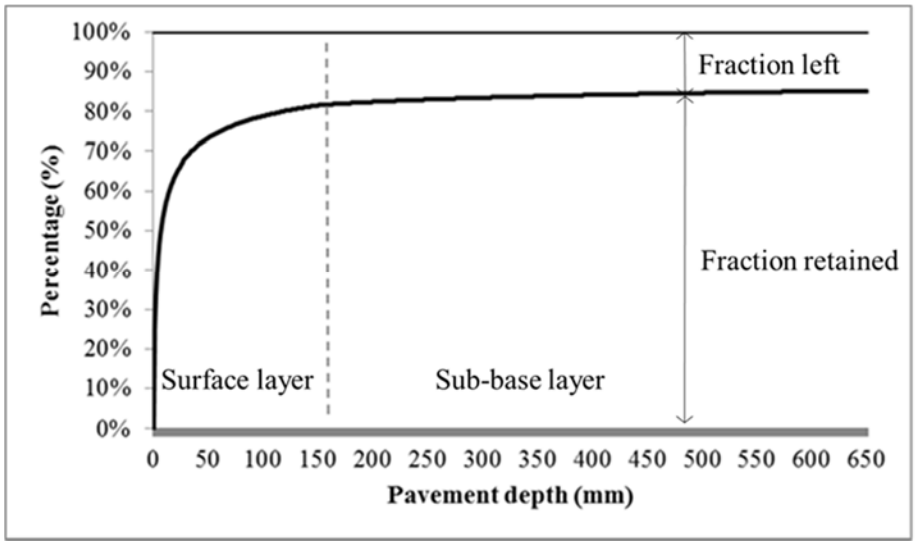

Figure 5.13. Percentage of TSS retained versus depth in PC for event 3

The developed model, which treats both the surface and sub-surface porosities as functions of time, has the capacity to capture the temporal variation of the hydraulic performance of the pavements. As shown in Table 5.1, the change of hydraulic performance in terms of a decrease in Q_p and increase in t_p along with time were, in general, observed from the three field-scale pavements. The role of pressure washing (occurring on May 13, 2013) was not only demonstrated in improving SIR but also in increasing Q_p and shortening t_p for PICP; whereas similar changes in Q_p and t_p were not detected for both PC and PA. The results from the model calibration and verification clearly shows that the proposed model effectively predicted the hydraulic changes, which can be largely attributed to the degradation of porosity of the pavements and/or the restoration of infiltration/porosity of pavement surface layer by pavement maintenance (e.g., pressure washing).

The good performance of the proposed model, which shows that it is capable of capturing the dynamics, does suggest it is applicable for modeling long-term performance of permeable pavements. Both the field observations and the modeling results from this chapter suggest the need to capture the dynamics of pavement performance as the physical properties of the pavements (e.g., porosity) that are subjected to the impact of external factors (e.g., traffic) are not stationary. From this point of view, the proposed model can effectively take the change in porosity resulting from the external factors (e.g., traffic and maintenance – pressure washing in this chapter) into consideration. The model currently applied the field monitored SIR and model calibration process, both of which are site-specific, to establish the functions for modeling the temporal variation of the porosities of surface and sub-surface layers. In general, the physically-based model is needed to capture the temporal variation of the porosities due to the external influential factors including traffic and pavement maintenance activities.

Overall, the proposed model is robust for predicting both hydraulic performance and TSS removal for all three types of permeable pavements. Although the thicknesses of the three pavements are the same (650 mm), the pavement structures are different in terms of surface layer, size of gravel, and thickness of each gravel layer. Regardless of the structural differences in the three pavements, the hydraulic and water quality performance appears to be similar (Table 5.1). Compared to the modeling results for PC and PA, the modeling results for PICP appear not to accurately capture the onset of the outflow hydrograph, as large delays in the modeled onset of outflow hydrograph can be seen in both calibration and verification events for PICP (Figures 8 and 12). Based on the modeling results from this chapter, it can be concluded that both the surface and sub-surface (gravel) layer of PA and PC are well modeled. The sub-surface layer of PICP is similar to those of PA and PC, although the gravels size used and the number of sub-surface layers is different. Thus, the relatively inferior performance of the proposed model for PICP might be due to the surface layer of PICP. The improvement on modeling the surface layer of PICP might help further enhance the model performance for PICP.

The proposed model was demonstrated to be very promising for practical use due to the fact that the model successfully captures the temporal variation of hydraulic performance of the pavements and thus, can be applied for long-term modeling of pavements. However, there are several issues that need to be improved upon for wider use of the proposed model: (1) field measurements of SIR and model calibration are needed to estimate surface and sub-surface porosities, thus a physically-based model for porosity is needed (as discussed previously); (2) field observations from 1:100 year simulated storm events were used to develop the model, thus the verification of the model for other magnitude of storm events is recommended; (3) the mean particle size estimated from PSD was used in the model. Ideally, difference particle sizes should

be taken into consideration. In stormwater management, the required service level for management technologies (such as best management practices and LIDs) is defined in terms of TSS removal rate given a specified particle size range. Therefore, further model verification and improvements are recommended for generalizing the modeling approach.

5.6 Conclusions

This chapter proposed a numerical model for permeable pavements and also proved its applicability by applying it to simulate both hydraulic and water quality (especially TSS) performance of pavements. Three types of permeable pavements: PA, PC and PICP, which are widely used nowadays in urban areas, were modeled. The results, overall, demonstrated very good agreement between field measurements and modeled results for all three types of pavement in terms of hydraulic and water quality variables including peak flow, time to peak, outflow volume and TSS removal rates. More importantly, the proposed model successfully captured the dynamics (temporal variation) of pavement performance by introducing functions to reflect the temporal changes in the porosities in both the surface and sub-surface layers of the pavements, which are resulted from external influential factors (e.g., traffic and maintenance activities). Therefore, the proposed model is very promising but simultaneously very practical in modeling long-term pavement performance and thus, aiding in the engineering design of permeable pavements. On the other hand to generalize the model for wide application, further investigations on several issues are recommended, such as a model for porosity as a function of external influencing factors (e.g., traffic and maintenance activities) rather than field measured SIR is recommended, in addition to verification on other magnitude storm events, and removal of different sizes of particle.

Chapter Six: Conclusions and Recommendations

6.1 General Conclusions

This dissertation aimed to provide knowledge of the hydrologic/hydraulic and water quality performance of permeable pavements in order to justify the feasibility of the use of permeable pavements for improving stormwater management in cold climate conditions, in addition to developing modeling tools to predict the performance of permeable pavements and to aid in the their design. More specifically, this dissertation made contributions in three aspects: (1) investigating and comparing the hydraulic and water quality performance of PA, PC and PICP under extreme storm events and in Calgary's cold climate conditions; (2) evaluating and comparing the ability of pollutant removal by individual layers of pavement structure and investigating the influence of pavement structure on the water quality performance; (3) developing modeling tools for predicting flow and pollutant removal by permeable pavements. The general conclusions obtained for each aspect are summarized as follows:

(1) Hydraulic and water quality performance of permeable pavements under cold climates: Storm runoff mitigation, surface infiltration capacity and pollutant removal were examined on field-scale PA, PC and PICP in the southwest of Calgary from 2011 to 2013. The infiltration data indicated that SIR of the three pavements degraded significantly along with time, especially due to the application of sanding materials during winter time. Among the three investigated permeable pavements, PC was found to be superior in terms of surface infiltration capacity. Pressure washing was proved to be an effective maintenance activity to restore SIR. The three pavements performed acceptably from hydraulic perspective and yielded little to no surface

ponding under 1:100 year design storms during Chinooks in winter times. They also proved their capability to attenuate peak flow and delay in time to peak from the outflow.

Regarding water quality performance, the three pavements effectively removed TSS, TP and heavy metals including Cu, Pb and Zn, under both winter and non-winter conditions. The observed removal rates for the above pollutants were approximately 70% and higher. Similar variation patterns were found between removal rates of TSS and those of TP and heavy metals. These finding suggests that TP and heavy metals are likely removed with TSS by physical process. The removal rates of TN were 30% on average and the low removal rates might be ascribed to the pavement age and climatic conditions such as pavement temperature, which is dependent on environment temperature. The different performance between TN and other examined pollutants implies that removal of TN might be governed by a different process.

(2) Water quality treatment efficacy by pavement structure: Laboratory experiments were conducted to evaluate the removal of TSS, TP and TN, and outflow PSD by surface layers and gravel layers with various thicknesses. The surface layers of three types of permeable pavements (PA, PC and PICP) were investigated in this study. The results show that PA and PICP surfaces have equivalent performance in removing TSS, TP and TN due to the same thickness (80 mm); while the superior performance of the PC surface layer is likely due to its greater thickness (150 mm) compared to PA and PICP.

Regarding the gravel layers, gravel sizes of 63 mm, 40 mm and 12 mm, which are typically used in permeable pavements, were used. Given a gravel size, the dependence of the pollutant removal efficiency on the thicknesses of gravel layers was found. When given a thickness of a gravel layer, smaller gravel yielded higher TSS and TP removal rates, which suggests that smaller

gravel is preferred from a water quality perspective. The TP removal rate was also strongly associated with the TSS removal rate. The TN removal rate appears more or less constant and thus, to be independent of gravel size. According to the PSD analysis, no significance difference in PSD was found among the surface layers of three pavements; whereas significant difference was found in the gravel layers with respect to gravel size and thickness.

A comparison of pollutant removal between the lab-scale and field-scale pavements with the same pavement structure was conducted. Equivalent performance was observed in terms of the TSS and TP removal; however, higher TN removal rates were found in the field–scale pavements. The difference in the TN removal rates between the lab-scale and field-scale pavements might be due to the different ages of the pavements. It is suspected that the removal of TN is likely associated with the biofilm in the pavements, which might be dependent on the age of the pavements. The results support that TP is removed along with TSS and TN is removed separately from TSS.

Based on the observations from the laboratory experiments, a mathematical model was proposed to predict the removal rates of TSS and TP when given a pavement structure. The model showed good performance in predicting the removal rates of TSS and TP through comparing the model predictions with the field measurements from field-scale pavements (prediction error < 5%). Therefore, the model can be a useful tool for assisting in the design and optimization of pavement structure considering water quality performance of permeable pavements.

(3) Permeable pavement modeling: In order to provide in-depth information on water movement and sediment removal through permeable pavement structure, a conceptual model was proposed. The proposed model is based on modified Kozeny-Carman equation and Yao equation,

which are solved using finite difference approximation. Original Kozeny-Carman equation is used in saturated flow and thus, a modified version of the equation was used in permeable pavement where flow movement is primarily unsaturated in the upper gravel layers. Data collected from the field experiments were used to calibrate and validate the model for PA, PC and PICP, respectively. A regression model for surface porosity of the three pavements was developed based on the measured SIR data from the field experiments. Good agreements were obtained between the measured data and model results in both model calibration and validation. Several variables including outflow hydrograph, peak flow, time to peak, runoff volume and TSS removal rate were used to evaluate the model performance. Water quality information such as TSS removal along the pavement structure and the major removal mechanism were able to obtain from the model. The modeling results suggest that the proposed model can be a practical and useful tool in simulating the hydraulic and water quality performance, and therefore aiding in the design and optimization of pavement structure. The limitations of the conceptual model lie in that: (1) the developed model was calibrated and verified based on site-specific observations collected in the thesis; thus further validation of the model is required using data sets collected from different magnitude storm events and other sites; and (2) it is assumed that flow is saturated in the modeling process, while the flow, especially at the beginning of a storm event, in the payment is primarily unsaturated.

6.2 Novel Contributions

In conclusion, the dissertation provides comprehensive information on the applicability of permeable pavement in Calgary's special climatic conditions that include cold dry weather and Chinooks. It also provides fundamental but very important knowledge of the linkage between water quality performance and pavement structure. In addition, the proposed modeling tools can be very useful in designing and optimizing permeable pavements considering their performance. The novel contribution of this dissertation is summarized as follows:

(1) Provided comprehensive knowledge on the performance of PA, PC and PICP under pollutant loadings and extreme storm events relevant to cold regions in Canada.

(2) Identified the role of three types of permeable pavements on the removal of various pollutants including TSS, TP, TN, Pb, Cu and Zn, and the different removal mechanisms associated with the pollutants.

(3) Observed the strong association between TP removal and TSS removal and the significant role of pavement temperature and age on TN removal.

(4) Evaluated the variations of outflow PSD and treatment efficiency of TSS, TP and TN by individual layers of pavement structure with various surface layers, gravel thicknesses, and gravel sizes.

(5) Developed both regression and numerical modeling tools to predict the performance of permeable pavement and aid in the design and optimization of pavement structure.

(6) Demonstrated the applicability of permeable pavement under cold climate conditions.

6.3 Recommendations for Future Research

Based on the research results, several further investigations are recommended:

(1) Removal rates of TN were suspected to be related to pavement temperature and to be likely dependent on pavement age. The removal of TN is different from TSS and TP removal. In order to understand the mechanisms controlling TN removal, further study focusing on the role of bio-film and the removal of different forms of nitrogen (e.g., N-NO^{3-}, N-NH_3) forms, as well as the organic content that potentially indicates the existence of biofilm, is suggested.

(2) Without maintenance (such as pressure washing), SIR was observed to continuously decrease. It will be required to continuously monitor SIR to determine maintenance frequency based on long term SIR data.

(3) After the permeable pavements were put into performance in this study, their surface porosity was determined by regression analysis assuming they were logarithmically linear to the observed SIR. In order to more precisely determine the surface porosity, further research on the relationship between SIR and surface porosity for permeable pavement is recommended.

(4) In this dissertation, the conceptual model was calibrated using available field data measured in simulated 1:100 year storm events, which was selected as the design storm for designing permeable pavements in the City of Calgary. However, lower magnitude storms occur more frequently. The frequent storm events in Calgary are typically under 5 mm (The City of Calgary, 2011). The pavements should also perform acceptably in more frequent and smaller storm events. As this thesis has been focused on infrequent

event, 1:100 storm event, the validation of the developed model using small events is needed to generalize the developed model for permeable pavements.

(5) Many stormwater management technologies (including permeable pavements) are required to provide service to remove a minimum of 85% TSS with particle sizes larger than 50 μm, for example. The proposed conceptual model however does not have the function to predict the PSD yet. Therefore, further improvement on the conceptual model to include PSD is recommended.

(6) When designing permeable pavement, the pavement structure should be designed to satisfy the requirements for structural purpose (e.g., traffic loading) and hydraulic and water quality performance. In such a design, further study on how to determine optimal structure along with initial SIR is needed in order to minimize potential structure issue caused by infiltrated water content during winter time (e.g., frost heave).

References

Abbott, C. L., and Comino-Mateos, L. (2003). "In-situ hydraulic performance of a permeable pavement sustainable urban drainage system." *Water Environ. J.,* 17(3), 187-190.

Al-Rubaei, A. M., Stenglein, A. L., Viklander, M., and Blecken, G. T. (2013). "Long-term hydraulic performance of porous asphalt pavements in northern Sweden." *J. Irrig. Drain. Eng.*, 139(6), 499-505.

Al-Rousan, T., Masad, E., Myers, L., and Speigelman, C. (2005). "New methodology for shape classification of aggregates." *Journal of the Transportation Research Board*, 11-23.

Arnold Jr, C. L., and Gibbons, C. J. (1996). "Impervious surface coverage: the emergence of a key environmental indicator." *J. Am. Plann. Assoc.*, 62(2), 243-258.

Andral M. C., Roger S., Montrejaud-Vignoles, M., and Herremans L. (1999). "Particle size distribution and hydrodynamic characteristics of solid matter carried by runoff from motorways." *Water Environ. Res.*, 71(4), 398-407.

APHA (1998). Standard methods for the examination of water and wastewater. 20th Edition. Published jointly by the American Public Health Association, American Water Works Association, and Water Environment Federation. Washington, D.C.

Balades, J., Legret, M., and Madiec, H. (1995). "Permeable pavements: pollution management tools." *Water Sci. Technol.*, 32(1), 49-56.

Ball, J., and Rankin, K. (2010). "The hydrological performance of a permeable pavement." *Urban Water J.*, 7(2), 79-90.

Barnes, K. B., Morgan, J., and Roberge, M. (2001). *Impervious surfaces and the quality of natural and built environments*. Thesis (M.Sc). Department of Geography and Environmental Planning, Towson University, Baltimore, USA.

Bean, E.Z. (2005). *A field study to evaluate permeable pavement surface infiltration rates, runoff quantity, runoff quality, and exfiltrate quality*. Thesis (M.Sc). North Carolina State University, Raleigh, USA.

Bean, E. Z., Hunt, W. D., and Bidelspach, D. A. (2004). "Study on the surface infiltration rate of permeable pavements." *Proc., 2004 World Water and Environmental Resources Congress: Critical Transitions in Water and Environmental Resources Management,* ASCE Environmental and Water Resources Institute (EWRI), Reston, Va., 749–758.

Bean, E. Z., Hunt, W. F., and Bidelspach, D. A. (2007a). "Field survey of permeable pavement surface infiltration rates." *J. Irrig. Drain. Eng.*, 133(3), 249-255.

Bean, E. Z., Hunt, W. F., and Bidelspach, D. A. (2007b). "Evaluation of four permeable pavement sites in eastern North Carolina for runoff reduction and water quality impacts." *J. Irrig. Drain. Eng.*, 133(6), 583-592.

Booth, D. B., and Leavitt, J. (1999). "Field evaluation of permeable pavement systems for improved stormwater management." *J. Am. Plann. Assoc.*, 65(3), 314-325.

Brabec, E. (2002). "Impervious surfaces and water quality: a review of current literature and its implications for watershed planning." *J. Plan. Lit.*, 16(4), 499-514.

Brattebo, B. O., and Booth, D. B. (2003). "Long-term stormwater quantity and quality performance of permeable pavement systems." *Water Res.*, 37(18), 4369-4376.

Brown, C. (2007). *Characterization of solids removal and clogging processes in two types of permeable pavement.* Thesis (M.Sc). University of Calgary, Calgary, Canada.

Brown, C., Chu, A., Van Duin, B., and Valeo, C. (2009). "Characteristics of sediment removal in two types of permeable pavement." *Water Qual. Res. J. Can.*, 44(1), 59-70.

Brown, R., Line, D., and Hunt, W. (2011). "LID treatment train: Pervious concrete with subsurface storage in series with bio-retention and care with seasonal high water tables." *J. Environ. Eng.*, 138(6), 689-697.

Chai, L., Kayhanian, M., Givens, B., Harvey, J. T., and Jones, D. (2012). "Hydraulic performance of fully permeable highway shoulder for storm water runoff management." *J. Environ. Eng.*, 138(7), 711-722.

Collins, K. A., Hunt, W. F., and Hathaway, J. M. (2008). "Hydrologic comparison of four types of permeable pavement and standard asphalt in eastern North Carolina." *J. Hydrol. Eng.*, 13(12), 1146-1157.

Collins, K. A., Hunt, W. F., and Hathaway, J. M. (2009). "Side-by-side comparison of nitrogen species removal for four types of permeable pavement and standard asphalt in eastern North Carolina." *J. Hydrol. Eng.*, 15(6), 512-521.

Davies, J. W., Pratt, C. J., and Scott, M. A. (2002). "Laboratory study of permeable pavement systems to support hydraulic modelling." *Proc. 9th Int. Conf. on Urban Drainage*, Portland, USA, 1-9.

Deo, O., Sumanasooriya, M., and Neithalath, N. (2010). "Permeability reduction in pervious concretes due to clogging: experiments and modeling." *J. Mater. Civ. Eng.*, 22(7), 741-751.

Dierkes, C., Kuhlmann, L., Kandasamy, J., and Angelis, G. (2002). "Pollution retention capability and maintenance of permeable pavements." *Proc. of the Ninth Int. Conf. on Urban Drainage: Global Solutions for Urban Drainage,* Portland, USA.

Dietz, M. E. (2007). "Low impact development practices: A review of current research and recommendations for future directions." *Water Air Soil Pollut*., 186(1-4), 351-363.

Dougherty, M., Hein, M., Martina, B. A., and Ferguson, B. K. (2010). "Quick surface infiltration test to assess maintenance needs on small pervious concrete sites." *J. Irrig. Drain. Eng.*, 137(8), 553-563.

Drake, J. A. P., Bradford, A., and Marsalek, J. (2013). "Review of environmental performance of permeable pavement systems: state of the knowledge." *Water Qual. Res. J. Can.,* 48(3), 203-222.

Dreelin, E. A., Fowler, L., and Ronald Carroll, C. (2006). "A test of porous pavement effectiveness on clay soils during natural storm events." *Water Res.*, 40(4), 799-805.

Eck, B. J., Winston, R. J., Hunt, W. F., and Barrett, M. E. (2011a). "Water quality of drainage from permeable friction course." *J. Environ. Eng.*, 138(2), 174-181.

Eck, B. J., Barrett, M. E., and Charbeneau, R. J. (2011b). "Coupled surface-subsurface model for simulating drainage from permeable friction course highways." *J. Hydraul. Eng.*, 138(1), 13-22.

Ellis, J. B., Revitt, D. M., and Lundy, L. (2012). "An impact assessment methodology for urban surface runoff quality following best practice treatment." *Sci. Total Environ.*, 416, 172-179.

Elliott, A. H., and Trowsdale S. A. (2007). "A review of models for low impact urban stormwater drainage." *Environ. Modell. Software*, 22, 394-405.

Fach, S., and Geiger, W. (2005). "Effective pollutant retention capacity of permeable pavements for infiltrated road runoffs determined by laboratory tests." *Water Sci. Technol.,* 51(2), 37-46.

Fassman, E. A., and Blackbourn, S. (2010). "Urban runoff mitigation by a permeable pavement system over impermeable soils." *J. Hydrol. Eng.*, 15(6), 475-485.

Ferguson, B. K. (1993). *Porous Pavements.* CRC Press, Boca Raton, USA.

Finkenbine, J., Atwater, J., and Mavinic, D. (2000). "Stream health after urbanization." *J. Am. Water Resour. Assoc*., 36(5), 1149-1160.

Gerrits, C. (2001). *Restoration of infiltration capacity of permeable pavers*. Thesis (MSc). University of Guelph, Guelph, Canada.

Gilbert, J. K., and Clausen, J. C. (2006). "Stormwater runoff quality and quantity from asphalt, paver, and crushed stone driveways in Connecticut." *Water Res.*, 40(4), 826-832.

Gonzalez-Angullo, N., Castro, D., Rodriguez-Hernandez, J., and Davies, J. (2008). "Runoff infiltration to permeable paving in clogged conditions." *Urban Water J.*, 5(2), 117-124.

Hatt, B. E., Fletcher, T. D., and Deletic, A. (2007). "Treatment performance of gravel filter media: implications for design and application of stormwater infiltration systems." *Water Res.*, 41(12), 2513-2524.

He, J., Huang, J., Valeo, C., and Chu, A. (2015). "Modeling water quality treatment efficacy of porous concrete pavement." *J. Water Resour. & Hydraul. Eng.*, accepted and to be published.

Hein, D. K., Swan, D. J., and Schaus, L. (2010). "Structural and hydrological design of permeable pavements." 2010 annual conference of the transportation association of Canada, Halifax, Canada.

Huang, J., Valeo, C., He, J., and Chu, A. (2012). "Winter performance of inter-locking pavers - stormwater quantity and quality." *Water*, 4(4), 995-1008.

Huang, J., Valeo, C., He, J., and Chu, A (2015a). "Three types of permeable pavements in cold climates: hydraulic and environmental performance." *J. Environ. Eng.*, in press.

Huang, J., Valeo, C., He, J., and Chu, A (2015b). "The influence of design parameters on stormwater pollutant removal in permeable pavements." *J. Hydrol. Eng.*, submitted for review.

Illgen, M., Schmitt, T. G., Welker, A., and Harting, K. (2007). "Runoff and Infiltration characteristics of permeable pavements - review of an intensive monitoring program." *Water Sci. Technol.*, 56(10), 133-40.

Imran, H. M., Shatirah, A., and Mohamed, R. K. (2013). "Permeable pavement and stormwater management systems: a review." *Environ. Technol.,* 34(18), 2649-2656.

Ismail, A., Hamzah, M. O., and Rashid, M. A. (2012). "Review of permeable pavement systems in Malaysia conditions." *OIDA International Journal of Sustainable Development*, 4(2), 27-36.

Jacobson, C. R. (2011). "Identification and quantification of the hydrological impacts of imperviousness in urban catchments: A review." *J. Environ. Manage.*, 92(6), 1438-1448.

James, W., and Langsdorff, H. (2003). "The use of permeable concrete block pavement in controlling environmental stressors in urban areas." 7th international conference on concrete block paving, Sun City, South Africa.

Kayhanian, M., McKenzie, E., Leatherbarrow, J., and Young, T. (2012). "Characteristics of road sediment fractionated particles captured from paved surfaces, surface run-off and detention basins." *Sci. Total Environ*., 439, 172-186.

Kuang, X., Sansalone, J., Ying, G., and Ranieri, V. (2011). "Pore-structure models of hydraulic conductivity for permeable pavement." *J. Hydrol.*, 399(3), 148-157.

Kuba, T., Smolders, G., Van Loosdrecht, M., and Heijnen, J. (1993). "Biological phosphorus removal from wastewater by anaerobic-anoxic sequencing batch reactor." *Wat. Sci. Tech.*, 27(5-6), 241-252.

LeFevre, N. J. B., Watkins Jr, D. W., Gierke, J. S., and Brophy-Price, J. (2009). "Hydrologic performance monitoring of an under-drained low-impact development storm-water management system." *J. Irrig. Drain. Eng.*, 136(5), 333-339.

Lee, J. H., and Bang, K. W. (2000). "Characterization of urban stormwater runoff." *Water Res.*, 34(6), 1773-1780.

Legret, M., and Colandini, V. (1999). "Effects of a porous pavement with reservoir structure on runoff water: water quality and fate of heavy metals." *Water Sci. Technol.*, 39(2), 111-117.

Legret, M., Colandini, V., and Le Marc, C. (1996). "Effects of a porous pavement with reservoir structure on the quality of runoff water and soil." *Sci. Total Environ.*, 189, 335-340.

Legret, M., and Pagotto, C. (1999). "Evaluation of pollutant loadings in the runoff waters from a major rural highway." *Sci. Total Environ.*, 235, 143-150.

Lucke, T., and Beecham, S. (2011). "Field investigation of clogging in a permeable pavement system." *Build. Res. Inf.*, 39(6), 603-615.

Macdonald, I., El-Sayed, M., Mow, K., and Dullien, F. (1979). "Flow through porous media-the Ergun equation revisited." *Ind. Eng. Chem. Fundam.*, 18(3), 199-208.

Marzulli, P., and Trigiante, D. (1995). "Stability and convergence of boundary value methods for solving ODE." *J. Differ. Equ. Appl.*, 1(1), 45-55.

McDowell-Boyer, L. M., Hunt, J. R., and Sitar, N. (1986). "Particle transport through porous media." *Water Resour. Res.*, 22(13), 1901-1912.

Montes, F., and Haselbach, L. (2006). "Measuring hydraulic conductivity in pervious concrete." *Environ. Eng. Sci.*, 23(6), 960-969.

Napier, F., D'Arcy, B., and Jefferies, C. (2008). "A review of vehicle related metals and polycyclic aromatic hydrocarbons in the UK environment." *Desalin.*, 226(1), 143-150.

Newman, A., Pratt, C., Coupe, S., and Cresswell, N. (2002). "Oil bio-degradation in permeable pavements by microbial communities." *Water Sci. Technol*., 45(7), 51-56.

New Jersey Department of Environmental Protection (2004). "New Jersey stormwater best management practises manual." Trenton, USA.

Pagotto, C., Legret, M., and Le Cloirec, P. (2000). "Comparison of the hydraulic behaviour and the quality of highway runoff water according to the type of pavement." *Water Res.*, 34(18), 4446-4454.

Pennsylvania Department of Environmental Protection. (2006). "Pennsylvania stormwater best management practices manual." Pennsylvania, USA.

Pezzaniti, D., Beecham, S., and Kandasamy, J. (2009). "Influence of clogging on the effective life of permeable pavements." *Water Management*, 162(3), 211-220.

Pratt, C. (1995). "A review of source control of urban stormwater runoff." *Water Environ. Manage.*, 9(2), 132-139.

Pratt, C., Mantle, J., and Schofield, P. (1995). "UK research into the performance of permeable pavement, reservoir structures in controlling stormwater discharge quantity and quality." *Water Sci. Technol.,* 32(1), 63-69.

Roger, S., Montrejaud-Vignoles, M., Andral, M. C., Herremans, L., and Fortune, J. P. (1998). "Mineral physical and chemical analysis of the solid matter carried by motorway runoff water." *Water Res.*, 32(4), 1119-1125.

Roseen, R. M., Ballestero, T. P., Houle, J. J., Briggs, J. F., and Houle, K. M. (2011). "Water quality and hydrologic performance of a porous asphalt pavement as a storm-water treatment strategy in a cold climate." *J. Environ. Eng.*, 138(1), 81-89.

Rushton, B. T. (2001). "Low-impact parking lot design reduces runoff and pollutant loads." *J. Water Resour. Plann. Manage.,* 127(3), 172-179.

Sansalone, J. J., and Buchberger, S. G. (1995). "An infiltration device as a best management practice for immobilizing heavy metals in urban highway runoff." *Water Sci. Technol.*, 32(1), 119-125.

Sansalone, J., Kuang, X., and Ranieri, V. (2008). "Permeable pavement as a hydraulic and filtration interface for urban drainage." *J. Irrig. Drain. Eng.*, 134(5), 666-674.

Sartor, J., Boyd, G. B., and Agardy, F. J. (1974). "Water pollution aspects of street surface contaminants." *Res. J. Water Pollut. C.*, 46(3), 458-465.

Schluter, W., and Jefferies, C. (2002). "Modelling the outflow from a porous pavement." *Urban Water*, 4(3), 245-253.

Scholz, M., and Grabowiecki, P. (2007). "Review of permeable pavement systems." *Build. Environ.*, 42(11), 3830-3836.

Shuster, W. D., Bonta, J., Thurston, H., Warnemuende, E., and Smith, D. R. (2005). "Impacts of impervious surface on watershed hydrology: a review." *Urban Water J.*, 4(2), 263-275.

Siriwardene, N. R., Deletic, A., and Fletcher, T. D. (2007). "Modeling of sediment transport through stormwater gravel filters over their lifespan." *Environ. Sci. Technol.*, 41(23), 8099-8103.

Stotz, G., and Krauth, K. (1994). "The pollution of effluents from pervious pavements of an experimental highway section: first results." *Sci. Total Environ.*, 146, 465-470.

Tan, S., Fwa, T., and Han, C. (2003). "Clogging evaluation of permeable bases." *J. Transp. Eng.*, 129(3), 309-315.

Teng, Z., and Sansalone, J. (2004). "In situ partial exfiltration of rainfall runoff. II: Particle separation." *J. Environ. Eng.*, 130(9), 1008-1020.

The City of Calgary. (2011). "Stormwater management and design manual." Calgary, Canada.

The City of Portland. (2014). "Portland stormwater management manual." Portland, USA.

Toronto and Region Conservation Authority. (2010). "Low impact development stormwater management planning and design guide." Ontario, Canada.

Tota-Maharaj, K., and Scholz, M. (2010). "Efficiency of permeable pavement systems for the removal of urban runoff pollutants under varying environmental conditions." *Environ. Prog. Sustainable Energy*, 29(3), 358-369.

Tuccillo, M. E. (2006). "Size fractionation of metals in runoff from residential and highway storm sewers." *Sci. Total Environ.*, 355, 288-300.

Tufenkji, N., and Elimelech, M. (2004). "Correlation equation for predicting single-collector efficiency in physicochemical filtration in saturated porous media." *Environ. Sci. Technol.*, 38(2), 529-536.

Urbonas, B. R. (1999). "Design of a sand filter for stormwater quality enhancement." *Water Environ. Res.*, 102-113.

Watanabe, S. (1995). "Study on storm water control by permeable pavement and infiltration pipes." *Water Sci. Technol.*, 32(1), 25-32.

Welker, A. L., Jenkins, J. K. G., McCarthy, L., and Nemirovsky, E. (2012). "Examination of the material found in the pore spaces of two permeable pavements." *J. Irrig. Drain. Eng.*, 139(4), 278-284.

Wiesmann, U. (1994). "Biological nitrogen removal from wastewater." *Adv. Bioch. Eng. Biotechnol*, 51, 113-154.

Winter, J., and Duthie, H. (1998). "Effects of urbanization on water quality, periphyton and invertebrate communities in a southern Ontario stream." *Can. Water Resour. J.*, 23(3), 245-257.

Watanabe, S. (1995). “Study on storm water control by permeable pavement and infiltration pipes.” *Water Sci. Technol.*, 32(1), 25-32.

Wong, T. H., Fletcher, T. D., Duncan, H. P., and Jenkins, G. A. (2006). “Modelling urban stormwater treatment - a unified approach.” *Ecol. Eng*., 27(1), 58-70.

Wu,Y. (1994). “An analysis of constant-pressure filtration.” *Chem. Eng. Sci.*, 49(6), 831-836.

Wu, F. C., and Huang, H. T. (2000). “Hydraulic resistance induced by deposition of sediment in porous medium.” *J. Hydraul. Eng.*, 126(7), 547-551.

Yao, K. M. (1968). *Influence of suspended particle size on the transport aspect of water filtration*. Thesis (Ph.D). University of North Carolina, Chapel Hill, USA.

Yao, K. M., Habibian, M. T., and O'Melia, C. R. (1971). “Water and waste water filtration: concepts and applications.” *Environ. Sci. Technol.*, 5(11), 1105-1112.

Yong, C., McCarthy, D., and Deletic, A. (2013). “Predicting physical clogging of porous and permeable pavements.” *J. Hydrol.*, 481, 48-55.

Zhu, Y., Fox, P. J., and Morris, J. P. (1999). “A pore-scale numerical model for flow through porous media.” *Int. J. Numer. Anal. Met.*, *23*(9), 881-904.

Appendix A: Raw Data for Field Experiments

SIR data for PA, PC and PICP (unit in mm/hr):

PA																		
2012-10-12	36000	28800	28800	36000	32000	33179.72	48000	36000	48000	40793.2	24784.85	20483.64	48000	24365.48	19591.84	48000	32000	27118.64
	31200			33726.57			44000			28687.23			30652.44			35706.21		
	43767.42																	
2012-11-06	14007.78	12193.06	14876.03	16382.25	17328.52	15205.91	13079.02	14048.78	13321	15789.47	14574.9	13994.17	10352.26	10843.37	11575.56	8510.638	9436.435	9580.838
	11980.03			15126.05			11659.92			13623.46			11347.52			9290.323		
	13264.23			16010.68			13027.18			14495.5			11029.68			9204.559		
	16991.57																	
2012-12-06	10730.25	8944.099	9670.92	8861.538	9657.948	8372.093	10027.86	9424.084	9356.725	8785.845	7615.019	7189.216	5792.438	6212.252	5491.991	5146.533	5401.35	4780.876
	10076.98			8561.237			8988.764			7411.22			5458.681			5050.859		
	9855.562			8863.204			9449.357			7750.325			5738.84			5094.905		
	11474.68																	
2013-01-07	5899.222	5108.194	4670.775	7160.617	7838.868	7350.689	5010.438	4433.498	4167.873	7868.852	7298.53	7492.196	4554.08	4201.926	4010.025	4137.931	4010.025	3837.953
	4824.121			6651.27			4234.049			6834.362			4241.532			3908.795		
	5125.578			7250.361			4461.464			7373.485			4251.891			3973.676		
	5988.788																	
2013-02-25	1806.549	1763.841	1710.011	1850.186	1687.17	1445.928	2177.858	2065.108	1978.837	3212.135	2975.207	2792.863	2471.679	2347.954	2250.703	2335.766	2089.379	1940.962
	1679.104			1421.24			1893.74			2705.75			2128.603			1883.83		
	1739.876			1601.131			2028.886			2921.488			2299.735			2062.485		
	2100.872																	
2013-04-01	1122.544	1061.086	979.8585	1465.052	1387.016	1335.188	1305.767	1255.668	1214.985	1896.484	1729.107	1651.755	1810.865	1731.185	1635.806	1543.739	1514.036	1455.428
	1013.585			1296.48			1196.908			1622.901			1606.605			1413.705		
	1044.268			1370.934			1243.332			1725.062			1696.115			1481.727		
	1318.621																	
2013-05-01	544.5676	506.1867	481.1065	870.2484	802.8098	753.0199	515.2426	460.8442	425.1927	775.1103	729.3724	707.9298	971.3322	932.8237	860.3178	1216.627	1297.999	1158.022
	510.6203			808.6927			467.0932			737.4709			921.4913			1224.216		
	725.6701																	
2013-05-13	12653.78	11285.27	10534.02	11603.55	9815.951	9079.445	13521.13	12339.33	10851.54	14574.9	16822.43	16609	14589.67	15368.2	14663.95	9683.927	10084.03	9555.408
Pressure Wash																		
	11491.02			10166.31			12237.33			16002.11			14873.94			9774.456		
	12424.2																	
2013-08-16	9849.521	9189.534	8933.002	8290.155	7995.558	7855.974	7104.095	6880.076	6682.135	8071.749	7834.603	7610.994	8791.209	8455.666	8256.881	8977.556	8386.721	8080.808
	8455.666			7610.994			6596.427			7449.56			7775.378			7977.839		
	9106.931			7938.17			6815.683			7741.726			8319.783			8355.731		
	8046.338																	
2013-09-21	7468.88	7515.658	7174.888	6560.364	6814.955	6440.072	6936.416	6566.347	6542.481	6492.335	6266.319	6093.948	6539.51	6083.65	5918.619	6492.335	6241.873	6055.509
	6946.454			6324.111			6363.235			5935.697			5723.37			5773.857		
	7276.47			6534.875			6602.12			6197.075			6066.287			6140.894		
	6469.62																	
2013-10-09	5263.158	5110.007	4765.056	4265.403	4071.247	3903.497	5487.805	5236.364	5115.453	5020.921	4774.536	4605.053	5240.175	5122.732	4926.445	5718.824	5460.751	5215.502
	4642.166			3724.78			4906.303			4379.562			4864.865			4991.334		
	4945.097			3991.232			5186.481			4695.018			5038.554			5346.603		
	4867.164																	
2013-11-08	1271.972	1122.282	1063.83	1463.861	1394.538	1305.649	1814.516	1729.522	1689.15	1595.214	1529.312	1388.621	2106.187	1962.923	1816.118	1271.299	1225.949	1148.417
	937.9274			1266.268			1621.256			1329.272			1690.935			1094.391		
	1099.003			1357.579			1713.611			1460.605			1894.041			1185.014		
	1451.642																	
2013-12-17	642.3696	606.6478	586.009	781.462	725.5505	701.2418	970.612	909.2057	831.2168	608.0054	571.7235	540.7232	708.8009	645.1902	621.5738	713.295	684.2155	653.3872
	568.2042			676.7553			797.8723			532.8202			603.3941			638.9493		
	600.8077			721.2524			877.2267			563.3181			644.7398			672.4618		
	679.9677																	

PICP																			
2011-10-17	11312	12765.96	13138.69	7792.208	6617.647	7500	7142.857	6122.449	6428.571	8144.796	7964.602	9574.468	3082.192	3278.689	2843.602	6545.455	7531.381	8071.749
	12408.47			7303.285			6564.626			8561.289			3068.161			7382.861		
	7548.115																	
2011-12-20	543.8066	649.8195	584.4156	328.4672	287.0813	309.2784	627.1777	526.3158	569.6203	434.7826	521.7391	566.0377	291.2621	300	285.7143	789.4737	829.4931	762.7119
	592.6806			308.2756			574.3712			507.5198			292.3255			793.8929		
	511.5109																	
2012-01-25	266.6667	278.6378	275.6508	186.9159	172.7447	182.1862	436.8932	443.3498	417.6334	285.2615	272.3147	281.25	254.5969	239.3617	242.5876	332.7172	338.3459	316.3445
	273.6518			180.6156			432.6255			279.6087			245.5154			329.1358		
	290.1921																	
2012-03-15	447.7612	390.4555	382.1656	183.2994	169.1729	179.6407	507.0423	485.1752	458.0153	489.1304	547.1125	543.8066	448.8778	414.7465	436.8932	608.1081	582.5243	664.2066
	279.4056			177.371			390.6194			526.6832			433.5059			618.2797		
2012-08-21	266.6667	413.7931	344.4976	786.8852	282.3529	209.3023	309.6774	110.176	69.83511	231.5113	122.0339	55.13017	424.7788	152.0591	84.30913	685.7143	375.9791	337.2365
	152.8662	102.5641		127.2085												204.8364		
	235.5647			351.4372			163.2295			136.2251			220.3823			400.9416		
	390.4442																	
2012-10-19	267.1614	338.0282	202.8169	452.8302	286.2823	157.8947	223.9502	174.9696	119.5021	202.2472	171.6329	144.8692	293.279	238.4106	171.4286	445.8204	243.2432	221.8798
	225.3521			174.7573			87.91209			110.6841			130.6715			211.1437		
	258.3396			267.9411			151.5835			157.3583			208.4474			280.5218		
	216.5358																	
2012-12-06	388.1402	299.3763	222.5657	293.279	196.7213	171.6329	171.0214	155.1724	153.0287	140.7625	165.3272	119.7007	243.2432	202.8169	178.882	243.6548	194.8579	177.1218
	196.7213			110.6841			140.625			87.80488			157.0338			208.0925		
	276.7009			193.0793			154.9619			128.3988			195.494			205.9317		
	210.7416																	
2013-01-07	305.7325	285.7143	262.7737	231.8841	206.0086	171.8377	272.2117	235.6792	208.0925	125.9843	111.3689	100.2088	208.3936	183.908	172.043	218.5129	238.806	222.5657
	247.4227			156.013			194.0701			83.38159			156.3518			207.1942		
	275.4108			191.4358			227.5134			105.2359			180.1741			221.7697		
	189.8302																	
2013-02-25	267.658	246.9983	238.806	242.8331	211.1437	202.5316	175.3959	167.0534	163.0804	140.2142	127.6596	121.519	169.6113	159.4684	156.1822	197.5309	186.7704	171.8377
	225.3521			184.379			169.6113			110.4294			149.8439			181.3602		
	244.7036			210.2218			168.7852			124.9556			158.7765			184.3748		
	189.273																	
2013-04-01	238.806	215.2466	199.7226	213.9673	199.7226	195.122	152.0591	155.6757	147.9959	172.2488	156.3518	152.8662	201.9635	192.2563	184.379	195.122	184.379	175.3959
	195.3867			187.5			143.7126			149.8439			179.1045			171.8377		
	212.2905			199.078			149.8608			157.8277			189.4258			181.6836		
	175.3303																	
2013-05-01	167.4419	147.8439	130.6715				151.1018	143.7126	137.2736	376.9634	298.7552	254.417	171.6329	158.2418	134.8315	153.682	134.2032	120.9068
	148.6524						144.0293			310.0452			154.902			136.264		
	166.949																	
2013-05-13	5458.681	4130.809	3953.871	6231.069	5651.491	5502.484	7358.201	6738.418	6593.407	5590.062	5117.271	4281.891	3854.39	3490.909	3209.987	4366.283	3944.125	3580.308
Pressure Wash																		
	4514.454			5795.015			6896.675			4996.408			3518.428			3963.572		
	4947.425																	
2013-08-16	2516.603	2383.317	2275.96	2105.879	1966.676	1843.318	2797.203	2600.217	2468.712	2386.477	2281.369	2156.657	1748.209	1689.744	1633.764	2509.148	2348.337	2216.066
	2170.309			1789.264			2390.835			2050.114			1574.631			2092.719		
	2336.547			1926.284			2564.242			2218.654			1661.587			2291.568		
	2166.48																	
2013-09-21	1676.173	1615.618	1529.149	1543.739	1420.539	1324.016	2236.719	2161.838	2010.331	1724.964	1642.523	1558.273	1706.566	1631.358	1574.287	1962.388	1765.355	1687.962
	1464.456			1271.411			1908.802			1489.296			1519.629			1567.603		
	1571.349			1389.926			2079.422			1603.764			1607.96			1745.827		
	1666.375																	
2013-10-09	1072.306	987.9931	957.7015	970.5466	939.5798	895.6338	1166.842	1117.579	1025.057	1020.625	978.9259	936.5854	1185.38	1055.1	998.2669	1304.702	1270.177	1217.656
	945.3161			864.9688			970.612			915.5646			953.2005			1176.086		
	990.8292			917.6822			1070.022			962.9252			1047.987			1242.155		
	1038.6																	
2013-11-08	512.9301	456.1148	433.8133	318.2109	295.8033	286.7669	484.8811	434.4285	423.3675	412.4656	384.9238	369.1456	386.92	353.2355	318.6475	398.2191	378.6783	367.6752
	421.3237			276.7315			418.167			356.2328			312.4932			347.5071		
	456.0455			294.3782			440.211			380.692			342.8241			373.0199		
	381.1951			`														
2013-12-17	249.0272	228.0718	224.1769	231.6006	220.4903	208.2881	270.4682	261.7849	252.4898	239.8521	235.1174	220.8216	207.6514	196.5468	190.8878	227.6752	215.4689	211.1096
	235.7564			202.4662			246.0445			207.6544			181.9514			203.7957		
	234.2581			215.7113			257.6969			225.8614			194.2593			214.5123		
	223.72																	

PC																			
2012-10-12	23263.33	22153.85	21951.22	96000	80898.88	92307.69	122033.9	93506.49	82285.71	47058.82	41142.86	42228.74	94117.65	87272.73	85207.1	80898.88	66055.05	64864.86
	22456.13			89735.52			99275.37			43476.81			88865.82			70606.26		
	112886																	
2012-11-06	19972.26	18414.32	20512.82	62608.7	49484.54	54339.62	24324.32	27799.23	26277.37	20224.72	18204.8	19459.46	66055.05	50174.22	47682.12	20253.16	22570.53	21984.73
	20689.66			58299.6			24956.67			18872.87			49484.54			21145.37		
	19897.26			56183.11			25839.4			19190.46			53348.98			21488.45		
	48274.17																	
2012-12-06	23920.27	25352.11	21428.57	35820.9	40111.42	37113.4	16161.62	15567.57	14968.81	15450.64	19618.53	20027.82	27067.67	24365.48	22360.25	14229.25	15384.62	14860.68
	20779.22			39889.2			15434.08			18390.8			23188.41			15205.91		
	22870.04			38233.73			15533.02			18371.95			24245.45			14920.11		
	36575.13																	
2013-01-07	12777.28	11492.42	11783.96	17183.77	13806.33	14342.63	19780.22	16252.82	15550.76	12664.91	10619.47	10105.26	19780.22	18181.82	17286.91	17391.3	19512.2	16628.18
	11009.17			13358.07			15205.91			10374.64			16881.59			16143.5		
	11765.71			14672.7			16697.43			10941.07			18032.64			17418.79		
	18273.76																	
2013-02-25	4117.815	3904.555	3718.048	4771.372	4118.993	4025.72	5077.574	5477.368	5206.074	4977.532	4859.939	4673.807	7834.603	7069.219	6707.033	6434.316	6169.666	6022.585
	3493.45			3947.368			4963.806			4274.265			5990.017			5801.773		
	3808.467			4215.863			5181.205			4696.386			6900.218			6107.085		
	5647.261																	
2013-04-01	2558.181	2384.896	2349.486	2921.485	2763.385	2679.568	2719.547	2658.789	2579.258	3665.988	3377.111	3280.93	4419.89	4189.7	4345.202	4081.633	3903.497	3940.887
	2355.25			2572.347			2555.911			3192.197			4118.993			3807.509		
	2411.953			2734.196			2628.376			3379.056			4268.446			3933.381		
	3386.651																	
2013-05-01	1492.847	1353.002	1276.03	2652.422	2178.517	2141.901	1509.592	1395.349	1316.632	6587.374	5299.963	4208.065	2327.461	1981.015	1938.611	1162.509	1048.111	990.5758
	1254.028			2164.112			1375.095			3958.219			1860.465			940.5003		
	1343.977			2284.238			1399.167			5013.405			2026.888			1035.424		
	1837.354																	
2013-05-13	22222.22	19834.71	18823.53	39130.43	36363.64	35294.12	29568.79	27961.17	26277.37	18067.75	16685.98	15686.27	22748.82	21396.73	20425.53	19972.26	19354.84	18390.8
Pressure Wash																		
	20293.49			36929.4			27935.78			16813.34			21523.69			19239.3		
	23789.16																	
2013-08-16	11365.43	10730.25	10263.72	11920.53	10983.98	10472.73	13899.61	13470.53	13846.15	15368.2	14443.33	13913.04	17433.41	15467.24	14574.9	13872.83	13055.3	12360.52
	10013.91			9696.97			13174.75			13508.44			13345.69			12777.28		
	10593.33			10768.55			13597.76			14308.25			15205.31			13016.48		
	12914.95																	
2013-09-21	9883.322	9461.235	9016.907	10770.38	10404.62	9896.907	10147.99	9677.419	10105.26	11603.55	11258.8	10698.37	11990.01	12224.11	11401.43	10843.37	10404.62	10027.86
	8737.864			10155.15			9580.838			10191.08			10541.73			9856.263		
	9274.832			10306.77			9877.878			10937.95			11539.32			10283.03		
	10369.96																	
2013-10-09	7847.411	8367.228	7663.651	8769.793	8566.33	8294.931	9160.305	8791.209	8515.671	8540.925	8338.159	7890.411	8076.276	7631.161	7365.729	8796.579	8290.155	7929.515
	7411.22			8026.756			8058.198			7563.025			7079.646			7696.419		
	7822.378			8414.452			8631.346			8083.13			7538.203			8178.167		
	8111.279																	
2013-11-08	4724.409	4480.398	4188.482	4018.979	3982.301	3910.918	3450.755	3210.702	3056.027	6307.49	5415.57	5122.732	2975.821	2749.666	2659.28	3483.309	3373.946	3737.348
	4085.106			3700.848			2907.916			4655.674			2550.027			3541.564		
	4369.599			3903.261			3156.35			5375.367			2733.698			3534.042		
	3845.386																	
2013-12-17	2268.431	1987.852	1892.247	1950.163	1840.961	1732.018	1668.211	1558.442	1482.549	1163.354	1080.513	1043.327	2236.372	2114.227	1949.371	1267.048	1121.757	1057.89
	1789.487			1684.802			1419.418			990.8484			1817.035			987.4511		
	1984.504			1801.986			1532.155			1069.511			2029.251			1108.537		
	1587.657																	

Water quality data for PC, PA and PICP:

Hydrologic data for PC, PA and PICP:

				Asphalt																			
		2012-10-15			2013-03-27			2013-09-20			2013-10-08			2013-11-07			2013-11-27					
		Inflow L/s		Outflow		Inflow L/s		Outflow	Inflow L/s		Outflow		Inflow L/s		Outflow		Inflow L/s		Outflow		Inflow L/s		Outflow
3.564	0	1.856		0.000	0	3.584		0	3.494		0.000	0	3.507		0.000	0	3.551		0.000	0	3.438		0.000
3.564	2	3.353		0.087	2	3.584		0	3.494		0.000	2	3.507		0.000	2	3.551		0.000	2	3.438		0.000
3.564	4	3.502		0.175	4	3.584		0.026	3.494		0.003	4	3.507		0.002	4	3.551		0.001	4	3.438		0.001
3.564	6	3.727		0.496	6	3.584		0.128	3.494		0.012	6	3.507		0.007	6	3.551		0.003	6	3.438		0.002
3.564	8	3.727		0.861	8	3.584		0.366	3.494		0.057	8	3.507		0.031	8	3.551		0.027	8	3.438		0.003
3.564	10	3.128		1.157	10	3.584		0.576	3.494		0.086	10	3.507		0.053	10	3.551		0.058	10	3.438		0.006
3.564	12	4.027		1.383	12	3.584		0.747	3.494		0.173	12	3.507		0.082	12	3.551		0.093	12	3.438		0.014
3.564	14	2.903		1.745	14	3.584		0.979	3.494		0.338	14	3.507		0.137	14	3.551		0.173	14	3.438		0.026
3.564	16	3.652		2.184	16	3.584		1.295	3.494		0.613	16	3.507		0.235	16	3.551		0.282	16	3.438		0.053
3.564	18	4.326		2.550	18	3.584		1.732	3.494		0.983	18	3.507		0.535	18	3.551		0.431	18	3.438		0.072
3.564	20	3.352		2.296	20	3.584		2.173	3.494		1.138	20	3.507		0.837	20	3.551		0.631	20	3.438		0.154
3.564	22	3.578		2.076	22			2.012			2.184	22			1.963	22			0.926	22			0.338
0.000	24			1.878	24			1.773			1.963	24			1.915	24			1.057	24			0.663
0.000	26			1.702	26			1.537			1.731	26			1.838	26			1.632	26			0.935
0.000	28			1.583	28			1.489			1.687	28			1.731	28			1.534	28			1.136
0.000	30			1.039	30			1.203			1.532	30			1.632	30			1.433	30			1.458
	32			0.680	32			1.035			1.343	32			1.443	32			1.329	32			1.375
	34			0.457	34			0.843			1.149	34			1.349	34			1.295	34			1.306
	36			0.377	36			0.836			1.003	36			1.203	36			1.119	36			1.285
	38			0.336	38			0.782			0.867	38			1.038	38			1.046	38			1.206
	40			0.302	40			0.702			0.732	40			0.953	40			0.994	40			1.173
	42			0.283	42			0.647			0.678	42			0.822	42			0.981	42			1.095
	44			0.178	44			0.583			0.427	44			0.715	44			0.842	44			1.072
	46			0.131	46			0.506			0.303	46			0.652	46			0.801	46			0.993
	48			0.089	48			0.451			0.305	48			0.527	48			0.763	48			0.981
	50			0.077	50			0.417			0.223	50			0.418	50			0.691	50			0.892
	52			0.052	52			0.432			0.225	52			0.383	52			0.559	52			0.828
	54			0.052	54			0.384			0.173	54			0.271	54			0.505	54			0.743
	56			0.052	56			0.317			0.182	56			0.253	56			0.492	56			0.713
	58			0.052	58			0.303			0.142	58			0.218	58			0.454	58			0.672
	60			0.052	60			0.292			0.119	60			0.199	60			0.394	60			0.635
	62			0.052	62			0.264			0.095	62			0.173	62			0.352	62			0.612
	64			0.052	64			0.231			0.072	64			0.152	64			0.343	64			0.583
	66			0.052	66			0.204			0.072	66			0.138	66			0.328	66			0.562
	68			0.052	68			0.192			0.072	68			0.114	68			0.311	68			0.531
	70			0.052	70			0.172			0.072	70			0.108	70			0.305	70			0.504
	72			0.052	72			0.169			0.072	72			0.093	72			0.297	72			0.456
	74			0.052	74			0.156			0.072	74			0.085	74			0.254	74			0.431
	76			0.052	76			0.098			0.072	76			0.075	76			0.233	76			0.418
	78			0.052	78			0.087			0.072	78			0.075	78			0.215	78			0.407
	80			0.052	80			0.066			0.072	80			0.075	80			0.197	80			0.372
	82			0.052	82			0.058			0.072	82			0.075	82			0.188	82			0.344
	84			0.052	84			0.058			0.072	84			0.075	84			0.184	84			0.360
	86			0.052	86			0.058			0.072	86			0.075	86			0.163	86			0.319
	88			0.052	88			0.058			0.072	88			0.075	88			0.152	88			0.281
	90			0.052	90			0.058			0.072	90			0.075	90			0.148	90			0.251
	92			0.052	92			0.058			0.072	92			0.075	92			0.133	92			0.248
	94			0.052	94			0.058			0.072	94			0.075	94			0.121	94			0.231
	96			0.052	96			0.058			0.072	96			0.075	96			0.117	96			0.217
	98			0.052	98			0.058			0.072	98			0.075	98			0.103	98			0.204
	100			0.052	100			0.058			0.072	100			0.075	100			0.116	100			0.194
	102			0.052	102			0.058			0.072	102			0.075	102			0.107	102			0.179
	104			0.052	104			0.058			0.072	104			0.075	104			0.108	104			0.173
	106			0.052	106			0.058			0.072	106			0.075	106			0.106	106			0.163
	108			0.052	108			0.058			0.072	108			0.075	108			0.105	108			0.158
	110			0.052	110			0.058			0.072	110			0.075	110			0.102	110			0.152
	112			0.052	112			0.058			0.072	112			0.075	112			0.096	112			0.145
	114			0.052	114			0.058			0.072	114			0.075	114			0.088	114			0.133
	116			0.052	116			0.058			0.072	116			0.075	116			0.088	116			0.130
	118			0.052	118			0.058			0.072	118			0.075	118			0.081	118			0.122
	120			0.052	120			0.058			0.072	120			0.075	120			0.079	120			0.118
	122			0.052	122			0.058			0.072	122			0.075	122			0.076	122			0.113
	124			0.052	124			0.058			0.072	124			0.075	124			0.076	124			0.105
	126			0.052	126			0.058			0.072	126			0.075	126			0.076	126			0.104
	128			0.052	128			0.058			0.072	128			0.075	128			0.076	128			0.103
	130			0.052	130			0.058			0.072	130			0.075	130			0.076	130			0.094
	132			0.052	132			0.058			0.072	132			0.075	132			0.076	132			0.082
	134			0.052	134			0.058			0.072	134			0.075	134			0.076	134			0.080
	136			0.052	136			0.058			0.072	136			0.075	136			0.076	136			0.074
	138			0.052	138			0.058			0.072	138			0.075	138			0.076	138			0.069
	140			0.052	140			0.058			0.072	140			0.075	140			0.076	140			0.054
	142			0.052	142			0.058			0.072	142			0.075	142			0.076	142			0.053
	144			0.052	144			0.058			0.072	144			0.075	144			0.076	144			0.050
	146			0.052	146			0.058			0.072	146			0.075	146			0.076	146			0.048
	148			0.052	148			0.058			0.072	148			0.075	148			0.076	148			0.048
	150			0.052	150			0.058			0.072	150			0.075	150			0.076	150			0.048
	152			0.052	152			0.058			0.072	152			0.075	152			0.076	152			0.048
	154			0.052	154			0.058			0.072	154			0.075	154			0.076	154			0.048
	156			0.052	156			0.058			0.072	156			0.075	156			0.076	156			0.048
	158			0.052	158			0.058			0.072	158			0.075	158			0.076	158			0.048
	160			0.052	160			0.058			0.072	160			0.075	160			0.076	160			0.048
	162			0.052	162			0.058			0.072	162			0.075	162			0.076	162			0.048
	164			0.052	164			0.058			0.072	164			0.075	164			0.076	164			0.048
	166			0.052	166			0.058			0.072	166			0.075	166			0.076	166			0.048
	168			0.052	168			0.058			0.072	168			0.075	168			0.076	168			0.048
	170			0.052	170			0.058			0.072	170			0.075	170			0.076	170			0.048
	172			0.052	172			0.058			0.072	172			0.075	172			0.076	172			0.048
	174			0.052	174			0.058			0.072	174			0.075	174			0.076	174			0.048
	176			0.052	176			0.058			0.072	176			0.075	176			0.076	176			0.048
	178			0.052	178			0.058			0.072	178			0.075	178			0.076	178			0.048
	180			0.052	180			0.058			0.072	180			0.075	180			0.076	180			0.048
	182			0.052	182			0.058			0.072	182			0.075	182			0.076	182			0.048
	184			0.052	184			0.058			0.072	184			0.075	184			0.076	184			0.048
	186			0.052	186			0.058			0.072	186			0.075	186			0.076	186			0.048
	188			0.052	188			0.058			0.072	188			0.075	188			0.076	188			0.048
	190			0.052	190			0.058			0.072	190			0.075	190			0.076	190			0.048
	192			0.052	192			0.058			0.072	192			0.075	192			0.076	192			0.048
	194			0.052	194			0.058			0.072	194			0.075	194			0.076	194			0.048
	196			0.052	196			0.058			0.072	196			0.075	196			0.076	196			0.048
	198			0.052	198			0.058			0.072	198			0.075	198			0.076	198			0.048
	200			0.052	200			0.058			0.072	200			0.075	200			0.076	200			0.048
	202			0.052	202			0.058			0.072	202			0.075	202			0.076	202			0.048
	204			0.052	204			0.058			0.072	204			0.075	204			0.076	204			0.048
	206			0.052	206			0.058			0.072	206			0.075	206			0.076	206			0.048
	208			0.052	208			0.058			0.072	208			0.075	208			0.076	208			0.048
	210			0.052	210			0.058			0.072	210			0.075	210			0.076	210			0.048
	212			0.052	212			0.058			0.072	212			0.075	212			0.076	212			0.048
	214			0.052	214			0.058			0.072	214			0.075	214			0.076	214			0.048
	216			0.052	216			0.058			0.072	216			0.075	216			0.076	216			0.048
	218			0.052	218			0.058			0.072	218			0.075	218			0.076	218			0.048
	220			0.052	220			0.058			0.072	220			0.075	220			0.076	220			0.048
	222			0.052	222			0.058			0.072	222			0.075	222			0.076	222			0.048
	224			0.052	224			0.058			0.072	224			0.075	224			0.076	224			0.048
	226			0.052	226			0.058			0.072	226			0.075	226			0.076	226			0.048
	228			0.052	228			0.058			0.072	228			0.075	228			0.076	228			0.048
	230			0.052	230			0.058			0.072	230			0.075	230			0.076	230			0.048
	232			0.039	232			0.058			0.072	232			0.075	232			0.076	232			0.048
	234			0.039	234			0.058			0.072	234			0.075	234			0.076	234			0.048
	236			0.039	236			0.058			0.072	236			0.075	236			0.076	236			0.048
	238			0.039	238			0.058			0.072	238			0.075	238			0.076	238			0.048
	240			0.039	240			0.058			0.072	240			0.075	240			0.076	240			0.048
	242			0.039	242			0.058			0.072	242			0.075	242			0.076	242			0.048
	244			0.039	244			0.058			0.072	244			0.075	244			0.076	244			0.048
	246			0.039	246			0.058			0.072	246			0.075	246			0.076	246			0.048
	248			0.039	248			0.058			0.072	248			0.075	248			0.076	248			0.048
	250			0.039	250			0.058			0.072	250			0.075	250			0.076	250			0.048
	252			0.039	252			0.058			0.072	252			0.075	252			0.076	252			0.048
	254			0.039	254			0.058			0.072	254			0.075	254			0.076	254			0.048
	256			0.039	256			0.058			0.072	256			0.075	256			0.076	256			0.048
	258			0.039	258			0.058			0.072	258			0.075	258			0.076	258			0.048
	260			0.039	260			0.058			0.072	260			0.075	260			0.076	260			0.048
	262			0.039	262			0.058			0.072	262			0.075	262			0.076	262			0.048
	264			0.039	264			0.058			0.072	264			0.075	264			0.076	264			0.048
	266			0.039	266			0.058			0.072	266			0.075	266			0.076	266			0.048
	268			0.039	268			0.058			0.072	268			0.075	268			0.076	268			0.048
	270			0.039	270			0.058			0.072	270			0.075	270			0.076	270			0.048
	272			0.039	272			0.058			0.072	272			0.075	272			0.076	272			0.048
	274			0.039	274			0.058			0.072	274			0.075	274			0.076	274			0.048
	276			0.039	276			0.058			0.072	276			0.075	276			0.076	276			0.048
	278			0.039	278			0.058			0.072	278			0.075	278			0.076	278			0.048
	280			0.039	280			0.058			0.072	280			0.075	280			0.076	280			0.048
	282			0.039	282			0.058			0.072	282			0.075	282			0.076	282			0.048
	284			0.039	284			0.058			0.072	284			0.075	284			0.076	284			0.048
	286			0.039	286			0.058			0.072	286			0.075	286			0.076	286			0.048
	288			0.039	288			0.058			0.072	288			0.075	288			0.076	288			0.048
	290			0.039	290			0.058			0.072	290			0.075	290			0.076	290			0.048
	292			0.039	292			0.058			0.072	292			0.075	292			0.076	292			0.048
	294			0.039	294			0.058			0.072	294			0.075	294			0.076	294			0.048
	296			0.039	296			0.058			0.072	296			0.075	296			0.076	296			0.048
	298			0.039	298			0.058			0.072	298			0.075	298			0.076	298			0.048
	300			0.039	300			0.058			0.072	300			0.075	300			0.076	300			0.048

				Concrete																	
		2012-10-19				2013-03-28				2013-09-24				2013-10-10				2013-11-13				2013-11-28			
		Inflow L/s		Outflow			Inflow L/s		Outflow		Inflow L/s		Outflow		Inflow L/s		Outflow		Inflow L/s		Outflow		Inflow L/s		Outflow
3.564	0	3.484		0.000	0	3.604		0.000	0	3.524		0.000	0	3.478		0.000	0	3.551		0.000	0	3.438		0.000
3.564	2	3.484		0.147	2	3.604		0.002	2	3.524		0.001	2	3.478		0.001	2	3.551		0.003	2	3.438		0.001
3.564	4	3.484		0.583	4	3.604		0.038	4	3.524		0.012	4	3.478		0.009	4	3.551		0.005	4	3.438		0.003
3.564	6	3.484		0.746	6	3.604		0.071	6	3.524		0.025	6	3.478		0.021	6	3.551		0.014	6	3.438		0.016
3.564	8	3.484		1.125	8	3.604		0.158	8	3.524		0.049	8	3.478		0.031	8	3.551		0.019	8	3.438		0.018
3.564	10	3.484		1.520	10	3.604		0.318	10	3.524		0.156	10	3.478		0.079	10	3.551		0.032	10	3.438		0.025
3.564	12	3.484		2.038	12	3.604		0.636	12	3.524		0.286	12	3.478		0.146	12	3.551		0.051	12	3.438		0.033
3.564	14	3.484		2.484	14	3.604		0.975	14	3.524		0.435	14	3.478		0.251	14	3.551		0.103	14	3.438		0.052
3.564	16	3.484		2.682	16	3.604		1.231	16	3.524		0.712	16	3.478		0.393	16	3.551		0.225	16	3.438		0.089
3.564	18	3.484		2.543	18	3.604		1.642	18	3.524		1.168	18	3.478		0.638	18	3.551		0.364	18	3.438		0.134
3.564	20	3.484		2.095	20	3.604		2.401	20	3.524		2.283	20	3.478		1.354	20	3.551		0.635	20	3.438		0.258
3.564	22			1.931	22			2.205	22			1.864	22			2.127	22			0.964	22			0.517
0.000	24			1.641	24			2.024	24			1.643	24			1.984	24			1.849	24			0.834
0.000	26			1.181	26			1.843	26			1.493	26			1.844	26			1.734	26			1.703
0.000	28			0.919	28			1.735	28			1.391	28			1.752	28			1.614	28			1.643
0.000	30			0.916	30			1.590	30			1.297	30			1.614	30			1.562	30			1.580
	32			0.524	32			1.487	32			1.163	32			1.487	32			1.403	32			1.528
	34			0.386	34			1.301	34			1.084	34			1.285	34			1.372	34			1.483
	36			0.187	36			1.207	36			0.976	36			1.183	36			1.305	36			1.404
	38			0.106	38			1.014	38			0.913	38			1.071	38			1.237	38			1.351
	40			0.091	40			0.735	40			0.825	40			1.003	40			1.154	40			1.314
	42			0.079	42			0.642	42			0.768	42			0.953	42			1.073	42			1.284
	44			0.051	44			0.421	44			0.703	44			0.901	44			0.997	44			1.235
	46			0.047	46			0.315	46			0.649	46			0.842	46			0.931	46			1.175
	48			0.047	48			0.253	48			0.591	48			0.783	48			0.885	48			1.083
	50			0.047	50			0.242	50			0.573	50			0.711	50			0.801	50			1.001
	52			0.047	52			0.216	52			0.501	52			0.632	52			0.751	52			0.934
	54			0.047	54			0.201	54			0.483	54			0.543	54			0.711	54			0.879
	56			0.047	56			0.173	56			0.437	56			0.503	56			0.693	56			0.809
	58			0.047	58			0.147	58			0.372	58			0.424	58			0.651	58			0.781
	60			0.047	60			0.132	60			0.318	60			0.331	60			0.604	60			0.744
	62			0.047	62			0.115	62			0.297	62			0.286	62			0.551	62			0.683
	64			0.047	64			0.104	64			0.258	64			0.301	64			0.520	64			0.603
	66			0.047	66			0.096	66			0.241	66			0.284	66			0.481	66			0.592
	68			0.047	68			0.085	68			0.221	68			0.274	68			0.448	68			0.533
	70			0.047	70			0.085	70			0.184	70			0.251	70			0.372	70			0.493
	72			0.047	72			0.085	72			0.153	72			0.205	72			0.331	72			0.471
	74			0.047	74			0.085	74			0.128	74			0.198	74			0.267	74			0.426
	76			0.047	76			0.085	76			0.117	76			0.177	76			0.231	76			0.401
	78			0.047	78			0.084	78			0.109	78			0.142	78			0.202	78			0.336
	80			0.047	80			0.082	80			0.096	80			0.129	80			0.183	80			0.301
	82			0.047	82			0.081	82			0.084	82			0.102	82			0.152	82			0.258
	84			0.047	84			0.062	84			0.074	84			0.086	84			0.129	84			0.238
	86			0.047	86			0.058	86			0.068	86			0.071	86			0.101	86			0.210
	88			0.047	88			0.056	88			0.068	88			0.063	88			0.092	88			0.194
	90			0.047	90			0.056	90			0.068	90			0.054	90			0.081	90			0.154
	92			0.047	92			0.056	92			0.068	92			0.054	92			0.067	92			0.139
	94			0.047	94			0.056	94			0.068	94			0.054	94			0.059	94			0.128
	96			0.047	96			0.056	96			0.068	96			0.054	96			0.055	96			0.106
	98			0.047	98			0.056	98			0.068	98			0.054	98			0.054	98			0.094
	100			0.047	100			0.056	100			0.068	100			0.054	100			0.054	100			0.085
	102			0.047	102			0.056	102			0.068	102			0.054	102			0.054	102			0.081
	104			0.047	104			0.056	104			0.068	104			0.054	104			0.054	104			0.076
	106			0.047	106			0.056	106			0.068	106			0.054	106			0.054	106			0.068
	108			0.047	108			0.056	108			0.068	108			0.054	108			0.054	108			0.063
	110			0.047	110			0.056	110			0.068	110			0.054	110			0.054	110			0.057
	112			0.047	112			0.056	112			0.068	112			0.054	112			0.054	112			0.051
	114			0.047	114			0.056	114			0.068	114			0.054	114			0.054	114			0.046
	116			0.047	116			0.056	116			0.068	116			0.054	116			0.054	116			0.044
	118			0.047	118			0.056	118			0.068	118			0.054	118			0.054	118			0.043
	120			0.047	120			0.056	120			0.068	120			0.054	120			0.054	120			0.042
	122			0.047	122			0.056	122			0.068	122			0.054	122			0.054	122			0.042
	124			0.047	124			0.056	124			0.068	124			0.054	124			0.054	124			0.042
	126			0.047	126			0.056	126			0.059	126			0.051	126			0.051	126			0.041
	128			0.047	128			0.056	128			0.059	128			0.051	128			0.051	128			0.040
	130			0.047	130			0.056	130			0.059	130			0.051	130			0.051	130			0.039
	132			0.047	132			0.056	132			0.059	132			0.051	132			0.051	132			0.038
	134			0.047	134			0.056	134			0.059	134			0.051	134			0.051	134			0.038
	136			0.047	136			0.056	136			0.059	136			0.051	136			0.051	136			0.038
	138			0.047	138			0.056	138			0.059	138			0.051	138			0.051	138			0.038
	140			0.047	140			0.056	140			0.059	140			0.051	140			0.051	140			0.038
	142			0.047	142			0.056	142			0.059	142			0.051	142			0.051	142			0.038
	144			0.047	144			0.056	144			0.059	144			0.051	144			0.051	144			0.038
	146			0.047	146			0.056	146			0.059	146			0.051	146			0.037	146			0.038
	148			0.047	148			0.056	148			0.059	148			0.051	148			0.037	148			0.038
	150			0.047	150			0.056	150			0.059	150			0.051	150			0.037	150			0.038
	152			0.047	152			0.056	152			0.059	152			0.051	152			0.037	152			0.038
	154			0.047	154			0.056	154			0.059	154			0.051	154			0.037	154			0.038
	156			0.047	156			0.056	156			0.059	156			0.051	156			0.037	156			0.037
	158			0.047	158			0.056	158			0.059	158			0.051	158			0.037	158			0.036
	160			0.047	160			0.056	160			0.059	160			0.051	160			0.037	160			0.033
	162			0.047	162			0.056	162			0.059	162			0.051	162			0.037	162			0.033
	164			0.047	164			0.056	164			0.059	164			0.051	164			0.037	164			0.033
	166			0.047	166			0.056	166			0.059	166			0.051	166			0.037	166			0.033
	168			0.047	168			0.056	168			0.059	168			0.051	168			0.037	168			0.033
	170			0.047	170			0.056	170			0.059	170			0.051	170			0.037	170			0.033
	172			0.047	172			0.056	172			0.059	172			0.051	172			0.037	172			0.033
	174			0.047	174			0.056	174			0.059	174			0.051	174			0.037	174			0.033
	176			0.047	176			0.056	176			0.059	176			0.051	176			0.037	176			0.033
	178			0.047	178			0.056	178			0.059	178			0.051	178			0.037	178			0.033
	180			0.047	180			0.056	180			0.059	180			0.051	180			0.037	180			0.033
	182			0.047	182			0.056	182			0.059	182			0.051	182			0.037	182			0.033
	184			0.047	184			0.056	184			0.059	184			0.051	184			0.037	184			0.033
	186			0.047	186			0.056	186			0.059	186			0.051	186			0.037	186			0.033
	188			0.047	188			0.056	188			0.059	188			0.051	188			0.031	188			0.033
	190			0.047	190			0.056	190			0.059	190			0.051	190			0.031	190			0.033
	192			0.047	192			0.056	192			0.059	192			0.051	192			0.031	192			0.033
	194			0.047	194			0.056	194			0.059	194			0.051	194			0.031	194			0.033
	196			0.031	196			0.056	196			0.059	196			0.051	196			0.031	196			0.033
	198			0.031	198			0.056	198			0.059	198			0.051	198			0.031	198			0.032
	200			0.031	200			0.056	200			0.059	200			0.051	200			0.031	200			0.031
	202			0.031	202			0.056	202			0.059	202			0.051	202			0.031	202			0.028
	204			0.031	204			0.056	204			0.059	204			0.051	204			0.031	204			0.028
	206			0.031	206			0.056	206			0.059	206			0.051	206			0.031	206			0.028
	208			0.031	208			0.056	208			0.059	208			0.051	208			0.031	208			0.028
	210			0.031	210			0.056	210			0.059	210			0.051	210			0.031	210			0.028
	212			0.031	212			0.056	212			0.059	212			0.051	212			0.031	212			0.028
	214			0.031	214			0.056	214			0.059	214			0.051	214			0.031	214			0.028
	216			0.031	216			0.056	216			0.059	216			0.051	216			0.031	216			0.028
	218			0.031	218			0.056	218			0.059	218			0.051	218			0.031	218			0.028
	220			0.031	220			0.056	220			0.059	220			0.051	220			0.031	220			0.028
	222			0.031	222			0.040	222			0.044	222			0.048	222			0.031	222			0.028
	224			0.031	224			0.040	224			0.044	224			0.042	224			0.031	224			0.028
	226			0.031	226			0.040	226			0.044	226			0.039	226			0.031	226			0.028
	228			0.031	228			0.040	228			0.044	228			0.039	228			0.031	228			0.028
	230			0.031	230			0.040	230			0.044	230			0.039	230			0.031	230			0.028
	232			0.031	232			0.040	232			0.044	232			0.039	232			0.031	232			0.028
	234			0.031	234			0.040	234			0.044	234			0.039	234			0.031	234			0.028
	236			0.031	236			0.040	236			0.044	236			0.039	236			0.031	236			0.028
	238			0.031	238			0.040	238			0.044	238			0.039	238			0.031	238			0.027
	240			0.031	240			0.040	240			0.044	240			0.039	240			0.031	240			0.027
	242			0.031	242			0.040	242			0.044	242			0.039	242			0.031	242			0.027
	244			0.031	244			0.040	244			0.044	244			0.039	244			0.031	244			0.027
	246			0.031	246			0.040	246			0.044	246			0.039	246			0.029	246			0.027
	248			0.031	248			0.040	248			0.044	248			0.039	248			0.029	248			0.027
	250			0.031	250			0.040	250			0.044	250			0.039	250			0.029	250			0.027
	252			0.031	252			0.040	252			0.044	252			0.039	252			0.029	252			0.027
	254			0.031	254			0.040	254			0.044	254			0.039	254			0.029	254			0.027
	256			0.031	256			0.040	256			0.044	256			0.039	256			0.029	256			0.027
	258			0.031	258			0.040	258			0.044	258			0.039	258			0.029	258			0.027
	260			0.031	260			0.040	260			0.044	260			0.039	260			0.029	260			0.027
	262			0.031	262			0.040	262			0.044	262			0.039	262			0.029	262			0.027
	264			0.031	264			0.040	264			0.044	264			0.039	264			0.029	264			0.027
	266			0.031	266			0.040	266			0.044	266			0.039	266			0.029	266			0.025
	268			0.031	268			0.040	268			0.044	268			0.039	268			0.029	268			0.025
	270			0.031	270			0.040	270			0.044	270			0.039	270			0.029	270			0.025
	272			0.031	272			0.040	272			0.044	272			0.039	272			0.029	272			0.025
	274			0.031	274			0.040	274			0.044	274			0.039	274			0.029	274			0.025
	276			0.031	276			0.040	276			0.044	276			0.039	276			0.029	276			0.025
	278			0.031	278			0.040	278			0.044	278			0.039	278			0.029	278			0.025
	280			0.031	280			0.040	280			0.044	280			0.039	280			0.029	280			0.025
	282			0.031	282			0.040	282			0.044	282			0.039	282			0.029	282			0.025
	284			0.031	284			0.040	284			0.044	284			0.039	284			0.029	284			0.025
	286			0.031	286			0.040	286			0.044	286			0.039	286			0.029	286			0.025
	288			0.031	288			0.040	288			0.044	288			0.039	288			0.029	288			0.025
	290			0.031	290			0.040	290			0.044	290			0.039	290			0.029	290			0.025
	292			0.031	292			0.040	292			0.044	292			0.039	292			0.029	292			0.025
	294			0.031	294			0.040	294			0.044	294			0.039	294			0.029	294			0.025
	296			0.031	296			0.040	296			0.044	296			0.039	296			0.029	296			0.025
	298			0.031	298			0.040	298			0.044	298			0.039	298			0.029	298			0.025
	300			0.031	300			0.040	300			0.044	300			0.039	300			0.029	300			0.025

	PICP										
	Inflow L/s										
0	3.680	0.000	0.000		0.000	0.000		0.000	0.000	0.000	0.000
2	3.680	0.828	0.641		0.019	0.041		0.001	0.001	0.001	0.001
4	3.680	1.063	0.723		0.094	0.075		0.001	0.001	0.001	0.001
6	3.680	1.424	1.064		0.117	0.087		0.001	0.002	0.003	0.002
8	3.680	1.950	1.154		0.135	0.094		0.001	0.001	0.007	0.003
10	3.680	2.512	1.284		0.136	0.104		0.002	0.001	0.011	0.009
12	3.680	2.751	1.532		0.112	0.106		0.003	0.004	0.093	0.043
14	3.680	2.917	1.943		0.144	0.136		0.003	0.005	0.167	0.084
16	3.680	2.863	2.194		0.198	0.156		0.004	0.005	0.246	0.114
18	3.680	2.743	2.631		0.287	0.188		0.007	0.006	0.308	0.148
20	3.680	2.545	2.512		0.749	0.593		0.008	0.006	0.411	0.205
22	0.000	2.069	2.481		1.534	0.919		0.014	0.009	0.482	0.274
24	0.000	1.350	2.319		2.055	1.437		0.016	0.009	0.571	0.341
26	0.000	0.806	2.016		2.327	1.753		0.018	0.013	0.663	0.385
28	0.000	0.447	1.732		2.211	1.865		0.060	0.021	0.719	0.441
30	0.000	0.224	1.431		2.057	1.777		0.091	0.046	0.880	0.552
32	0.000	0.144	0.843		1.924	1.642		0.148	0.071	0.938	0.693
34	0.000	0.103	0.631		1.743	1.542		0.181	0.089	1.036	0.773
36	0.000	0.069	0.510		1.551	1.430		0.261	0.096	1.285	0.837
38	0.000	0.050	0.429		1.368	1.409		0.294	0.105	1.537	0.936
40	0.000	0.040	0.392		1.218	1.322		0.326	0.157	1.638	1.085
42	0.000	0.029	0.342		1.120	1.207		0.352	0.195	1.578	1.258
44	0.000	0.024	0.213		0.963	1.169		0.397	0.226	1.491	1.542
46	0.000	0.019	0.143		0.877	1.097		0.486	0.286	1.402	1.463
48	0.000	0.019	0.102		0.856	1.046		0.571	0.316	1.336	1.396
50	0.000	0.014	0.084		0.846	1.034		0.658	0.388	1.226	1.248
52	0.000	0.011	0.079		0.801	0.971		0.771	0.412	1.157	1.139
54	0.000	0.011	0.061		0.792	0.923		0.977	0.587	1.037	1.074
56	0.000	0.011	0.059		0.788	0.911		1.289	0.652	0.947	0.983
58	0.000	0.011	0.059		0.742	0.896		1.456	0.784	0.836	0.932
60	0.000	0.011	0.059		0.704	0.873		1.397	1.047	0.784	0.813
62	0.000	0.011	0.059		0.675	0.861		1.207	1.107	0.731	0.762
64	0.000	0.011	0.059		0.625	0.852		1.153	1.196	0.684	0.653
66	0.000	0.011	0.059		0.582	0.846		1.083	1.287	0.629	0.619
68	0.000	0.011	0.059		0.557	0.811		1.018	1.186	0.598	0.527
70	0.000	0.011	0.059		0.524	0.810		0.936	1.096	0.552	0.482
72	0.000	0.011	0.059		0.497	0.808		0.921	0.937	0.512	0.431
74	0.000	0.011	0.059		0.465	0.807		0.905	0.883	0.487	0.387
76	0.000	0.011	0.059		0.445	0.807		0.894	0.851	0.458	0.356
78	0.000	0.011	0.059		0.475	0.805		0.875	0.794	0.446	0.314
80	0.000	0.011	0.059		0.459	0.805		0.871	0.763	0.438	0.298
82	0.000	0.011	0.059		0.445	0.753		0.841	0.741	0.417	0.287
84	0.000	0.011	0.059		0.422	0.704		0.794	0.732	0.408	0.286
86	0.000	0.011	0.059		0.400	0.692		0.779	0.718	0.399	0.262
88	0.000	0.011	0.059		0.389	0.681		0.758	0.694	0.391	0.257
90	0.000	0.011	0.059		0.381	0.681		0.751	0.683	0.381	0.251
92	0.000	0.011	0.059		0.364	0.669		0.742	0.671	0.368	0.244
94	0.000	0.011	0.059		0.353	0.669		0.738	0.662	0.363	0.243
96	0.000	0.011	0.059		0.343	0.658		0.722	0.656	0.351	0.237
98	0.000	0.011	0.059		0.325	0.658		0.717	0.650	0.342	0.230
100	0.000	0.011	0.059		0.301	0.646		0.712	0.621	0.337	0.228
102	0.000	0.011	0.059		0.291	0.634		0.695	0.604	0.328	0.224
104	0.000	0.011	0.059		0.297	0.611		0.648	0.584	0.319	0.221
106	0.000	0.011	0.059		0.290	0.600		0.622	0.571	0.301	0.217
108	0.000	0.011	0.041		0.291	0.588		0.610	0.564	0.278	0.213
110	0.000	0.011	0.041		0.274	0.531		0.600	0.557	0.261	0.207
112	0.000	0.011	0.041		0.265	0.519		0.573	0.550	0.247	0.198
114	0.000	0.011	0.041		0.268	0.519		0.541	0.542	0.237	0.194
116	0.000	0.011	0.041		0.261	0.508		0.518	0.536	0.225	0.185
118	0.000	0.011	0.041		0.250	0.508		0.486	0.511	0.224	0.179
120	0.000	0.011	0.041		0.246	0.496		0.456	0.504	0.224	0.174
122	0.000	0.011	0.041		0.248	0.496		0.432	0.494	0.217	0.173
124	0.000	0.011	0.041		0.252	0.473		0.425	0.482	0.205	0.173
126	0.000	0.011	0.041		0.242	0.450		0.414	0.472	0.192	0.171
128	0.000	0.011	0.041		0.245	0.438		0.411	0.461	0.188	0.168
130	0.000	0.011	0.041		0.241	0.427		0.407	0.446	0.184	0.168
132	0.000	0.011	0.041		0.234	0.404		0.403	0.431	0.174	0.168
134	0.000	0.011	0.041		0.225	0.404		0.399	0.418	0.172	0.168
136	0.000	0.011	0.041		0.225	0.392		0.394	0.410	0.169	0.168
138	0.000	0.011	0.041		0.224	0.392		0.386	0.402	0.166	0.168
140	0.000	0.011	0.041		0.219	0.381		0.381	0.395	0.163	0.168
142	0.000	0.011	0.041		0.212	0.381		0.376	0.392	0.158	0.168
144	0.000	0.011	0.041		0.203	0.369		0.373	0.388	0.155	0.167
146	0.000	0.011	0.041		0.194	0.369		0.366	0.384	0.152	0.165
148	0.000	0.011	0.041		0.178	0.358		0.364	0.381	0.148	0.161
150	0.000	0.011	0.041		0.169	0.358		0.358	0.374	0.145	0.160
152	0.000	0.011	0.041		0.155	0.346		0.348	0.361	0.142	0.159
154	0.000	0.011	0.041		0.138	0.346		0.341	0.347	0.139	0.154
156	0.000	0.011	0.041		0.127	0.335		0.336	0.327	0.133	0.142
158	0.000	0.011	0.041		0.113	0.335		0.329	0.311	0.130	0.138
160	0.000	0.011	0.041		0.108	0.323		0.322	0.302	0.127	0.135
162	0.000	0.011	0.041		0.098	0.311		0.316	0.295	0.122	0.131
164	0.000	0.011	0.041		0.088	0.300		0.304	0.288	0.113	0.128
166	0.000	0.011	0.041		0.088	0.300		0.297	0.273	0.110	0.125
168	0.000	0.011	0.041		0.088	0.288		0.274	0.258	0.106	0.124
170	0.000	0.011	0.041		0.088	0.288		0.235	0.240	0.102	0.122
172	0.000	0.011	0.041		0.088	0.277		0.228	0.226	0.097	0.120
174	0.000	0.011	0.041		0.088	0.265		0.214	0.215	0.096	0.118
176	0.000	0.011	0.041		0.088	0.265		0.205	0.215	0.096	0.115
178	0.000	0.011	0.041		0.088	0.254		0.197	0.215	0.096	0.114
180	0.000	0.011	0.041		0.088	0.242		0.190	0.215	0.096	0.113
182	0.000	0.011	0.041		0.088	0.242		0.179	0.215	0.096	0.112
184	0.000	0.011	0.041		0.088	0.242		0.171	0.215	0.096	0.112
186	0.000	0.011	0.041		0.088	0.231		0.164	0.215	0.096	0.112
188	0.000	0.011	0.041		0.088	0.231		0.158	0.215	0.096	0.112
190	0.000	0.011	0.041		0.088	0.231		0.154	0.215	0.096	0.112
192	0.000	0.011	0.041		0.088	0.219		0.149	0.215	0.096	0.112
194	0.000	0.011	0.041		0.088	0.219		0.146	0.215	0.096	0.112
196	0.000	0.011	0.041		0.088	0.219		0.134	0.215	0.096	0.112
198	0.000	0.011	0.041		0.088	0.219		0.124	0.215	0.096	0.112
200	0.000	0.011	0.041		0.088	0.219		0.124	0.211	0.096	0.112
202	0.000	0.011	0.041		0.088	0.219		0.124	0.208	0.096	0.112
204	0.000	0.011	0.041		0.088	0.219		0.124	0.201	0.096	0.108
206	0.000	0.011	0.041		0.088	0.219		0.124	0.195	0.096	0.107
208	0.000	0.011	0.041		0.088	0.219		0.124	0.190	0.096	0.105
210	0.000	0.011	0.041		0.088	0.219		0.124	0.182	0.096	0.103
212	0.000	0.011	0.041		0.088	0.219		0.124	0.181	0.096	0.102
214	0.000	0.011	0.033		0.088	0.219		0.124	0.175	0.096	0.102
216	0.000	0.011	0.033		0.088	0.219		0.124	0.170	0.095	0.102
218	0.000	0.011	0.033		0.088	0.219		0.124	0.169	0.093	0.102
220	0.000	0.011	0.033		0.088	0.219		0.124	0.166	0.091	0.102
222	0.000	0.011	0.033		0.088	0.219		0.124	0.166	0.088	0.102
224	0.000	0.011	0.033		0.088	0.190		0.123	0.166	0.086	0.102
226	0.000	0.011	0.033		0.088	0.190		0.121	0.166	0.085	0.102
228	0.000	0.011	0.033		0.088	0.190		0.119	0.166	0.084	0.102
230	0.000	0.011	0.033		0.088	0.190		0.119	0.166	0.084	0.102
232	0.000	0.011	0.033		0.088	0.190		0.119	0.166	0.084	0.102
234	0.000	0.011	0.033		0.088	0.190		0.119	0.166	0.084	0.102
236	0.000	0.011	0.033		0.088	0.138		0.119	0.166	0.084	0.102
238	0.000	0.011	0.026		0.088	0.138		0.119	0.166	0.084	0.102
240	0.000	0.011	0.026		0.088	0.138		0.119	0.166	0.084	0.102
242	0.000	0.011	0.026		0.088	0.138		0.119	0.166	0.084	0.102
244	0.000	0.011	0.026		0.088	0.138		0.119	0.166	0.084	0.102
246	0.000	0.011	0.026		0.088	0.137		0.119	0.166	0.084	0.102
248	0.000	0.011	0.026		0.088	0.138		0.119	0.166	0.084	0.102
250	0.000	0.011	0.026		0.088	0.138		0.119	0.166	0.084	0.102
252	0.000	0.011	0.026		0.088	0.145		0.119	0.166	0.084	0.102
254	0.000	0.011	0.026		0.088	0.138		0.119	0.166	0.084	0.101
256	0.000	0.011	0.026		0.088	0.139		0.119	0.166	0.084	0.100
258	0.000	0.011	0.026		0.083	0.138		0.119	0.166	0.084	0.097
260	0.000	0.011	0.026		0.081	0.115		0.119	0.166	0.084	0.097
262	0.000	0.011	0.026		0.079	0.115		0.119	0.166	0.084	0.097
264	0.000	0.011	0.026		0.076	0.115		0.119	0.166	0.084	0.097
266	0.000	0.011	0.026		0.075	0.115		0.119	0.166	0.084	0.097
268	0.000	0.011	0.026		0.075	0.115		0.119	0.166	0.084	0.097
270	0.000	0.011	0.026		0.075	0.115		0.119	0.166	0.084	0.097
272	0.000	0.011	0.026		0.075	0.115		0.119	0.164	0.084	0.097
274	0.000	0.011	0.026		0.075	0.115		0.119	0.163	0.084	0.097
276	0.000	0.011	0.026		0.075	0.115		0.119	0.163	0.084	0.097
278	0.000	0.011	0.026		0.075	0.115		0.119	0.163	0.084	0.097
280	0.000	0.011	0.026		0.075	0.115		0.119	0.163	0.084	0.097
282	0.000	0.011	0.026		0.075	0.115		0.119	0.163	0.084	0.097
284	0.000	0.011	0.026		0.075	0.115		0.119	0.163	0.084	0.097
286	0.000	0.011	0.026		0.075	0.115		0.119	0.163	0.084	0.097
288	0.000	0.011	0.026		0.075	0.115		0.119	0.163	0.084	0.097
290	0.000	0.011	0.026		0.075	0.115		0.119	0.163	0.084	0.097
292	0.000	0.011	0.026		0.075	0.115		0.119	0.163	0.084	0.097
294	0.000	0.011	0.026		0.051	0.115		0.119	0.163	0.084	0.097
296	0.000	0.011	0.026		0.051	0.115		0.119	0.163	0.084	0.097
298	0.000	0.011	0.026		0.050	0.115		0.119	0.163	0.084	0.097
300	0.000	0.011	0.026		0.050	0.115		0.119	0.163	0.084	0.097

Appendix B: Raw Data for Lab Experiments

Pollutant concentrations with respect to different lab-scale modules:

63 mm gravels

	TSS			TP		TN	
sample (ml)	100						
		Raw storm		Raw storm		Raw storm	
raw water		533		2.54		4.13	
		481		2.78		4.25	
		548		2.82		4.08	
		488		2.85		4.31	
		563		2.58		4.46	
		502		2.79		4.61	
		518		2.45		4.52	
		479		2.73		4.47	
		457		2.86		4.27	
		558		2.94		4.09	
		521		2.88		4.25	
		503		2.58		4.33	
Depth of layer (mm)		Outflow Conc.		Outflow Conc.		Outflow Conc.	
100	1	199	1	1.97	1	4.22	
		180		1.85		4.27	
		213		2.03		4.24	
		195		1.82		4.19	
	2	200	2	1.91	2	4.28	
		226		1.85		4.24	
		184		2.01		4.22	
		196		1.92		4.20	
	3	216	3	1.89	3	4.17	
		190		2.04		4.23	
		189		1.93		4.17	
		173		2.07		4.26	
	4	199	4	1.85	4	4.29	
		163		1.97		4.24	
		214		1.91		4.20	
		171		1.85		4.26	
200	1	165	1	1.52	1	4.21	
		148		1.58		4.19	
		134		1.69		4.26	
		157		1.52		4.13	
	2	167	2	1.47	2	4.25	
		154		1.60		4.16	
		137		1.72		4.21	
		142		1.56		4.12	
	3	132	3	1.69	3	4.25	
		154		1.57		4.09	
		161		1.52		4.19	
		143		1.48		4.20	
	4	118	4	1.61	4	4.15	
		122		1.47		4.25	
		104		1.49		4.13	
		134		1.64		4.14	
300	1	129	1	1.32	1	4.12	
		96		1.18		4.18	
		125		1.25		4.16	
		119		1.34		4.18	
	2	107	2	1.41	2	4.10	
		110		1.22		4.14	
		119		1.05		4.12	
		103		1.32		4.21	
	3	92	3	1.39	3	4.25	
		99		1.27		4.18	
		106		1.12		4.11	
		113		1.25		4.17	
	4	117	4	1.29	4	4.24	
		97		1.31		4.13	
		101		1.13		4.16	
		89		1.15		4.19	
400	1	81	1	0.84	1	4.14	
		70		1.05		4.07	
		73		0.97		4.17	
		104		0.89		4.19	
	2	101	2	1.04	2	4.15	
		88		0.93		4.21	
		102		1.09		4.12	
		93		1.06		4.17	
	3	74	3	0.97	3	4.10	
		86		1.15		4.18	
		101		1.03		4.07	
		67		0.89		4.18	
	4	81	4	0.95	4	4.19	
		74		1.07		4.03	
		68		0.95		4.15	
		96		1.13		4.13	
500	1	72	1	0.84	1	4.13	
		82		0.71		4.03	
		91		0.78		4.08	
		87		0.75		4.19	
	2	66	2	0.73	2	4.18	
		65		0.58		4.09	
		59		0.81		4.15	
		42		0.67		4.15	
	3	63	3	0.69	3	4.13	
		52		0.83		4.07	
		41		0.63		4.11	
		75		0.76		4.16	
	4	61	4	0.52	4	4.18	
		46		0.58		4.14	
		73		0.61		4.20	
		58		0.71		4.11	

40 mm gravels

	TSS			TP		TN	
sample (ml)	100						
		Raw storm		Raw storm		Raw storm	
raw water		553		2.54		4.13	
		531		2.78		4.25	
		518		2.82		4.18	
		489		2.85		4.31	
		493		2.58		4.46	
		506		2.79		4.41	
		521		2.85		4.47	
		486		2.83		4.34	
		533		2.86		4.41	
		513		2.94		4.14	
		483		2.62		4.15	
		548		2.81		4.33	
Depth of layer (mm)		Outflow Conc.		Outflow Conc.		Outflow Conc.	
50	1	235	1	2.18	1	4.24	
		259		2.12		4.27	
		274		2.11		4.19	
		242		2.23		4.22	
	2	255	2	2.19	2	4.25	
		245		2.15		4.27	
		238		2.11		4.16	
		243		2.13		4.27	
	3	221	3	2.01	3	4.29	
		252		2.16		4.26	
		273		2.25		4.30	
		248		2.13		4.18	
	4	224	4	2.27	4	4.24	
		236		2.27		4.19	
		265		2.18		4.26	
		252		2.21		4.27	
100	1	182	1	1.81	1	4.19	
		155		1.96		4.27	
		176		1.85		4.26	
		152		2.03		4.21	
	2	183	2	1.88	2	4.29	
		179		2.02		4.18	
		185		1.93		4.16	
		191		1.94		4.22	
	3	205	3	1.85	3	4.24	
		185		1.77		4.26	
		159		1.73		4.20	
		164		1.97		4.26	
	4	172	4	1.82	4	4.27	
		156		1.92		4.17	
		172		1.71		4.27	
		153		1.88		4.17	
150	1	144	1	1.62	1	4.25	
		152		1.67		4.28	
		140		1.55		4.19	
		155		1.68		4.25	
	2	179	2	1.75	2	4.16	
		144		1.63		4.19	
		156		1.78		4.20	
		148		1.62		4.27	
	3	139	3	1.84	3	4.15	
		118		1.59		4.18	
		157		1.64		4.19	
		137		1.72		4.30	
	4	122	4	1.78	4	4.21	
		129		1.63		4.26	
		138		1.57		4.24	
		152		1.49		4.16	
200	1	136	1	1.33	1	4.25	
		141		1.47		4.21	
		124		1.51		4.13	
		111		1.43		4.20	
	2	126	2	1.39	2	4.21	
		111		1.32		4.23	
		106		1.50		4.14	
		117		1.41		4.26	
	3	93	3	1.36	3	4.28	
		132		1.42		4.20	
		120		1.55		4.17	
		108		1.58		4.23	
	4	101	4	1.53	4	4.21	
		111		1.52		4.26	
		96		1.68		4.17	
		104		1.47		4.18	
250	1	113	1	1.22	1	4.22	
		105		1.46		4.16	
		117		1.38		4.26	
		84		1.23		4.27	
	2	102	2	1.12	2	4.14	
		90		1.26		4.20	
		105		1.38		4.15	
		115		1.31		4.26	
	3	97	3	1.42	3	4.21	
		88		1.39		4.26	
		103		1.46		4.17	
		79		1.37		4.18	
	4	92	4	1.21	4	4.24	
		110		1.28		4.10	
		75		1.41		4.17	
		89		1.24		4.22	

12 mm gravels

	TSS			TP		TN	
sample (ml)	100						
		Raw storm		Raw storm		Raw storm	
raw water		522		2.44		4.28	
		507		2.71		4.38	
		473		2.83		4.55	
		510		2.36		4.26	
		531		2.57		4.43	
		538		2.91		4.51	
		492		2.85		4.26	
		503		2.59		4.05	
		527		2.74		4.21	
		511		2.94		4.26	
		548		2.81		4.51	
		531		2.99		4.10	
Depth of layer (mm)		Outflow Conc.		Outflow Conc.		Outflow Conc.	
30	1	275	1	2.16	1	4.31	
		261		2.21		4.21	
		269		2.26		4.26	
		255		2.12		4.30	
	2	263	2	2.18	2	4.25	
		279		2.09		4.20	
		248		2.13		4.28	
		237		2.08		4.32	
	3	261	3	2.18	3	4.32	
		270		2.20		4.31	
		235		2.20		4.29	
		227		2.27		4.27	
	4	249	4	2.07	4	4.25	
		236		2.14		4.32	
		252		2.17		4.31	
		248		2.11		4.30	
50	1	228	1	2.04	1	4.31	
		203		2.18		4.32	
		182		2.05		4.24	
		223		1.95		4.21	
	2	217	2	2.06	2	4.32	
		230		2.11		4.30	
		248		1.91		4.27	
		218		2.06		4.27	
	3	225	3	1.98	3	4.27	
		216		2.01		4.24	
		223		2.14		4.28	
		194		2.03		4.30	
	4	169	4	2.11	4	4.22	
		189		2.13		4.31	
		203		2.05		4.32	
		195		1.89		4.27	
70	1	173	1	1.93	1	4.27	
		205		1.90		4.32	
		156		1.79		4.30	
		176		1.88		4.22	
	2	159	2	1.96	2	4.25	
		166		2.05		4.27	
		142		1.82		4.28	
		157		1.94		4.31	
	3	192	3	1.88	3	4.32	
		173		1.92		4.26	
		155		1.99		4.18	
		189		1.96		4.27	
	4	201	4	2.01	4	4.29	
		164		1.86		4.30	
		146		1.74		4.25	
		171		1.97		4.31	
90	1	132	1	1.69	1	4.27	
		110		1.87		4.23	
		147		1.96		4.32	
		138		1.70		4.29	
	2	172	2	1.74	2	4.25	
		149		1.73		4.32	
		166		1.83		4.28	
		122		1.75		4.31	
	3	131	3	1.68	3	4.22	
		144		1.87		4.24	
		127		1.92		4.19	
		137		1.89		4.24	
	4	171	4	1.93	4	4.20	
		138		1.78		4.28	
		152		1.96		4.25	
		136		1.77		4.30	
110	1	145	1	1.75	1	4.31	
		128		1.60		4.22	
		103		1.68		4.18	
		142		1.82		4.26	
	2	108	2	1.63	2	4.25	
		103		1.72		4.30	
		110		1.80		4.21	
		137		1.73		4.27	
	3	93	3	1.85	3	4.20	
		118		1.73		4.25	
		104		1.93		4.30	
		142		1.68		4.27	
	4	101	4	1.77	4	4.25	
		95		1.59		4.23	
		117		1.66		4.32	
		135		1.56		4.26	

Surface

	TSS		TP		TN	
sample (ml)	100					
		Raw storm		Raw storm		Raw storm
raw water		521		2.44		4.28
		528		2.71		4.38
		502		2.83		4.55
		536		2.36		4.26
		502		2.57		4.43
		482		2.91		4.51
		533		2.85		4.26
		519		2.59		4.05
		527		2.74		4.21
		512		2.94		4.26
		485		2.81		4.51
		518		2.99		4.10

Pavement		Outflow Conc.		Outflow Conc.		Outflow Conc.
PA	1	464	1	2.55	1	4.25
		451		2.59		4.17
		423		2.62		4.32
		439		2.60		4.30
	2	461	2	2.51	2	4.27
		455		2.61		4.20
		447		2.68		4.14
		432		2.57		4.28
	3	447	3	2.62	3	4.26
		458		2.68		4.21
		435		2.45		4.15
		439		2.59		4.28
	4	431	4	2.66	4	4.32
		449		2.61		4.29
		463		2.55		4.22
		436		2.64		4.24
PC	1	403	1	2.53	1	4.32
		374		2.46		4.20
		432		2.61		4.12
		421		2.48		4.23
	2	395	2	2.55	2	4.16
		418		2.69		4.25
		404		2.57		4.21
		413		2.41		4.32
	3	432	3	2.39	3	4.11
		417		2.55		4.23
		389		2.63		4.30
		411		2.44		4.12
	4	415	4	2.41	4	4.17
		408		2.51		4.31
		422		2.65		4.23
		401		2.46		4.14
PICP	1	422	1	2.66	1	4.17
		453		2.61		4.23
		435		2.53		4.22
		458		2.59		4.32
	2	439	2	2.68	2	4.25
		431		2.53		4.17
		426		2.68		4.24
		441		2.58		4.21
	3	431	3	2.51	3	4.25
		455		2.48		4.19
		447		2.64		4.18
		428		2.64		4.24
	4	451	4	2.54	4	4.29
		470		2.47		4.30
		433		2.66		4.19
		427		2.58		4.31

Full Structure

	TSS		TP		TN	
sample (ml)	100					
		Raw storm		Raw storm		Raw storm
raw water		473		2.83		4.41
		510		2.91		4.23
		531		2.76		4.19
		538		2.71		4.38
		492		2.68		4.47
		502		2.59		4.22
		518		2.80		4.35
		479		2.69		4.46
		457		2.88		4.26
		558		2.43		4.17
		521		2.66		4.33
		527		2.78		4.40

Pavement		Outflow Conc.		Outflow Conc.		Outflow Conc.
PA	1	51	1	0.32	1	4.01
		64		0.49		3.86
		32		0.61		4.13
		45		0.55		4.18
	2	27	2	0.42	2	4.10
		47		0.58		4.02
		66		0.44		3.95
		48		0.58		4.02
	3	33	3	0.61	3	4.17
		61		0.56		4.08
		38		0.47		4.03
		48		0.63		4.19
	4	35	4	0.59	4	4.11
		41		0.43		4.03
		27		0.46		3.99
		46		0.55		3.93
PC	1	49	1	0.47	1	4.03
		66		0.61		4.11
		29		0.61		3.95
		34		0.44		4.08
	2	50	2	0.51	2	4.17
		57		0.58		3.88
		42		0.63		3.96
		24		0.48		4.04
	3	40	3	0.42	3	4.01
		57		0.49		4.15
		53		0.54		3.85
		37		0.57		3.92
	4	32	4	0.51	4	3.92
		32		0.66		4.05
		39		0.68		4.07
		52		0.58		3.93
PICP	1	36	1	0.33	1	4.08
		52		0.49		4.13
		57		0.38		3.91
		33		0.51		4.11
	2	43	2	0.61	2	3.97
		51		0.40		4.03
		26		0.47		4.12
		40		0.35		4.09
	3	54	3	0.44	3	4.14
		31		0.61		4.07
		28		0.39		4.11
		53		0.54		3.92
	4	47	4	0.53	4	4.16
		24		0.48		4.11
		35		0.64		4.07
		31		0.29		3.94